NORSAR

ROYAL NORWEGIAN COUNCIL FOR SCIENTIFIC AND INDUSTRIAL RESEARCH

Scientific Report No. 5-74/75

FINAL TECHNICAL REPORT
NORSAR PHASE 3

1 July 1974 – 30 June 1975

Prepared by
K. A. Berteussen

Kjeller, 8. August 1975

Sponsored by
Advanced Research Projects Agency
ARPA Order No. 2551

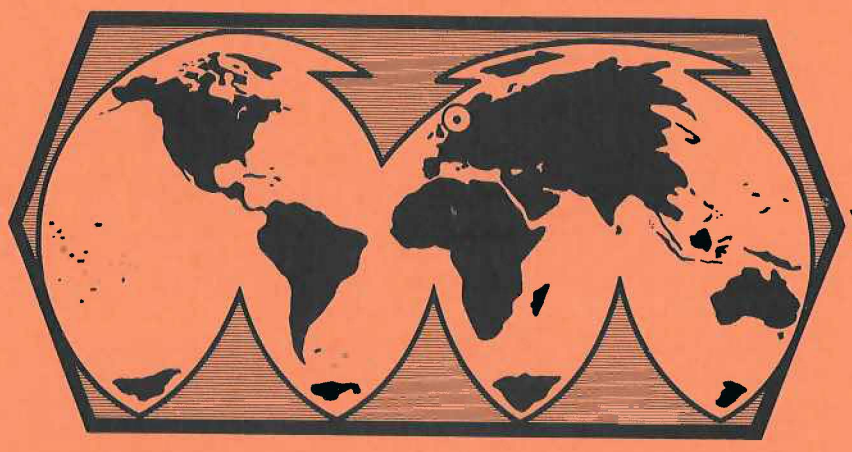

SECURITY CLASSIFICATION OF THIS PAGE *(When Data Entered)*

REPORT DOCUMENTATION PAGE

READ INSTRUCTIONS BEFORE COMPLETING FORM

1. REPORT NUMBER: F08606-74-C-0049	2. GOVT ACCESSION NO.
3. RECIPIENT'S CATALOG NUMBER	
4. TITLE *(and Subtitle)*: Final Report - NORSAR Phase 3 1 July 1974 - 30 June 1975	5. TYPE OF REPORT & PERIOD COVERED: Technical Report 1 July 74 - 30 June 75
	6. PERFORMING ORG. REPORT NUMBER: Sci. Rep. No. 5-74/75
7. AUTHOR(s): K.A. Berteussen (editor)	8. CONTRACT OR GRANT NUMBER(s): F08606-74-C-0049
9. PERFORMING ORGANIZATION NAME AND ADDRESS: NTNF/NORSAR Post Box 51 2007 Kjeller, Norway	10. PROGRAM ELEMENT, PROJECT, TASK AREA & WORK UNIT NUMBERS: NORSAR Phase 3
11. CONTROLLING OFFICE NAME AND ADDRESS: Vela Seismological Center 312 Montgomery Street Alexandria, Va. 22314	12. REPORT DATE: 8 August 1975 13. NUMBER OF PAGES: 109
14. MONITORING AGENCY NAME & ADDRESS *(if different from Controlling Office)*	15. SECURITY CLASS. *(of this report)* 15a. DECLASSIFICATION/DOWNGRADING SCHEDULE

16. DISTRIBUTION STATEMENT *(of this Report)*

Approved for public release; distribution unlimited.

17. DISTRIBUTION STATEMENT *(of the abstract entered in Block 20, if different from Report)*

18. SUPPLEMENTARY NOTES

19. KEY WORDS *(Continue on reverse side if necessary and identify by block number)*

NORSAR, Seismic Array, Seismology

20. ABSTRACT *(Continue on reverse side if necessary and identify by block number)*

This report covers research and operation activities at the Norwegian Seismic Array (NORSAR) for the period 1 July 1974 - 30 June 1975. The research activities are described in chapters A-S, while chapters T-Y report on data processing, programming, ARPANET activities, computer center operation and array maintenance.

DD FORM 1 JAN 73 1473 EDITION OF 1 NOV 65 IS OBSOLETE

SECURITY CLASSIFICATION OF THIS PAGE *(When Data Entered)*

AFTAC Project Authorization No.: VT/5702/B/ETR

ARPA Order No.	:	2551
Program Code No.	:	5F10
Name of Contractor	:	Royal Norwegian Council for Scientific and Industrial Research
Effective Date of Contract	:	1 July 1974
Contract Expiration Date	:	30 June 1975
Contract No.	:	F08606-74-C-0049
Project Manager	:	Nils Marås (02) 71 69 15
Title of Work	:	Norwegian Seismic Array (NORSAR) Phase 3
Amount of Contract	:	$900 000
Contract period covered by the report	:	1 July 1974-30 June 1975

This research was supported by the Advanced Research Projects Agency of the Department of Defense and was monitored by AFTAC/VSC, Patrick AFB FL 32925, under Contract No. F08606-74-C-0049.

TABLE OF CONTENTS

TABLE OF CONTENTS
(Cont.)

SUMMARY

This report covers research and operation activities at the Norwegian Seismic Array (NORSAR) for the period 1 July 1974-30 June 1975. The research activities are described in chapters A-S, while chapters T-Y report on data processing, programming, ARPANET activities, computer center operation and array maintenance.

In the reporting period seismological research covering a wide range of topics has been going on at NORSAR. Some projects are continued from the previous period, while some new projects represent topics previously not covered by this institution. Scattering of teleseismic signals has been given a great deal of attention the last few years both at NORSAR and other institutions. Chapters A, B and C represent a continuation of previous work in this field, while Chapter H discusses the effect of scattering of signals from local events. The location of the source of array-recorded slowness, azimuth and internal time anomalies has been discussed ever since they first were discovered. In Chapters D and E it is demonstrated that both for NORSAR and LASA these are mainly of local origin. The details of the local structure causing these anomalies are investigated 3-dimensionally in Chapter F, while the next Chapter (G) reports on a study of the upper mantle in the vicinity of the NORSAR array.

A new method for a parameterized description of both seismic signals (Chapter I) and noise (Chapter J) is presented. Chapter K reports on an earthquake/explosion discrimination study using the m_b:M_s method, while it is demonstrated in Chapter L that the method described in Chapters I and J can be used to improve the discrimination capability of the array. The 'Kirnos project' for comparison of 'east' and 'west' magnitudes is now finished and the results are presented in Chapter M. Chapter N is a report on the problem of using various statistical tests for discriminating

between seismic noise and signals.

Chapters O, P and Q are devoted to surface wave studies. The first of these (Chapter O) is a study of surface wave dispersion between Kirkenes and Kings Bay. The second one (Chapter P) is a study of anisotropy using higher mode surface waves, while the last (Chapter Q) is a study of source spectra and scaling laws.

In Chapter R it is demonstrated that seismic 'noise' produced by a hydroelectric power plant may be used for studies of in situ stress. The last of the research chapters (S) is a study of the seismicity in Fennoscandia.

Chapters T-Y report on the operation of the array. Chapters T and U describe the event detection and processing activities. It is demonstrated that previous research efforts reported herein has successfully been included in the daily operation. Although the programming staff has been reduced, Chapter V can report on a large activity of this group in several fields. One such example is their work on the ARPANET (Chapter W) which has become an integrated part of the NORSAR daily life. Chapters X and Y report on the operation of the data center and the array maintenance, respectively.

K.A.Berteussen

A. STUDIES OF PRECURSORS

The correct interpretation of precursor signals associated with the seismic phases PP, PKIKP, PKPPKP and others has an important bearing on the delineation of structure within the Earth . Of particular importance is the problem of identifying and analysing seismic waves which have resulted by scattering by small-scale random irregularities in density and elastic parameters inside the Earth. Many previous studies of precursors have implicitly discriminated against the possibility of scattering type interpretations in their data selection and analysis methods. Experiments capable of discriminating between scattering and other possible interpretations of precursor signals on the basis of estimates of the slownesses and azimuths of the various arrivals must necessarily involve array data sampled densely and simultaneously in space.

A.1 Processing of Seismic Precursor Data

A program (BEAMAN) has been developed which calculates continuously beam power/second over a symmetrical dense grid of slowness-azimuth values. This processing procedure has two main attributes in the analysis of precursor signals. Firstly, significant peaks in the power distribution images provide robust estimates of slowness, azimuth and time even for the small and variable signals generally encountered in precursor wave trains. In many cases the concordance or discordance of these estimates with theoretical expectations can, even after generous allowance is made for measurement uncertainties, discriminate sharply between scattering and alternative (deterministic) interpretations. The second attribute of the processing method used is that it yields a continuous three dimensional mapping of the power distribution; this is additionally valuable insofar as the distribution of any power subsidiary to the major power peaks

can potentially substantiate a scattering interpretation but generally finds no explanation in alternative hypotheses. Conventional least squares methods for estimating slowness and azimuth essentially rely on signal energy being highly concentrated in slowness-azimuth space and yield only discrete slowness-azimuth estimates. In consequence, such methods are not fully appropriate for the analysis of signals having a potential scattering origin. An example of a beam power plot in slowness-azimuth space is shown in Fig. A.2.

D.W. King, E.S. Husebye,
R.A.W. Haddon

A.2 Precursors to PP

A detailed study of so-called precursors to PP ($90^{\circ} \lesssim \Delta \lesssim 110^{\circ}$) has been completed (King et al, 1975). In summary, the results of a theoretical study of the interpretation of the precursors in terms of scattering by small-scale random irregularities in the crust and uppermost mantle have been compared with observational data from 2 nuclear explosions recorded at the Warramunga array and 3 earthquakes recorded at the NORSAR array. The NORSAR data comprises mainly onset times and duration, slowness, azimuth and amplitude variations determined using BEAMAN analysis of precursor wave trains such as those illustrated in Fig. A.1. The comparison of theoretical and observational results reveals that the scattering interpretation offers a plausible and adequate explanation of the detailed observational data. In contrast, previous interpretations fail to account for the extended duration of observed wave trains, and for the wide azimuthal distribution of energy incident at the receiver. The scattering interpretation of PP precursors removes the need for postulating many sharp reflecting discontinuities in the uppermost few hundred kilometers of the crust and upper mantle.

D.W. King, R.A.W. Haddon,
E.S. Husebye

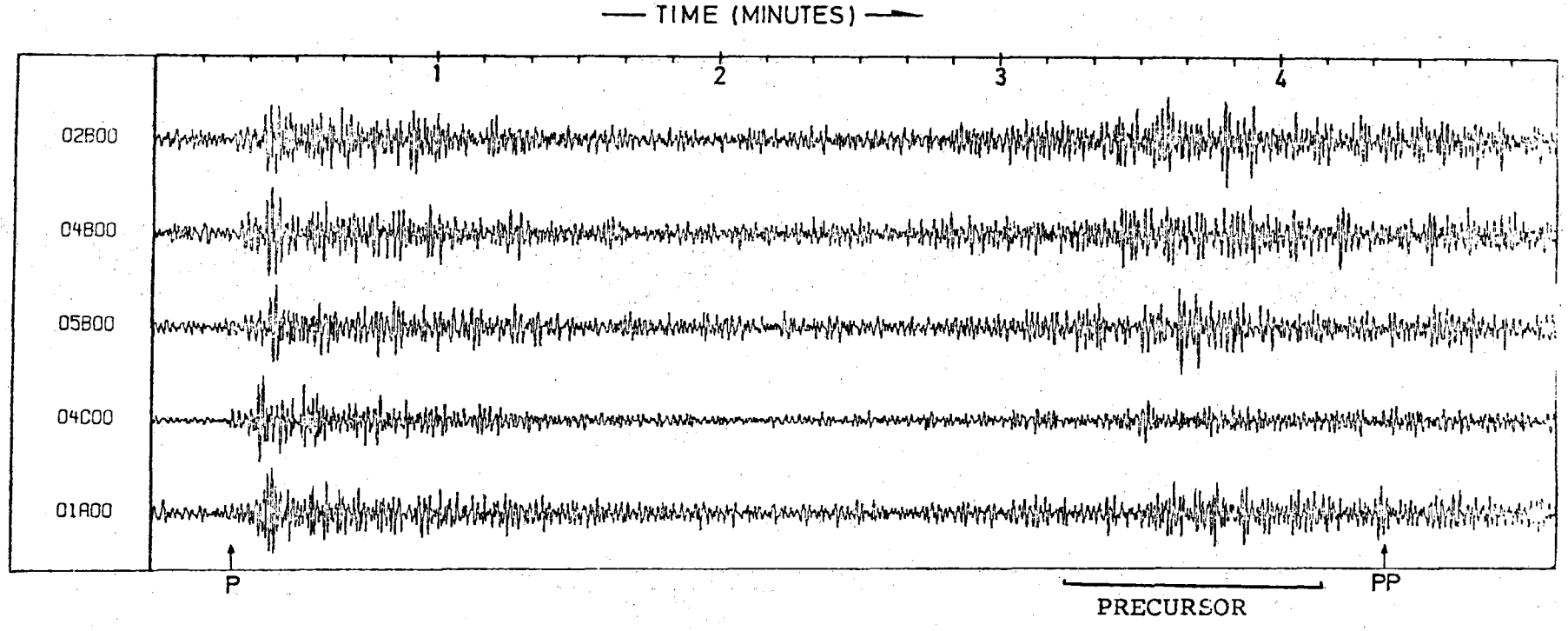

Fig. A.1 Seismograms from 5 selected subarray central instruments (as labelled) for an event in Molucca Passage ($\Delta \sim 100^{\circ}$). The traces have been filtered in the range 0.6-3.0 Hz. Note the extended duration and variable nature of PP precursor wave train.

A.3 Precursors to PKIKP

The distribution of slowness, azimuth and amplitude along PKIKP precursor wave trains ($125^{\circ} \lesssim \Delta \lesssim 143^{\circ}$) recorded at NORSAR has been investigated and shown to be fully consistent with that entailed by a theoretical treatment of the scattering of P waves by small-scale random inhomogeneities in the lowest mantle near where P waves enter into and exit from the core. It has been established that the azimuth of arrival of precursor energy can migrate with increasing time from values near to the primary PKP azimuth to values differing from the PKP azimuth by as much as 30°. The migration of peak precursor beam power in both slowness and time is illustrated in the consecutive frames of Fig. A.2. The theoretical slowness-azimuth distribution entailed by scattering at the mantle-core boundary is superimposed on this figure, and the agreement between observed and predicted values is remarkably good. In marked constrast with the precursor data, the main PKIKP arrivals are stable and compact over several seconds. These and similar data are particularly strong evidence in support of a scattering interpretation. Furthermore, they discriminate sharply against traditional interpretations involving transition layers within the outer core. Since in addition data previously interpreted as corroborating the existence of sharp reflecting discontinuities within the outer core can be adequately accounted for on the scattering interpretation, there appears to be no seismological evidence which requires distinct layering of the Earth's outer core.

E.S. Husebye, D.W. King,
R.A.W. Haddon

A.4 Precursors to PKPPKP

Seismic scattering by small-scale random inhomogeneities in the lower and upper mantle has already been shown to account for observed precursors to the seismic phases PKIKP and PP. The theoretical implications

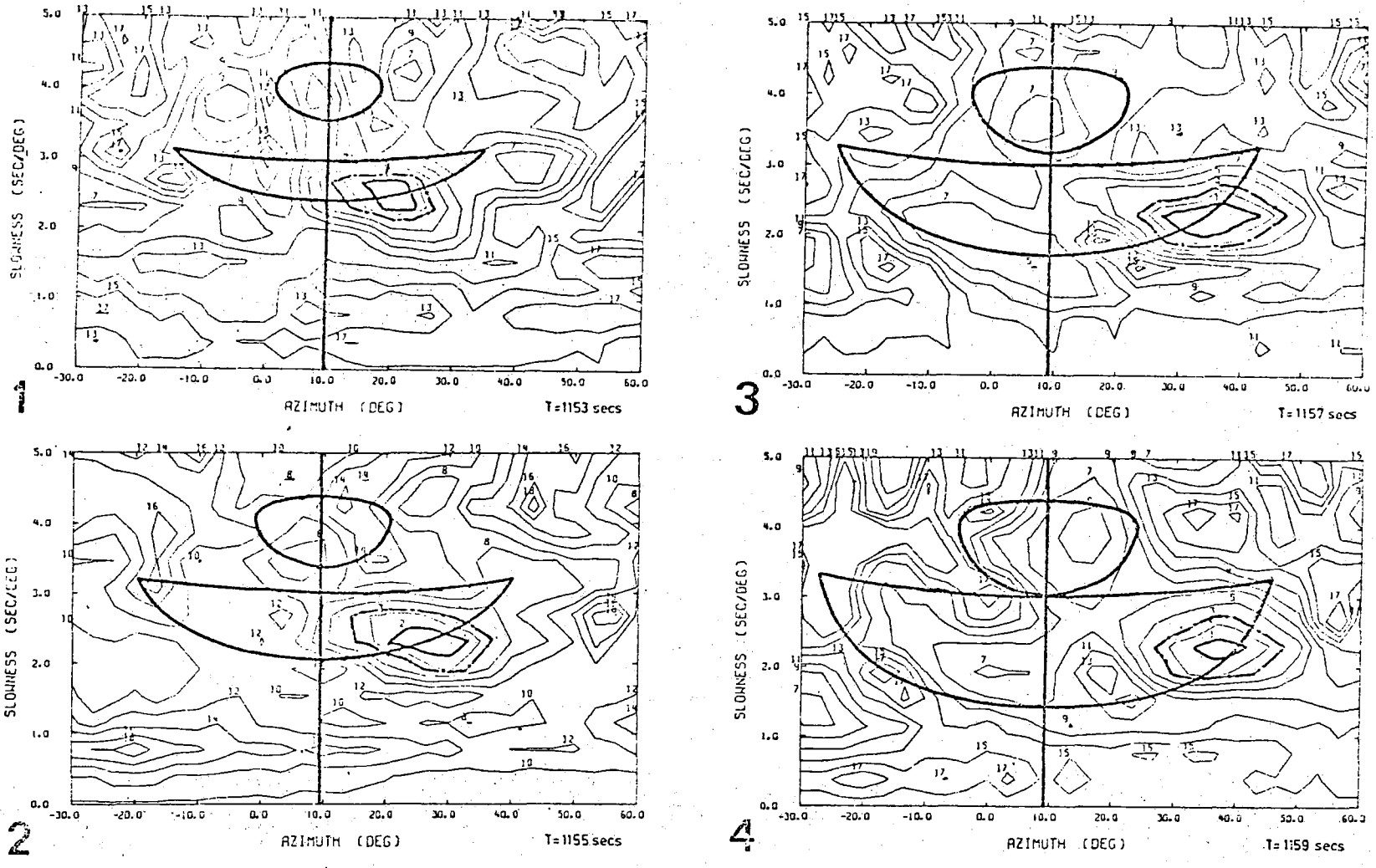

Fig. A.2 Contoured beam power levels in slowness-azimuth space for continguous 2 second intervals of PKIKP precursors with mean corrected travel times as indicated for an event at $\Delta=135.7^{\circ}$. The contours represent power levels in dB below a maximum of 25.7 dB. Contours enclosing dominant peaks in each frame are darkened. Theoretical slowness-azimuth curves for scattered waves of corresponding travel time are plotted centered on the measured primary PKP azimuth.

of these random inhomogeneities in respect of scattering of P'P' phases are being examined in detail and compared with observational data on P'P' precursors at NORSAR. It has been found that observed P'P' precursors having lead times up to about 50 seconds before the main P'P' phases are consistent with having the same scattering origins as precursors to PP and PKIKP. As with the scattering interpretation of precursors to PP, the scattering interpretation of precursors to P'P' removes the need for postulating certain reflecting discontinuities in the upper mantle.

R.A.W. Haddon, E.S. Husebye
D.W. King

Synopsis of precursor studies compiled by D.W.King.

REFERENCES

R.A.W. Haddon, E.S. Husebye, D.W. King. Origins of precursors to P'P', manuscript in preparation.

E.S. Husebye, D.W. King, R.A.W. Haddon. Precursors to PKIKP and scattering near the mantle-core boundary, submitted for publication.

D.W. King, E.S. Husebye, R.A.W. Haddon. Precursors to PP, Phys. Earth Planet. Int., in press.

D.W. King, E.S. Husebye, R.A.W. Haddon. Processing of seismic precursor data, manuscript in preparation.

B. WAVE SCATTERING THEORY IN ANALYSIS OF P-WAVE ANOMALIES AT NORSAR AND LASA

Observed travel time and amplitude anomalies at the NORSAR and LASA arrays are significantly larger than the measurement errors, and cannot be explained in terms of deterministic crust and upper mantle structural models for the respective siting areas. In this study (Berteussen et al, 1975) the Chernov (1960) theory has been used in modelling the crust and upper mantle as a random medium, and also to estimate to what extent such models can account for the observed anomalies. In Table B.1 the basic assumptions underlying the Chernov (1960) theory for acoustical wave propagation in random media is summarized, while Tables B.2 and B.3 show the results obtained for the crust and upper mantle under NORSAR and LASA respectively. It is found that the random medium modelling can explain 50 to 60% of the variance of the time and amplitude anomalies at NORSAR. The corresponding results for LASA are 50-60% and 25% respectively. In contrast, reasonable deterministic models cannot account for even 25% of this variance. While the random medium model can provide a satisfactory explanation of the observational data, extensive tests have revealed that the parameters characterizing the random medium cannot be uniquely determined from the data.

K.A. Berteussen, A. Christoffersson,
E.S. Husebye, A. Dahle

REFERENCES

Aki, K. (1973): Scattering of P-waves under the Montana LASA, J. Geophys. Res., 78, 1334-1346.

Berteussen, K.A., A. Christoffersson, E.S. Husebye and A. Dahle (1975): Wave scattering theory in analysis of P-wave anomalies at NORSAR and LASA, Geophys. J.R. Astr. Soc., in press.

Capon, J. (1974): Characterization of crust and upper mantle structure under LASA as a random medium, Bull. Seism. Soc. Am., 64, 235-266.

Chernov, L. (1960): Wave propagation in random media, trans. by R.A. Silverman, McGraw-Hill Book Company, New York.

TABLE B.1

Basic assumptions underlying the Chernov (1960) theory for acoustical wave propagation in random media.

1. Small velocity variations, $\overline{\mu^2} << 1$
2. Statistically homogeneous
3. Statistically isotropic
4. Gaussian correlation function for index of refraction, $N(r) = e^{-r^2/a^2}$
5. Extent of medium much greater than correlation distance, $L >> a$
6. Large scale inhomogeneities (Fresnel-approximation) $ka >> 1$
7. Rytov (Born) approximation
   $\frac{\Delta I}{I} << 1$ per wavelength (for the whole medium

TABLE B.2

Results obtained in modelling the crust and upper mantle beneath NORSAR as a Chernov medium. An asterisk indicates that the standard deviation of the refractive index corresponds to the lower limit of the extent of the medium.

DATA		CHERNOV MEDIUM MEASUREMENT			
Configuration	Amp/phase	S.d. of refraction index (%)	Correlation Distance (km)	Extent of Medium (km)	Variance Reduction (%)
1A,1B	P	1.6 *	17	≥ 100	97
2B,3B	P	0.8	12	300	84
1B,7B	P	1.0	16	250	96
4B,5B	P	0.9	18	200	93
1A,6B	P	0.9	25	350	96
1A,1B	A	1.2	14	100	60
2B,3B	A	1.4	15	100	57
1B,7B	A	1.3 *	8	≥ 250	36
4B,5B	A	1.0 *	≥ 25	≥ 250	20
1A,6B	A	1.0 *	17	≥ 150	60
1A,1B-4B	P	0.5	30	≥ 250	71
1A,1B-4B	A	0.9	30	≥ 250	73
1A,1B-7B	P	2.0	60	≥ 250	66
1A,1B-7B	A	0.8	35	≥ 100	60

TABLE B.3

Results obtained in modelling the crust and upper mantle beneath LASA as a Chernov random medium. Corresponding results obtained by Aki (1973) and Capon (1974) are also given.

DATA		CHERNOV MEDIUM MEASUREMENTS			
Configuration	Amp/Phase	S.d. of refraction index (%)	Correlation Distance (km)	Extent of Medium (km)	Variance Reduction (%)
A0,B1,B4	P	0.6 0.3	15	50 150	25
A0,B1,B4	A	3.0 2.0	15	50 150	58
66 instruments (Aki, 1973)	A&P	4.0	10	60	
A,B,C ring (Capon, 1974)	A&P	2.0	12	120	

C. TIME AND AMPLITUDE FLUCTUATIONS OF TELESEISMIC P-SIGNALS AT NORSAR IN VIEW OF WAVE SCATTERING THEORY

In the study of Berteussen et al (1975) it was demonstrated that a considerable part of the time and amplitude anomalies observed at the large seismic arrays can be explained using the Chernov (1960) theory for wave propagation in a random medium. In this study (Dahle, 1975) more emphasis is given to the theoretical aspect of applying this theory and on the validity of doing so. There is limited success with regard to the proposed scattering hypothesis; however, it is believed that the scattering approach deserves considerable attention. Such a conclusion is justified by the fact that the seismic wave field exhibits to a satisfactory degree some of the statistical qualities predicted by the theory. For example, the theory predicts a positive correlation between phase and amplitude anomalies, which also is observed. The assertion of forward wave scattering and mode conversion being basically P→P turns out to be an important point. There is reason to suspect the crust and upper mantle locally being inhomogeneous in a way not pertaining to Chernov's (1960) theory for weak inhomogeneities equally distributed throughout the medium. Stronger inhomogeneities giving rise to back-scattering, conversion to modes other than P and higher order scattering (scattered-scattered waves) are possible explanations of an observed discrepancy between theory and experience.

Substantial support to the scattering hypothesis is provided by the correlation functions depicted in Fig. C.1, which shows the correlation of time and amplitude anomalies respectively as a function of spatial lag. These are the features leading to the space predictive procedure described in Quarterly Report no. 3 in 1973. The prediction procedure is important for two reasons. Firstly, because it shows the anomaly percentage explainable by correlated stochastic terms, and secondly it provides a means of finding the optimum correlation matrix for the data.

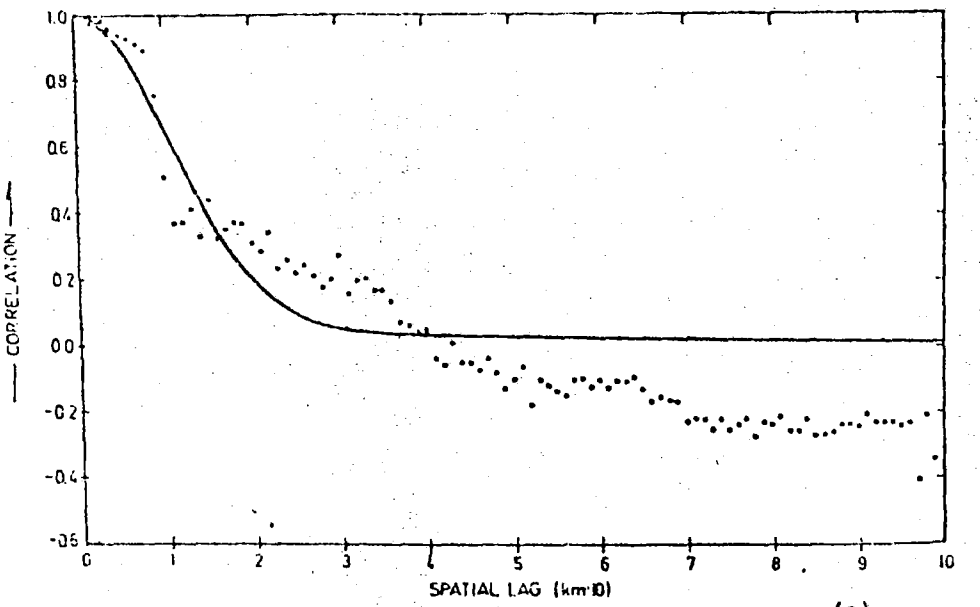

(a)

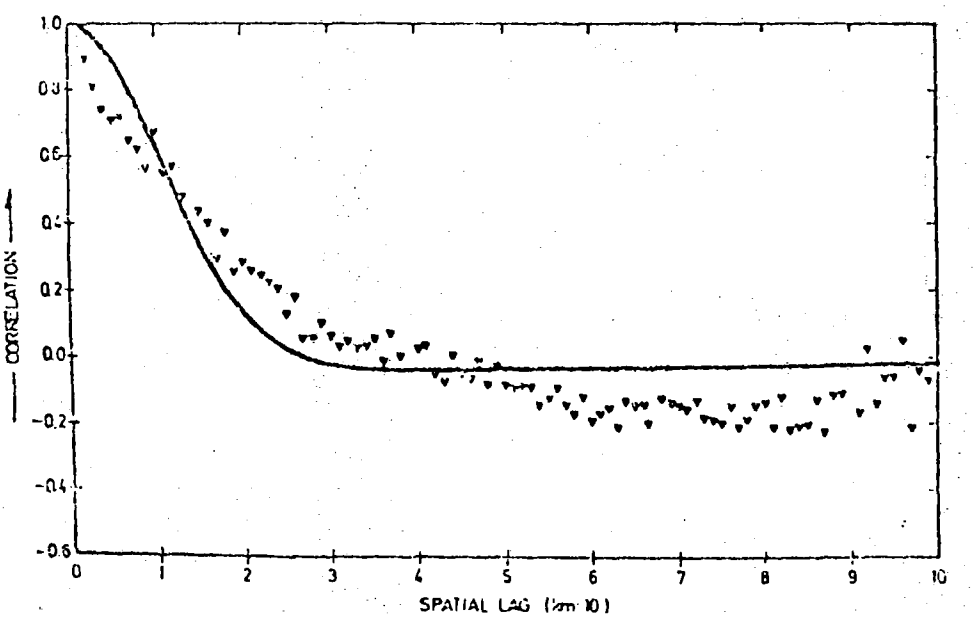

(b)

Fig. C.1 Empirical transverse correlation functions for travel time fluctuations (a) and logamplitude fluctuations (b) together with the theoretical Chernov (1960) functions with correlation distance 15 km and wave parameter 10.

The realization of randomly corrugated seismic wave fronts is undoubtedly important in small aperture array seismology. In this study one has successfully related the fluctuations in body wave travel time, local wave front normal and amplitude to wave scattering in an inhomogeneous crust and upper mantle. A quantitative description of the inhomogeneous medium is inconclusive for the moment, but the results show that attention must be paid to scattering effects when observed times or amplitudes are inverted into structural models.

A. Dahle

REFERENCES

Berteussen, K.A., A. Christoffersson, E.S. Husebye and A. Dahle (1975): Wave scattering theory in analysis of P-wave anomalies at NORSAR and LASA, Geophys. J.R. Astr. Soc., in press.

Chernov, L. (1960): Wave propagation in random media, trans. by R.A. Silverman, McGraw-Hill Book Company, New York.

Dahle, A. (1975): Time and amplitude fluctuations of teleseismic P-signals at NORSAR in view of wave scattering theory, Scientific Report No. 4-74/75, NTNF/NORSAR, in press.

D. ON THE ORIGIN OF SLOWNESS AND AZIMUTH ANOMALIES OF TELESEISMIC SIGNALS

Using slowness and azimuth anomalies observed from P and PKP phases at NORSAR, it has been demonstrated (Berteussen, 1975) that as much as 90% of the corresponding anomalies for PP and PcP phases can be predicted. It is thus concluded that anomalies caused by inhomogeneities at the source side or at the deepest part of the ray path cannot be observed at NORSAR, i.e., for PP phases inhomogeneities on the source side of the surface reflection point and for PcP phases inhomogeneities on the source side or at the mantle-core reflection point are not strong enough to produce anomalies which can be identified in this type of data. Even after having corrected for the first order effect of the local structure (a dipping plane interface), there is no significant part of the anomalies left that can be ascribed to inhomogeneities at the source side. It has further been demonstrated that locating a significant part of the anomalies deep in the mantle would require unreasonable velocity contrasts; one thus has to conclude that most of these anomalies are caused by structures in the very upper part of the mantle or in the crust.

An additional piece of information (Berteussen, 1975) has been time residual and wave front slowness and azimuth measurements of long period P-waves inside three different frequency bands, 0.1 Hz highpass, all pass, and 0.05-0.1 Hz bandpass. It is found that the location error vectors gradually diminish as the frequency decreases. For the 0.1 Hz highpass data the vectors are essentially the same as for short period data, and then they change to about half the size but keep their direction for the longest wavelengths. Assuming that the linear extent of structures causing measurable anomalies have to be, say at least half a wavelength, it is thus found that since the longest wavelengths used (160-80 km) have 58%

of the ($dT/d\Delta$, Φ) anomalies of the short period data, 58% of these have to be caused by inhomogeneities with a linear extent of at least say 1/2 ($\frac{160+80}{2}$) = 60 km. Then there are 42% of the anomalies which these long waves do not 'see', thus indicating that the inhomogeneities causing these anomalies must have a linear extent too small for these waves, i.e., 42% of the slowness and azimuth anomalies are caused by inhomogeneities of linear extent less than 60 km. From the 0.1 Hz highpass filtered data (wavelength ~ 80 km) it is further concluded that 17% (75-58) of the anomalies are caused by inhomogeneities of linear extent between 60 and 40 km. The remaining 25% of the slowness and azimuth anomalies and virtually 100% of the plane wave front deviations then have to be caused by inhomogeneities which have characteristic sizes of less than 40 km. It has been shown (Berteussen, 1975) that at NORSAR the best plane wave front reduces the variance of the time anomalies relative to the wave front predicted from the PDE event location by approximately 50% and that thus the time deviation around this best plane wave front accounts for the remaining 50%. If one therefore instead of thinking in terms of ($dT/d\Delta$, Φ) anomalies and plane wave front deviations thinks of time deviations relative to the wave front predicted from the PDE event location the following picture emerges. 29% (58/2) of these are caused by inhomogeneities larger than 60 km, 9% are caused by inhomogeneities between 60 km and 40 km, and the remaining 62% ($\frac{100+25}{2}$) are caused by inhomogeneities of size less than 40 km. From the previous section we know that virtually all the anomalies are caused by inhomogeneities in the very upper mantle under the receiver, say above 600 km. We are now in a position to also set an upper limit to these inhomogeneities. Assuming that the anomalies are caused by structures as close to the receiver as possible, we find that a maximum of 71% (62+9) of these are produced within the last 40 km, and in order to include the remaining 29% we then have to go down to a depth of at least 60 km.

K.A. Berteussen

REFERENCES

Berteussen, K.A. (1975): The origin of slowness and azimuth anomalies at large arrays, submitted for publication.

E. THE EFFECT OF ARRAY CONFIGURATION ON SLOWNESS AND AZIMUTH ANOMALIES

The multitude of sensors characterizing the large seismic arrays makes it possible to test what effect a change in array configuration has on the slowness and azimuth anomalies for P-phases recorded at the arrays. In two recent papers this effect has been studied both for LASA (Berteussen, 1975a) and NORSAR (Berteussen, 1975b).

On Fig. E.1 the 'array diagram' for a set of well-recorded P-phases at LASA using all 21 subarrays is shown. The tail of the arrows represents the slowness and azimuth ($dT/d\Delta$, Φ) estimated at the array, while the head represents the values entailed by a (laterally homogeneous) standard earth model. On Fig. E.2 the same array diagram is then shown when only odd numbered LASA subarrays have been used. The configuration is somewhat 'thinner' than the full array, but has approximately the same aperture (200 km). Comparing Figs. E.1 and E.2, it is immediately apparent that certain sectors (especially azimuth $90^{\circ} \lesssim \Phi \leq 270^{\circ}$) of the two array diagrams are significantly different. In particular, the anomalies associated with rays which bottom in the vicinity of proposed plume structures under Hawaii ($\Phi \sim 265^{\circ}$) at LASA and the Galapagos Islands ($\Phi \sim 155^{\circ}$) (Davies and Sheppard, 1972, Kanasewich et al, 1973) are markedly different in the two figures. Anomalies associated with rays bottoming in the lowest mantle beneath Iceland ($\Phi \sim 20^{\circ}$) are essentially consistent on Figs. E.1 and E.2; however, array diagrams for other configurations (Berteussen, 1975a) demonstrate conclusively that these anomalies are also critically dependent on the spatial sampling of the wavefront.

The same effects may also be demonstrated at NORSAR. On Fig. E.3 the array diagram for the full NORSAR array is shown, while Fig. E.4 shows a diagram using subarrays 1, 5-8, 15-20, giving us an array of aperture 70 km instead of the 100 km aperture of the whole NORSAR. For the azimuth section

330-120 degrees it is seen that the vectors have been rotated by almost 90 degrees relative to those on Fig. E.3. Also note that for azimuth 300 degrees (the direction to Iceland) Fig. E.4 shows rapid variations in the anomaly pattern. Given a NORSAR array consisting of only these eleven sub-arrays, one could, following Davies and Sheppard (1972) and Kanasewich et al (1973), be tempted to associate these rapid changes with, for example, a hot spot under Iceland. However, a more complete picture (Fig. E.3) demonstrates that such an interpretation would be erroneous. Using smaller arrays and fewer subarrays even more drastic variations can of course be induced. On Fig. E.5 the array diagram for the NORSAR subarray combination 2, 3, 9, 10, 11, giving an aperture of some 45 km, which still is larger than most of the medium-sized arrays, is shown. For the direction towards Iceland, the arrows are now seen to be turned quite opposite to those on Fig. E.4. Also for the rest of the slowness-space large differences are observed relative to the data on Figs. E.3 and E.4. Finally, (Fig. E.6) an array diagram is shown using only the subarrays 6, 17, 20. This configuration is approximately the same as that of the Hagfors array in Sweden, and demonstrates that for such a small array almost 'any' type of location errors may be found. On Fig. E.6 one interesting detail should be noted. One of the arrows (azimuth~0) is seen to be turned in almost the same direction as the core phases between azimuth 0° and 90°, and directly opposite to the surrounding P-wave vectors, thus indicating that the anomaly for the core phases is a function only of direction of approach of the ray.

Clearly, there are a lot of details in each of these figures which it would be tempting to associate with structures far away from the receiver. The fact that these details are not retained as one changes configuration suggests, however, that in reality the wavefronts are locally delayed or speeded up for example by rapid Moho depth variations and/or scattering by small-scale randomly distributed inhomogeneities close

to the receiver. The final estimates of slowness and azimuth are then very much dependent on which sites are sampled and which are not. Of course, source side or deep mantle effects may be present in the data, but local structural effects have been shown to be so dominant and so difficult to characterize (and therefore to correct for) that there can be no justification for speculating on structures well removed from the array on the basis of these data.

K.A. Berteussen

REFERENCES

Berteussen, K.A. (1975a): Array analysis of lateral inhomogeneities in the deep mantle, submitted for publication.

Berteussen, K.A. (1975b): The origin of slowness and azimuth anomalies at large arrays, submitted for publication.

Davies, K., and R.M. Sheppard (1972): Lateral heterogeneity in the earth's mantle, Nature, 239, 318-323.

Kanasewich, E.R., R.M. Ellis, C.H. Chapman, P.R. Gutowski (1973): Seismic array evidence of a core-boundary source for the Hawaiian linear volcanic chain, J. Geophys. Res., 78, 1361-1371.

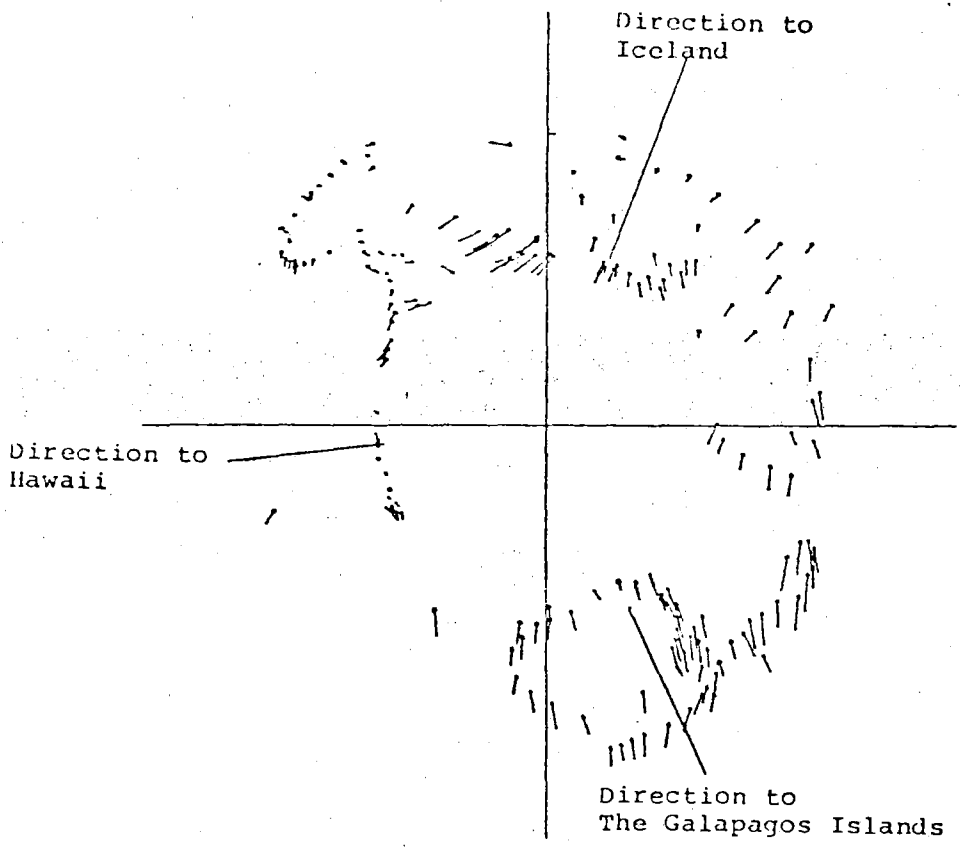

Fig. E.1 Array diagram for a configuration consisting of all 21 LASA subarrays. The tail of the arrows represents the observed ($dT/d\Delta$, Φ), i.e., the slowness-space location measured at LASA. The head of the arrows represents the ($dT/d\Delta$, Φ) one expects using the PDE event location and standard distance-slowness tables.

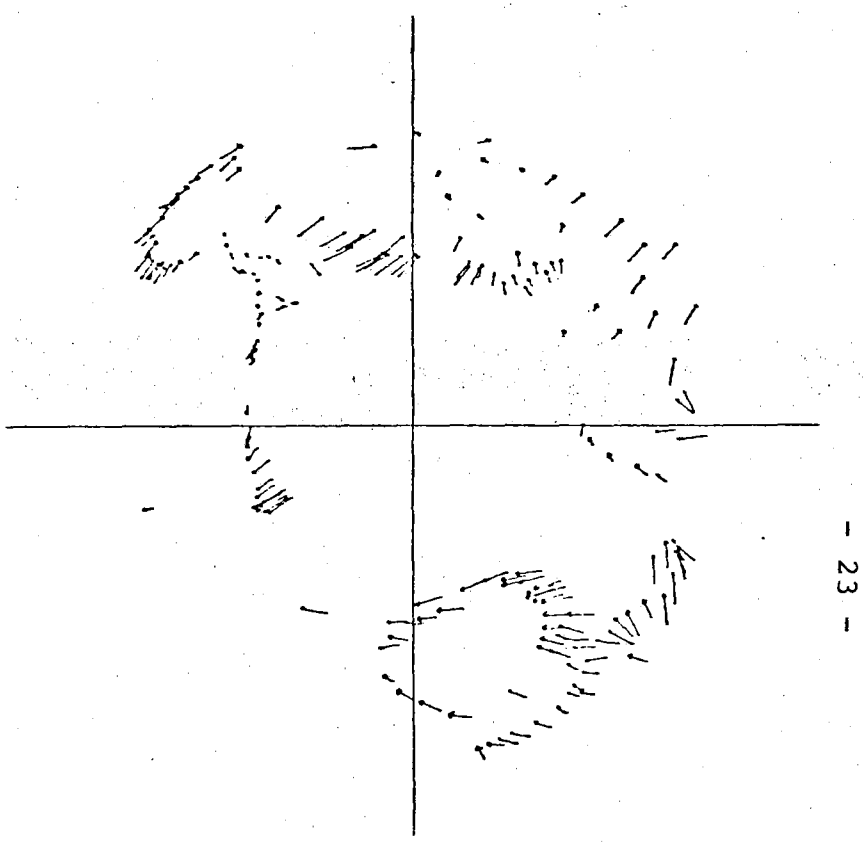

Fig. E.2 Same as Fig. E.1 for the LASA subarrays 1,3,5,7,9,11,13,15,17,19,21 (A0,B2,B4,C2,C4,D2,D4,E2,E4,F2,F4).

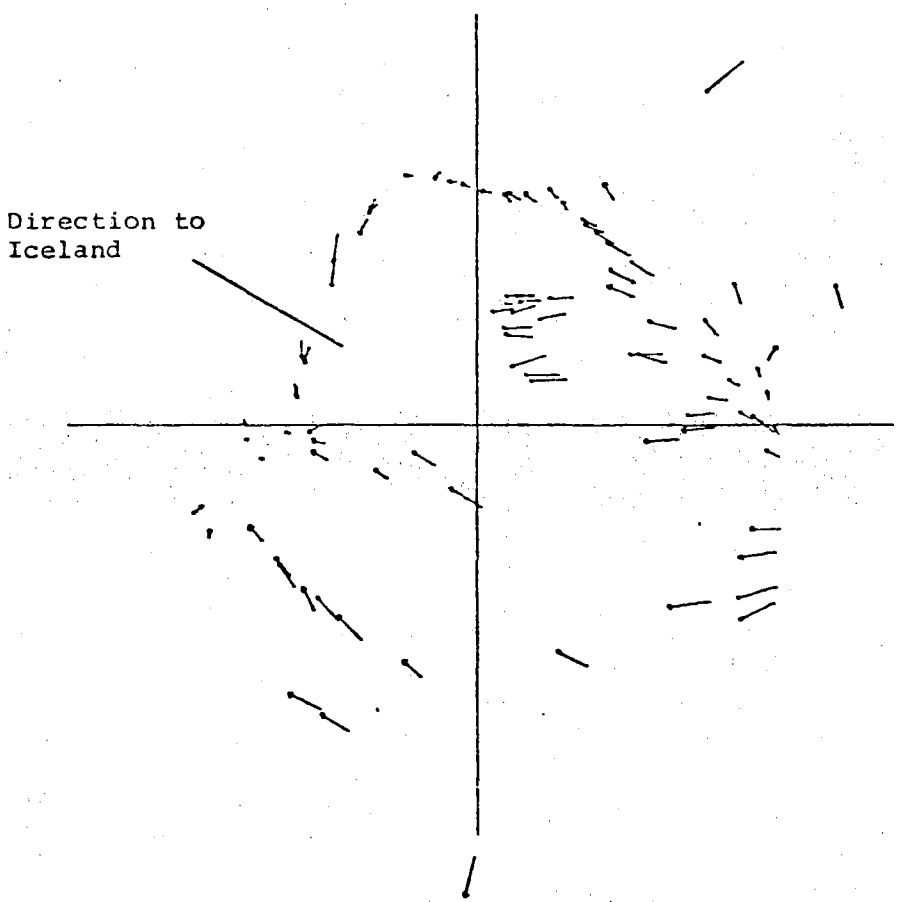

Fig. E.3 Same as Fig. E.1 for all 22 NORSAR subarrays.

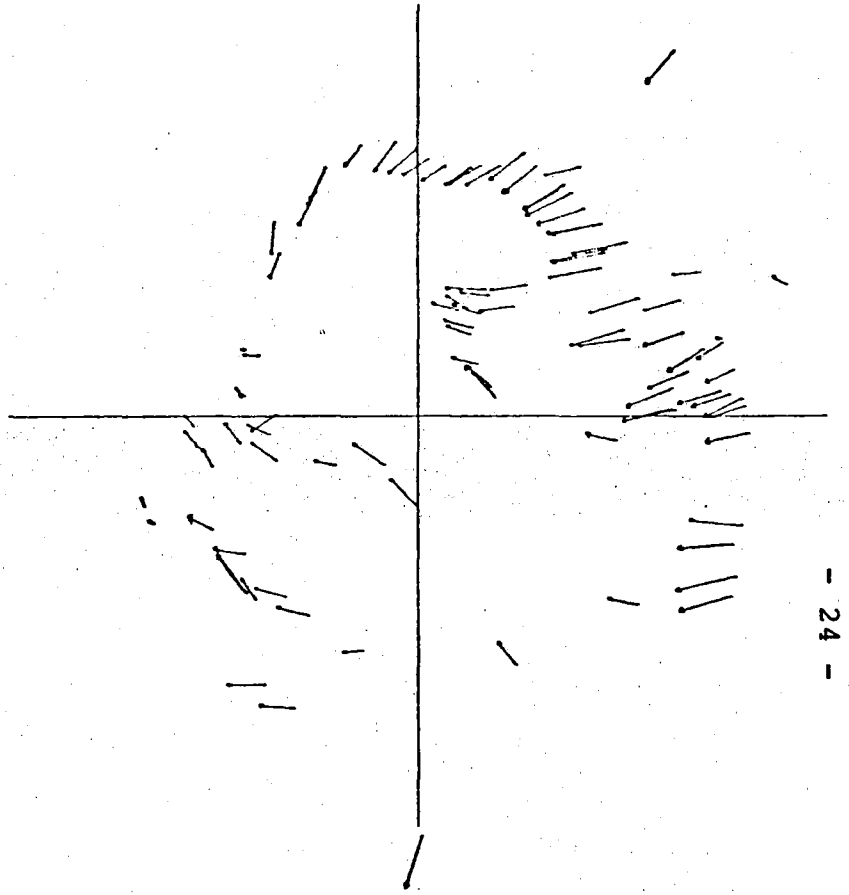

Fig. E.4 Same as Fig. E.1 for the NORSAR subarrays 1, 5-8, 15-20 (1A, 4B-7B, 7C-12C).

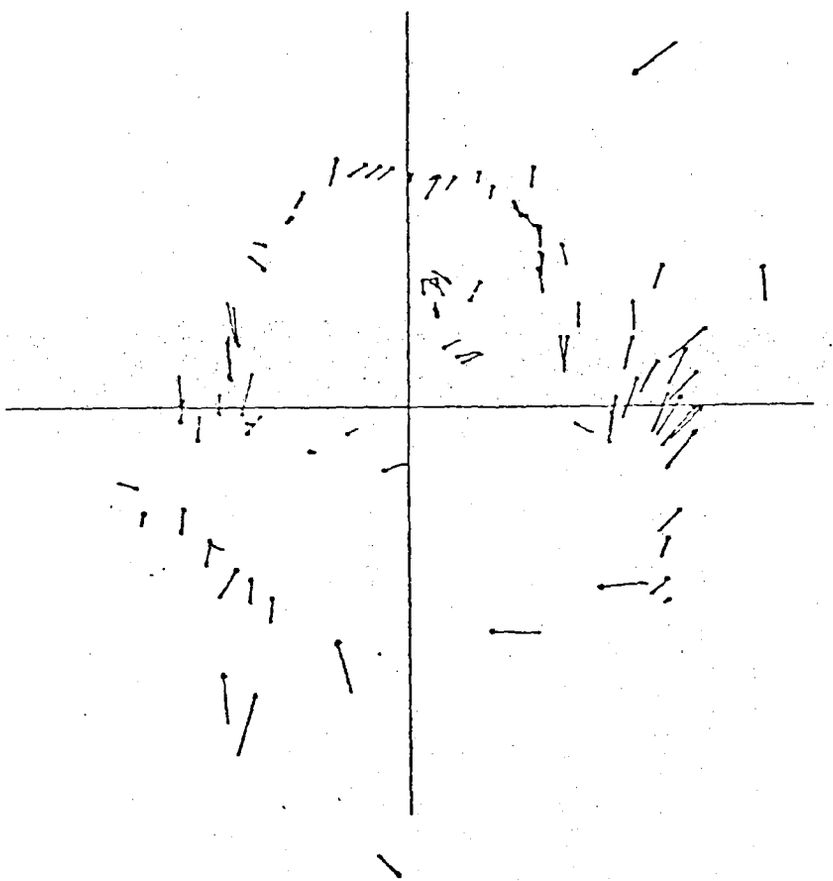

Fig. E.5 Same as Fig. E.1 for the NORSAR subarrays 2,3,9,10,11 (1B,2B,1C,2C,3C).

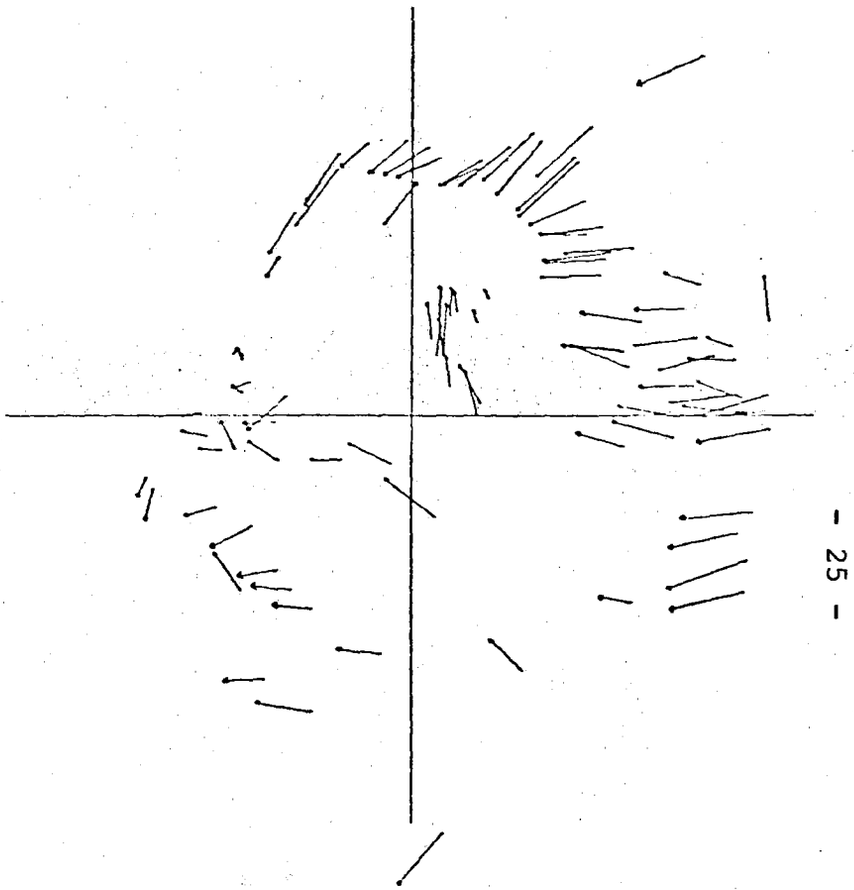

Fig. E.6 Same as Fig. E.1 for the NORSAR subarrays 6, 17, 20 (5B, 9C,12C).

F. DETERMINATION OF THE THREE-DIMENSIONAL SEISMIC STRUCTURE OF THE LITHOSPHERE

A new three-dimensional earth modelling is formulated in order to meet an increasing demand for more detailed and accurate information about the earth's interior. We start with a layered medium of classic seismology, but divide each layer into many blocks and assign a parameter to each block which describes the velocity perturbation from the average for the layer. Our data is the teleseismic P travel time residuals observed at an array of seismographs distributed on the surface above the earth's volume we are modelling. By isolating various sources of errors and biases, we arrive at a system of equations to determine the model parameters. The solution was obtained by the use of generalized inverse and stochastic inverse methods with the analysis of resolution and errors in estimates. Our method also gives a lower limit of the true r.m.s. velocity fluctuation in the actual earth under the assumption of ray-theory.

Using NORSAR P-wave residuals, we have determined the three-dimensional seismic structure of the lithosphere under the array to the depth of 126 km. The true r.m.s. velocity fluctuation was found to be at least 3.4%. This is in agreement with estimates obtained from statistical analysis of P time fluctuation based on the Chernov theory. The three-dimensional velocity anomalies are presented both by the generalized inverse and by the stochastic inverse solutions. We preferred the dual presentation, because it gives the reader greater freedom in judging the results than a single "optimal" solution. Both methods gave essentially the same results. The discrepancies, when they existed, were always explainable in terms of differences in the smoothing procedure which is explicitly given in the resolution matrix.

We found clear evidence of pipe-like structures under NORSAR, dipping northward and away from the surface contour of the Oslo graben (Fig. F.1). These pipe-like structures were interpreted as vestiges of magma ascent by penetrative convections associated with the Permian volcanism of the Oslo graben. The inclination of the pipe-like structures is interpreted as a result of plastic deformation of the lithosphere due to the shear exerted by the asthenosphere convection current driving the plate motion.

In case of LASA, the most conspicuous feature of the estimated three-dimensional velocity anomaly is a N60^{o}E trend which persists from the upper crust to depths greater than 100 km. Relatively high velocities are found towards SE and low velocities in the cenral array siting area and towards NW. We are tempted to associate the N60^{o}E trending velocity anomalies with shearing caused by the Nevadan and Laramie orogenies in the western United States. The shear may be concentrated in a zone of weakness which in turn causes a broad low velocity anomaly throughout the lithosphere.

K. Aki, A. Christoffersson
E.S. Husebye

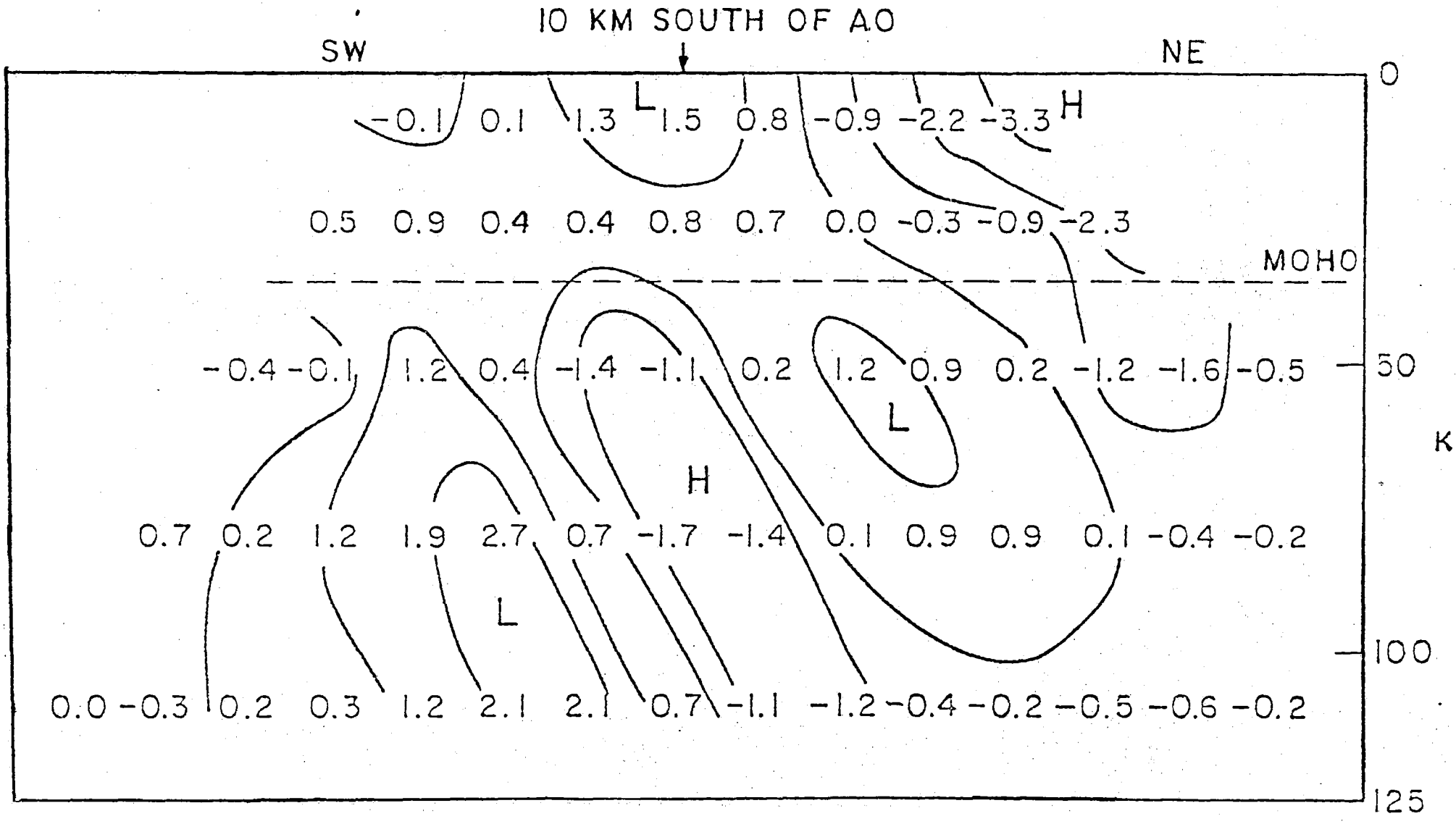

Fig. F.1 A vertical section through the NORSAR area. The values listed are deviations in per cent from average P-velocity. Negative numbers mean high velocity.

G. UPPER MANTLE P WAVE VELOCITIES

The beam-power processing program described elsewhere in this report (section A) has been used to estimate apparent slownesses and azimuths of short period P signals from some 40 Russian explosions ($12^{\circ} \lesssim \Delta \lesssim 40^{\circ}$) and a comparable number of Atlantic earthquakes. Those data which have sampled only continental paths exhibit consistent evidence for multibranching in the approx. distance range $15^{\circ} < \Delta < 28^{\circ}$. These data are broadly consistent with a slightly modified version of the B1 model of Jordan and Anderson (1974). The observed slownesses and travel times of the explosion data are plotted in compact form on Fig. G.1 in comparison with the T-Δ curve entailed by a B1-type model with a modified velocity gradient in the uppermost mantle and with the discontinuities near 400 and 650 km reduced in size and smoothed. A model of this type explains the principal features of the data (although the need for further refinement and travel-time adjustment is recognized), and equally important does not entail features blatantly inconsistent with the data. The notable absence of arrivals corresponding to the prograde end of the triplication associated with 'the 650 km discontinuity' may be explained by postulating an increase in Q to accompany the velocity increase at that depth (see Mereu et al, 1974).

P waves from the North Atlantic earthquakes have upwards of half of their travel paths in oceanic structures. These data differ from the continental data insofar as evidence for multibranching is much less pronounced. The absence of clear secondary arrivals places some constraint on the size and nature of possible velocity discontinuities at depth.

Smooth models such as those presented by Kulhanek and Brown (1974) adequately explain most of the observed times and slownesses.

G. Calcagnile and D.W. King

REFERENCES

Jordan, T., and D.L. Anderson (1974): Earth structure from free oscillations and travel times, Geophys. J., 36, 411-459.

Mereu, R.F., D.W. Simpson and D.W. King (1974): Q and its effect on the observation of upper mantle travel-time branches, Earth Planet. Sci. Lett., 21, 439-447.

Kulhanek, O., and R.J. Brown (1974): P wave velocity anomalies in the Earth's mantle from the Uppsala array observations, Pure and Appl. Geophys., 112, 597-617.

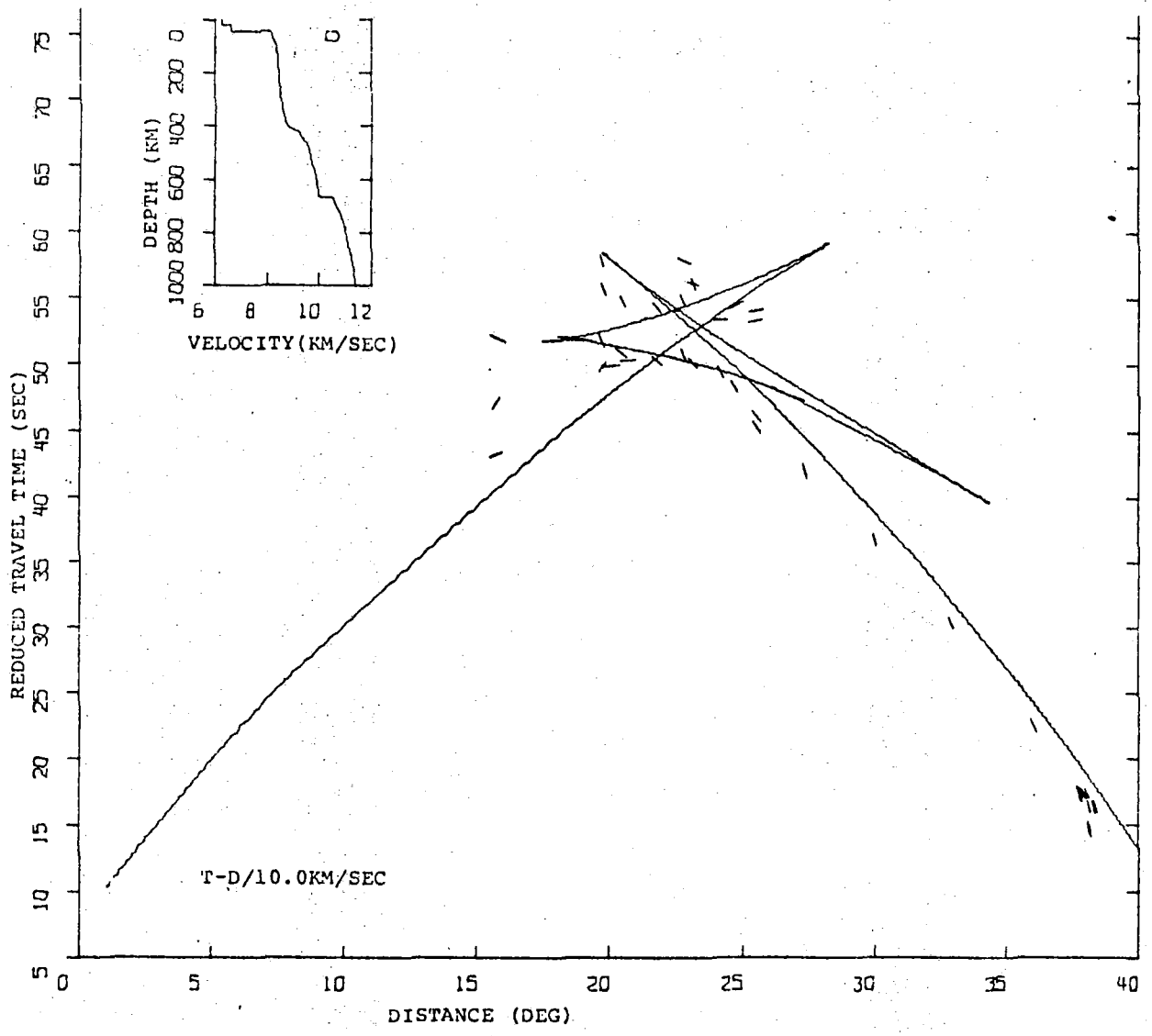

Fig. G.1 Observed slownesses and (reduced) travel times from Russian explosions in comparison with the T-Δ curve entailed by a modified B1 velocity model (inset).

H. IMPLICATIONS OF CRUSTAL SCATTERING ON SEISMIC PROFILING

There is evidence from numerous disparate sources for the presence of small-scale random irregularities in the crust and upper mantle. Estimated characteristic sizes of irregularities are typically in the range from 4.5 meters (Jeffreys, 1970) to several tens of kilometers (e.g. Berteussen et al, 1975), but are subject to great uncertainties (Berteussen et al, 1975; King et al, 1975). Notwithstanding the uncertainties which prevail as to the characteristic size of the irregularities, their presence would be expected to scatter relatively strongly the short wavelength P (and S) waves commonly recorded in seismic profiling surveys. It is a simple matter to estimate the range of sizes of irregularities within which the fundamental assumptions underlying profiling methods are so seriously violated that a statistical (diffraction) theory is strictly necessary in any interpretation. For instance, for a typical signal wavelength of 2 km and a path length of 300 km, it can be shown from the acoustic wave scattering theory of Chernov (1960) that only inhomogeneities smaller than 0.1 km or greater than 18 kms would permit the application of standard ray theory.

A number of previous studies have indicated that a significant part of the irregularities in the vicinity of NORSAR have characteristic sizes less than about 20 km. It is to be expected then that recordings of local ($\Delta \lesssim 5^{\circ}$) events should exhibit features not readily interpretable in terms of ray theory. A number of local explosions and earthquakes recorded at NORSAR have been plotted as distance sections and the durability of various arrivals scrutinized. Almost all arrivals exhibit a great variability over small surface areas. As an example, data from an earthquake approx. 320 km away

from two subarrays separated laterally by only 40 kms are plotted on a common section in Fig. H.1. Interpretations of crustal layering based on subsets of this data would undoubtedly have grossly different features. This example is by no means atypical -- records from within 7 km-aperture subarrays commonly exhibit a comparable variability, particularly with regard to secondary arrivals. It is planned to re-examine the uncertainties in crustal interpretations using the NORSAR recordings from local earthquakes and explosions distributed widely in azimuth.

D.W. King and K.A. Berteussen

REFERENCES

Berteussen, K.A., A. Christoffersson, E.S. Husebye and A. Dahle (1975): Wave scattering theory in analysis of P-wave anomalies at NORSAR and LASA, Geophys. J.R. Astr. Soc., in press.

Chernov, L.A. (1960): Wave propagation in a random medium, trans. by R.A. Silverman, McGraw-Hill Book Company, New York.

King, D.W., R.A.W. Haddon and E.S. Husebye (1975): Precursors to PP, Phys. Earth and Planet. Int., in press.

Jeffreys, H. (1970): The Earth, 5th Ed., Cambridge Univ. Press, New York.

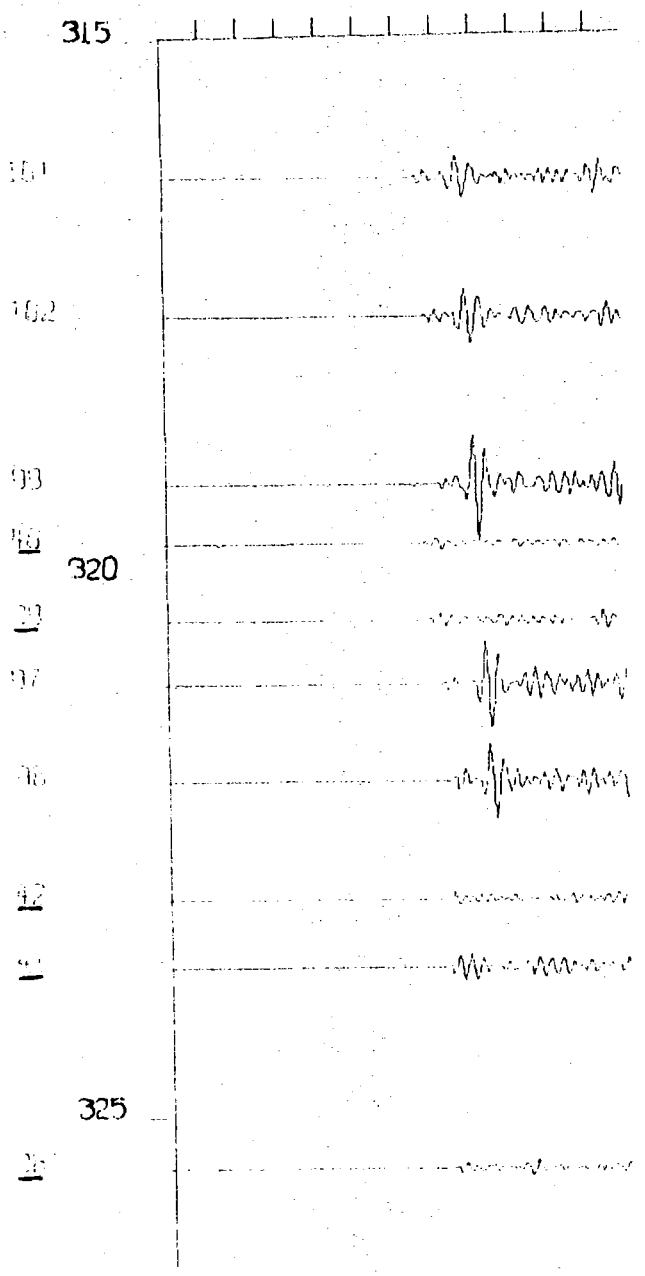

Fig. H.1 NORSAR recorded P-signals for event close to Haugesund, Norway, 03 April 1975. The leftmost numbers give instrument number (those underlined are from subarray 06B while the others are from subarray 09C). The numbers close to the vertical axis give kilometer from the source. The distance between the marks on the horizontal axis is one second. The data has been filtered with a 1.6-4.4 Hz bandpass filter.

I. AUTOREGRESSIVE REPRESENTATION OF SEISMIC P-WAVE SIGNALS AND SHORT-PERIOD DISCRIMINATION

It is shown that seismic P-wave signals can be represented by parametric models of autoregressive type. These are models having the form

$$X(t) - a_1 X(t-1) - \ldots - a_p X(t-p) = Z(t)$$

where $X(t)$ is the digitized short-period data time series defined by the P-wave signal, and $Z(t)$ is a white noise series. The autoregressive analysis was undertaken for 40 underground nuclear explosions and 45 earthquakes from Eurasia. For each event a separate analysis of the noise preceding the event as well as of the P-wave coda has been included. It is found that in most cases a reasonable statistical fit is obtained using a low order autoregressive model.

The autoregressive parameters characterize the power spectrum (equivalently, the autocorrelation function) of the P-wave signal. In fact, for an autoregressive process of order p, the theoretical power spectrum is given by

$$G(f) = \frac{\sigma_z^2/f_c}{\left| 1 - a_1 e^{-\pi i (f/f_c)} - \ldots - a_p e^{-p\pi i (f/f_c)} \right|^2}$$

for $0 \leq f \leq f_c$, where i is the imaginary unit, and $f_c = 1/2h$ is the cutoff frequency, h being the time interval between samples. These parameters should form a convenient basis for studying the possibilities of short-period discrimination between nuclear explosions and earthquakes, since given the autoregressive parameters one is able to reconstruct the power spectrum for the considered event. In principle, therefore, the study of discriminants using power spectral properties should reduce to a study of the associated autoregressive parameters, that is, essentially to a study

of plots such as the one given in Fig. I.1. From this figure and various similar plots we reach the tentative conclusion that it seems difficult to construct really good discriminants based solely on power-spectral properties. However, the autoregressive parameters are of value when combined with other discriminants such as the m_b:M_s criterion (Bungum and Tjøstheim, 1975).

D. Tjøstheim

REFERENCES

Bungum, H., and D. Tjøstheim (1975): Discrimination between Eurasian earthquakes and underground explosions using the m_b:M_s method and short period autoregressive parameters, This report.

Tjøstheim, D. (1975): Autoregressive representation of seismic P-wave signals with an application to the problem of short-period discriminants, Geophys. J. R. Astr. Soc., in press.

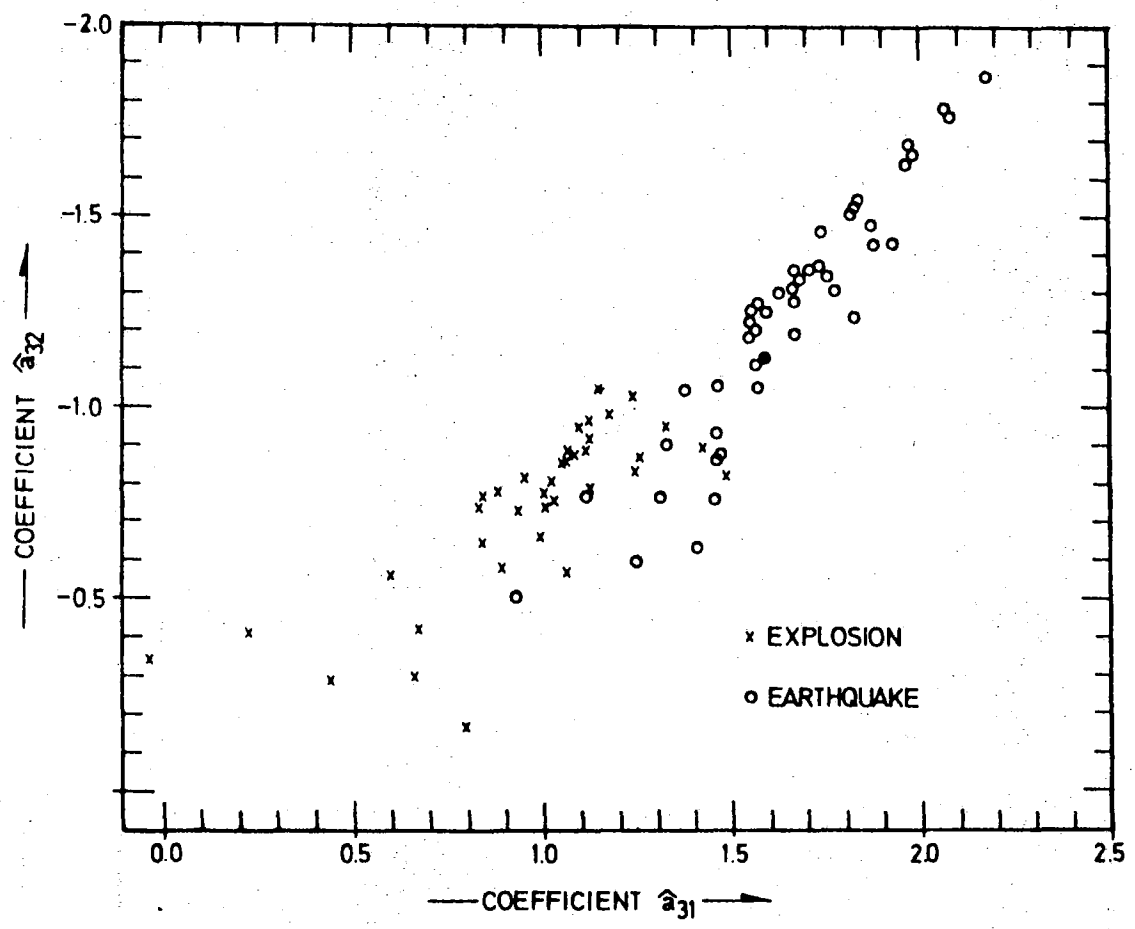

Fig. I.1 Estimated coefficients $\hat{a}_{31}$ and $\hat{a}_{32}$ assuming a 3rd order autoregressive model.

$$X(t)-a_{31}\,X(t-1)-a_{32}\,X(t-2)-a_{33}\,X(t-3) = Z(t).$$

J. SOME AUTOREGRESSIVE MODELS FOR SHORT-PERIOD SEISMIC NOISE

Several investigations have been made into the structure of seismic noise in general and of the seismic noise at NORSAR in particular. These studies have been nonparametric in nature in the sense that they have been concerned with the general properties of the spectrum and autocorrelation function of the process. The advantage of having a parametric model should be obvious. If a good model can be found, the noise process can be characterized by the numerical values of a few parameters as opposed to a study of plots of the spectrum and the autocorrelation function.

It turns out that the short-period seismic noise at NORSAR can be described by a parametric model having the form

$$X(t) - a_1(t)X(t-1) - \ldots - a_p(t)X(t-p) = Z(t)$$

where $X(t)$ is used to denote the noise process. This is a nonstationary generalization of the standard autoregressive models allowing time-varying autoregressive coefficients and a nonstationary white-noise residual process $Z(t)$. It is found that the short-period noise at NORSAR is in most cases quite satisfactorily described by a third order ($p=3$) model. Also, it is seen from Table J.1 that the nonstationary character of the noise is due primarily to time variations of the residual variance and the lower order autoregressive coefficients.

D. Tjøstheim

REFERENCE

Tjøstheim, D. (1975): Some autoregressive models for short-period seismic noise, Bull. Seism. Soc. Am., 65, pp. 677-691.

TABLE J.1

Mean, standard deviation and stability parameters of autoregressive coefficients and residual variances for various subarrays. The parameters are obtained by averaging the estimated autoregressive coefficients and residual variances over 34 two-minute noise samples from August 1973. For each two-minute sample a third order autoregressive model has been assumed. The stability parameter gives an indication of the time variations in the model. Low stability means large time variations and vice versa.

Sub-array	$\hat{a}_{31}$			$\hat{a}_{32}$			$\hat{a}_{33}$			$\hat{\sigma}_z^2$		
	Mean	St.Dev.	Stab.	Mean	St.Dev.	Stab.	Mean	St.Dev.	Stab.	Mean	St.Dev.	Stab.
01A	1.68	0.15	11.2	-0.97	0.28	3.5	0.18	0.15	1.2	16323	10584	1.6
01B	1.79	0.13	13.8	-1.01	0.28	3.6	0.15	0.16	0.9	10785	6352	1.7
02B	1.80	0.10	18.0	-1.09	0.20	5.5	0.20	0.10	2.0	9203	4665	2.0
03B	1.63	0.19	8.6	-0.82	0.36	2.3	0.09	0.18	0.5	21438	14072	1.5
05B	1.70	0.17	10.0	-0.95	0.32	2.9	0.14	0.16	0.9	12240	9426	1.3
06B	1.70	0.12	14.2	-0.92	0.22	4.2	0.11	0.12	0.9	10185	6158	1.6
07B	1.73	0.22	7.9	-1.00	0.30	3.3	0.17	0.13	1.3	13402	12839	1.0
01C	1.73	0.10	17.3	-1.00	0.20	5.0	0.18	0.11	1.6	8135	3522	1.3
02C	1.71	0.11	16.5	-0.93	0.28	3.3	0.12	0.15	0.8	9246	5127	1.8
03C	1.64	0.22	7.5	-0.83	0.39	2.1	0.09	0.17	0.5	11633	11273	1.0
04C	1.60	0.19	8.4	-0.74	0.38	1.9	0.04	0.17	0.2	9837	8865	1.1
05C	1.73	0.23	7.5	-0.95	0.37	2.6	0.16	0.17	0.9	10436	8135	1.3
06C	1.72	0.13	13.2	-0.94	0.26	3.6	0.13	0.14	0.9	8457	5656	1.5
07C	1.54	0.18	8.6	-0.68	0.29	2.3	0.02	0.13	0.2	11666	8685	1.3
09C	1.42	0.34	3.9	-0.57	0.47	1.2	-0.00	0.20	0.0	21412	26591	0.8
10C	1.76	0.11	16.0	-1.02	0.17	6.0	0.17	0.10	1.7	10415	6655	1.7
11C	1.72	0.09	19.1	-0.95	0.18	5.3	0.12	0.11	1.1	17061	10639	1.6
12C	1.75	0.13	13.5	-1.00	0.23	4.3	0.14	0.12	1.2	9942	5412	1.8
13C	1.53	0.18	8.4	-0.56	0.25	2.2	-0.08	0.14	0.6	12779	12013	1.0
14C	1.43	0.30	4.8	-0.65	0.35	1.9	0.08	0.14	0.6	23544	8942	2.6

K. FURTHER m_b:M_s STUDIES AT NORSAR

A comprehensive m_b:M_s analysis has been undertaken using a data base of 60 presumed nuclear explosions and 45 presumed earthquakes in Eurasia recorded at NORSAR between 1971 and 1974. The data have been selected subject to the requirement that both PDE location and magnitude estimates should be available in addition to the recordings at NORSAR. The geographic distribution of these events is given in Fig. K.1; notice that 35 of the presumed explosions are confined to a small area in Eastern Kazakh.

The m_b:M_s relationship was investigated using both NORSAR and PDE estimates for the body wave magnitude m_b. It was found that while m_b(NORSAR) gave a slightly better separation for the Eastern Kazakh data (see Fig. K.1), m_b(PDE) gave significantly better results when applied to the complete data set, this being due to a magnitude bias caused by a larger power loss in array beamforming for events with smaller travel distance ($<30^{\circ}$).

The basic results of this m_b:M_s analysis are given in Fig. K.2, where m_b(PDE) is plotted versus M_s(NORSAR). It was possible to estimate M_s for 44 of the presumed explosions, for the other 16 an upper bound is given, determined by the noise level at that particular time. Among the 44 explosions there are 3 difficult events, all on the edge of the earthquake population. Two of those are from the Ural Mountains (March 22, 1971, and October 26, 1973), while the smallest and most difficult one to identify is from Novaya Zemlya (July 22, 1974). Several of the events for which no Rayleigh waves have been identified occurred during a period when the noise level was low enough to allow identification based on negative evidence, while others are falling between the two populations.

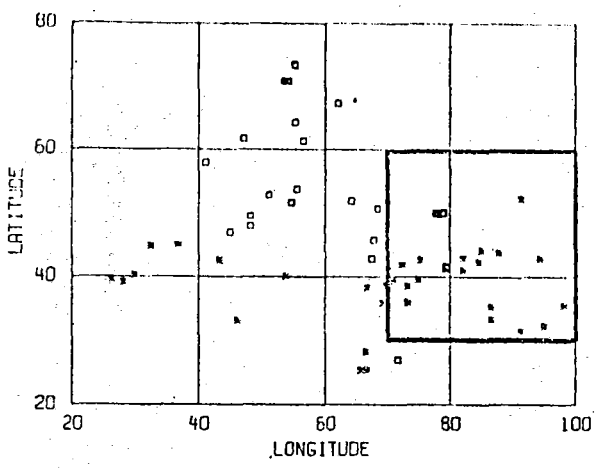

Fig. K.1 The geographic distribution of the 60 explosions and 45 earthquakes used in this study. Explosions are depicted by squares and earthquakes by stars. The area between 30° - 60°N and 70° - 100°E is that called 'Eastern Kazakh'.

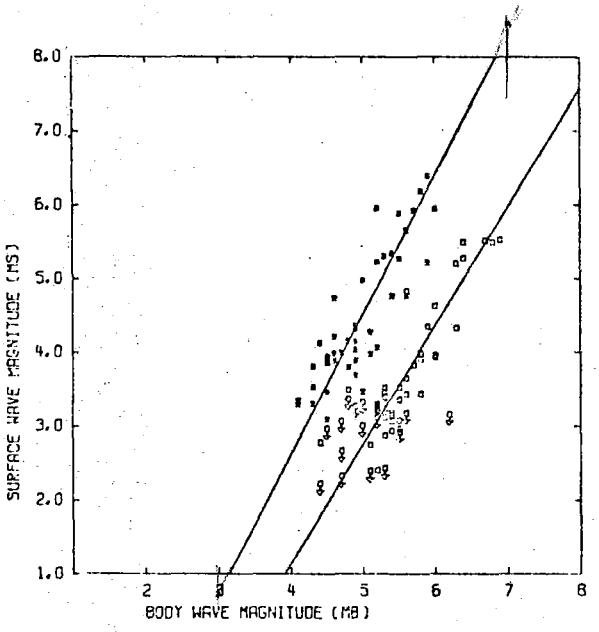

Fig. K.2 m_b:M_s diagram for the complete data base of 60 explosions and 45 earthquakes from Eurasia, including 16 explosions for which no Rayleigh waves have been detected at NORSAR. The symbol for each of these 16 events includes an arrow to indicate that the M_s value has been replaced by a noise estimate representing the largest possible M_s value.

In order to evaluate numerically the separation in Fig. K.2, a discriminant was defined which is a linear combination of m_b and M_s such that it is zero everywhere on the explosion regression line. From the distributions of the explosion and earthquake discriminant values the identification probability can be estimated for any particular false alarm rate. It was found for the data in Fig. K.2 that for a false alarm rate of 1% one would have an identification probability of 90.3%. Furthermore, if the 16 explosions with no Rayleigh waves detected were removed, the identification probability would increase to 95.4%, still for a false alarm rate of 1%.

The 16 noise measurements in Fig. K.2 are distributed almost randomly in time over about 4 years. The average value, which is M_s=2.9, can therefore be used as a measure of the detectability level for explosion Rayleigh waves from Eurasia, and the standard deviation is estimated to $\pm$ 0.4 M_s units. This large standard deviation is caused by large long term fluctuations in the noise level, and in order to investigate that effect more thoroughly, the on-line system at NORSAR was extended to allow for calculation of the average long period noise level. One year of such analysis is shown in Fig. K.3, and a separate calculation of the distribution shows that 70% of the time the variation is within $\pm$8 dB of the median. Provided that there is an inverse linear relationship between noise level and detectability this corresponds to a standard deviation of about $\pm$0.4 M_s units in detectability, which is equal to the value we estimated using the direct method.

H. Bungum

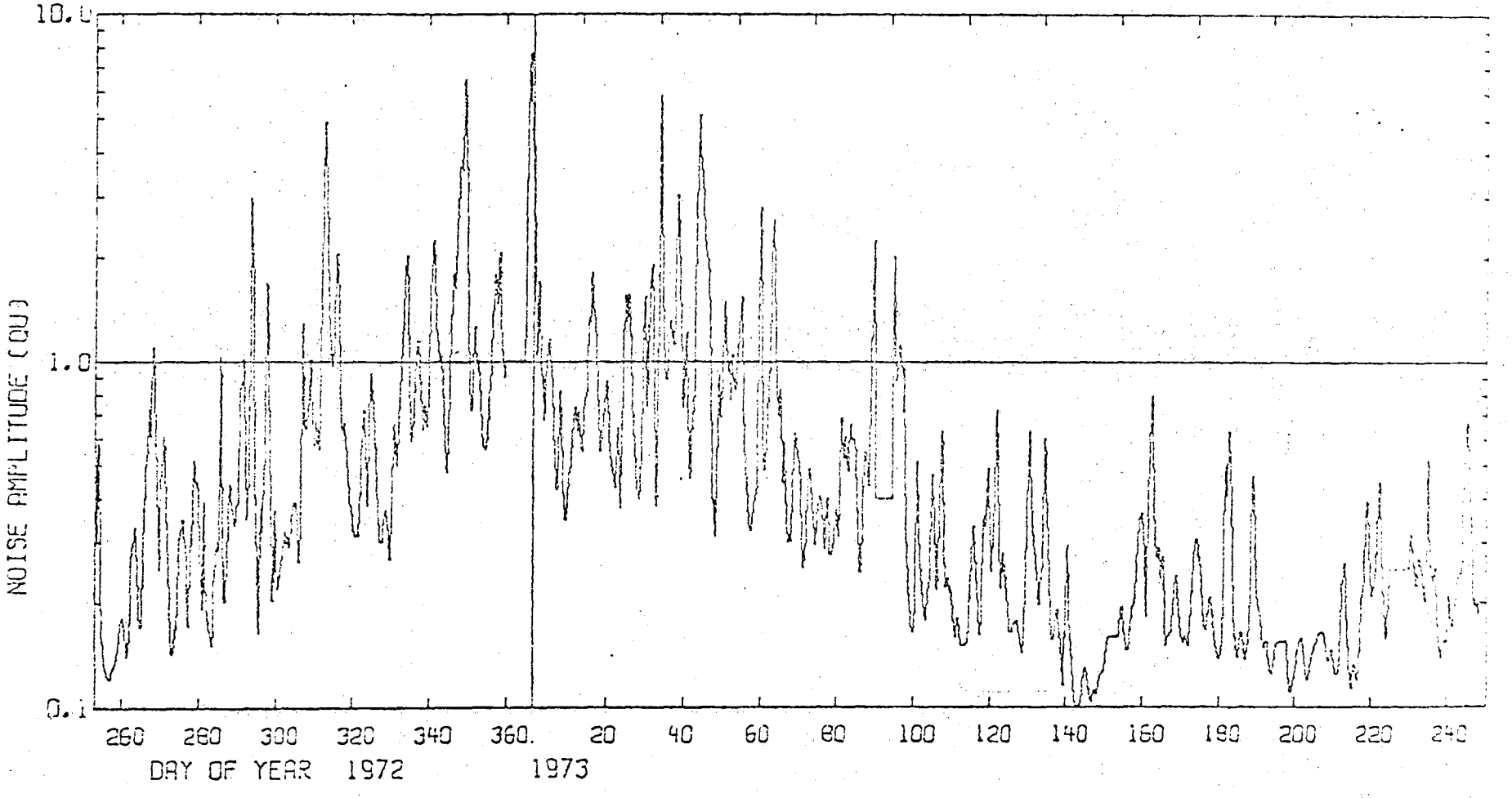

Fig. K.3 Average long period noise level at NORSAR for one year from day 253/72 to day 252/73. The data are actually the average of the noise levels at 14 vertical long period seismometers, where, for each noise sample the highest four and lowest four of the 22 subarrays have been excluded for reasons of stability. The amplitudes are given in arbitrary units, and the sampling rate is 20 per day.

L. IMPROVED IDENTIFICATION USING COMBINED CRITERIA

In Section K a relatively large data base was presented in an m_b:M_s analysis of seismic events from Eurasia. The same data base will be used in this section, only that we have proceeded one step further and combined the m_b:M_s data with more short period information in order to further improve the separation between earthquakes and explosions. Such combinations are often done through successive application of discriminants, starting with the best one. Combining discriminants linearly, however, results in several advantages. First of all, the same analysis applies to all events so that the analyst can enter with his interpretation at a higher level; secondly, a combined discriminant is easier to evaluate than a step-wise procedure. In this study we have defined a new two-dimensional discriminant which in many ways can be compared with the m_b:M_s discriminant.

The new discriminant is constructed by combining the m_b:M_s data with some parameters obtained by modelling the short period data, noise as well as main signal and coda, as auto-regressive time series. For more details we refer to Tjøstheim (1975); see also Section I, where it was found that such modelling is in fact possible, and in most cases a good approximation is obtained using a third order model. The three resulting coefficients then essentially describe the second order structure or the power spectrum of the particular time series under consideration.

The optimal linear combinations have been obtained through an extensive trial-and-error procedure, where a large number of combinations have been tested. The best one was obtained by defining the two parameters of the new discriminant as

$$X1 = m_b - B \cdot \hat{a}_1(S)$$
$$X2 = M_s + B \cdot (\hat{a}_1(C) - \hat{a}_1(N)) \qquad \text{(L.1)}$$

where $\hat{a}_1(S)$ is the first order coefficient from the main signal, and C and N denote coda and preceding noise respectively. It was reassuring to note that the above discriminant gave the best results even when applied to different data bases and different regions (in Eurasia, that is), and the same kind of stability was observed for the scaling coefficient B, whose optimal value usually was found to be around 0.5.

An example of the new two-dimensional discriminant as applied to data from around Eastern Kazakh is given in Figs. L.1 and L.2, where the m_b:M_s and the corresponding X1:X2 diagrams are given respectively. It is easily seen that the improvement in separation is considerable.

H. Bungum and D. Tjøstheim

REFERENCES

Tjøstheim, D. (1975): Autoregressive representation of seismic P-wave signals with an application to the problem of short-period discriminants, Geophys. J.R. Astr. Soc., in press.

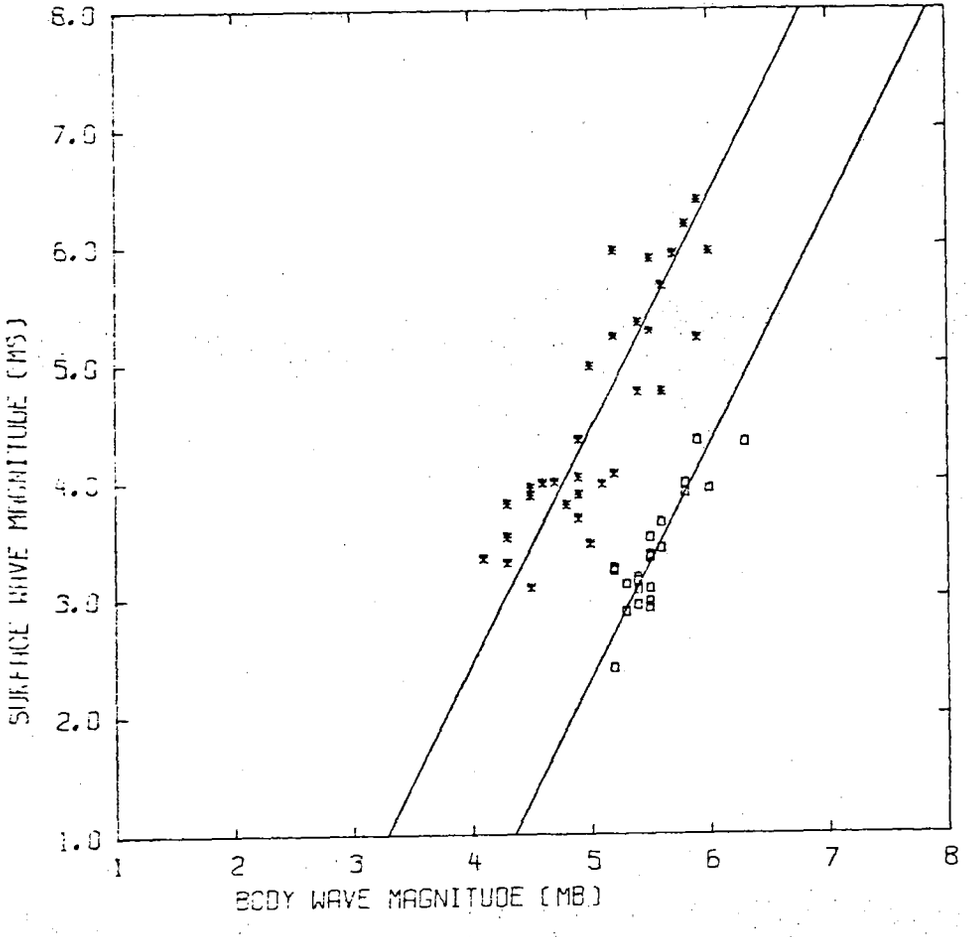

Fig. L.1

m_b:M_s diagram for the 'Eastern Kazakh' data base of 35 explosions and 31 earthquakes.

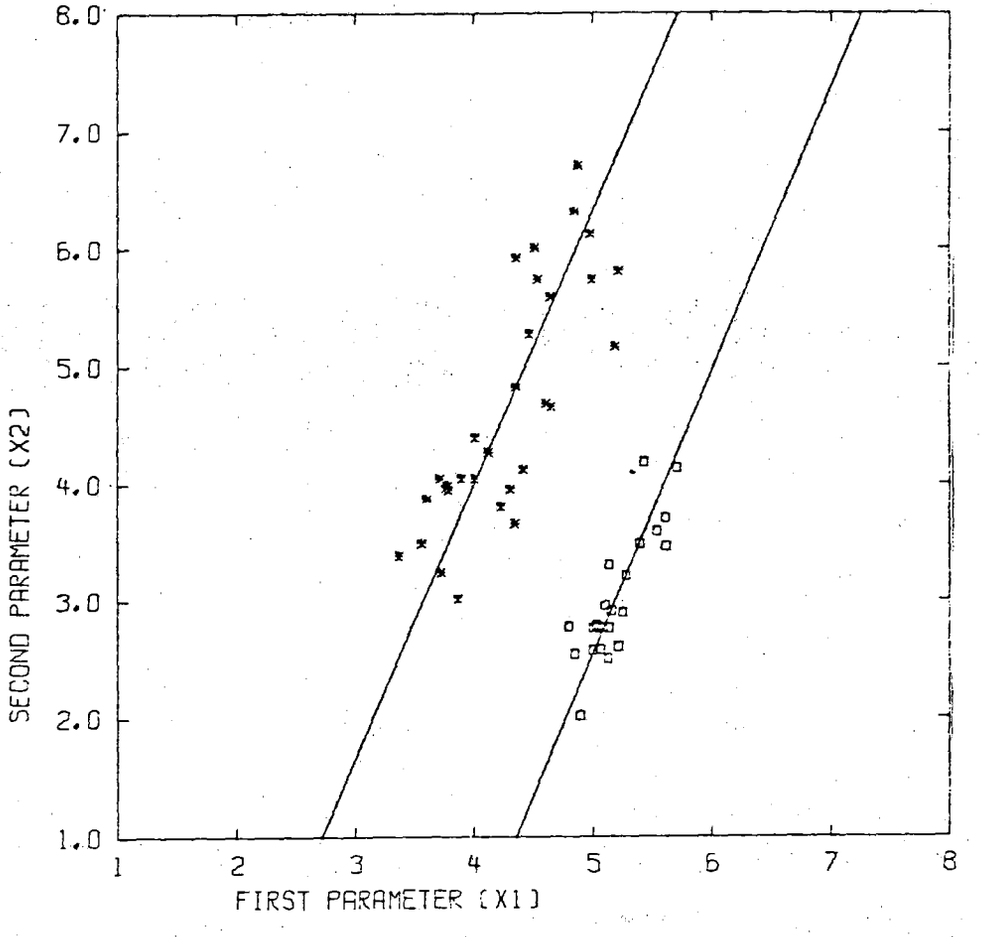

Fig. L.2

X1:X2 diagram for the same data as in Fig. L.1, using formula (L.1) with B = 0.5.

M. A KIRNOS SEISMOGRAPH IN THE NORSAR SEISMIC ARRAY

The differences in earthquake magnitudes measured from wide band (Kirnos) seismographs, such as are widely installed in the USSR ('East') and narrow band seismographs used in 'Western' installations have been discussed at great lengths in the Geneva test ban negotiations (CCD). The displacement response for the two instrument types are shown in Fig. M.1. Operation of Hall-Sears (U.S.A.) and Kirnos (U.S.S.R.) seismometers at the same site suggests itself as a useful experiment directed to clarifying the discrepancies between 'Eastern' and 'Western' body wave magnitudes.

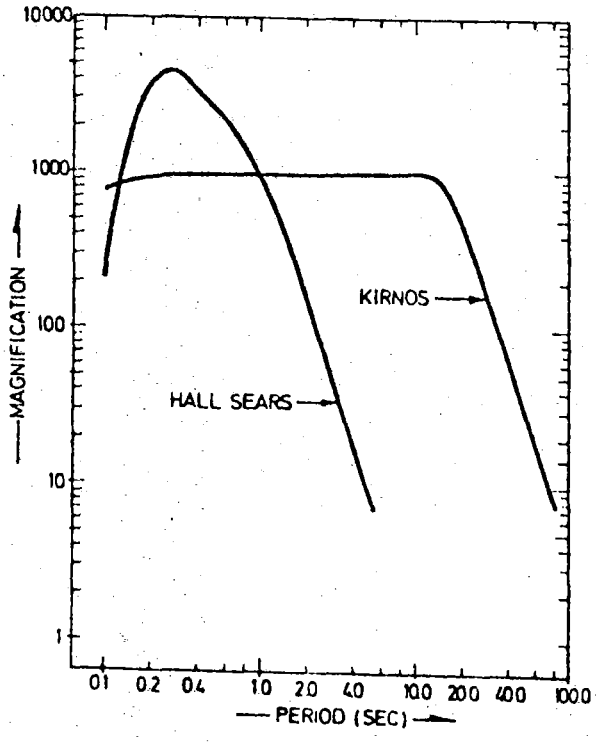

Fig. M.1 Displacement response for Kirnos SVK-2 compared to the NORSAR seismometer response (Hall-Sears). Equal magnification at 1 sec period.

As a part of a Nordic project on detection seismology, a Kirnos vertical broadband instrument was installed at NORSAR subarray 04B and operated over a period of about nine months. During the period of operation (Jan-Sep 1974) the seismograms from the Kirnos instrumentation have been read in comparison with the NORSAR bulletin. On an average some twelve events have been identified every month, with more events detected in summer than in winter. Fig. M.2 shows the decision histogram together with the maximum likelihood estimated thresholds of 5.7 and 6.4 body wave magnitude for 50 and 90 per cent probability of detection, respectively. All wave modes are included in the detection decision in this case. When only body waves (P, PP, PcP, PKP) are considered, the results are even more modest for the Kirnos seismograph detectability, namely, 5.9 and 6.5 m_b units. However, it has to be pointed out that the reliability of the estimates decreases when sample size is significantly less than one hundred.

Due to poor detectability, the Kirnos seismograph system would need years of operation in Norway in order to establish a reasonable data base suitable for statistical magnitude studies. However, it might be interesting to see if the limited data available follow the general trend that would be expected from a broadband instrument of the SVK-2 type. Due to the paucity of observations, no regionalization was attempted, and, moreover, core phases are excluded from the magnitude considerations in the following. Altogether 25 events in the distance range 18-91 degrees were jointly recorded as P-waves by the Kirnos and the NORSAR Hall-Sears instrument at subarray site 04B00, the two instruments being separated physically by only 2 meters. The body wave magnitude m_b^E computed by the 'Eastern' broadband instrument versus m_b^W computed by the 'Western' SP instrument is shown in Fig. M.3. According to Davies (1968), the difference $m_b^E - m_b^W$ should be around 0.5 magnitude units, while Marshall et al (1972)

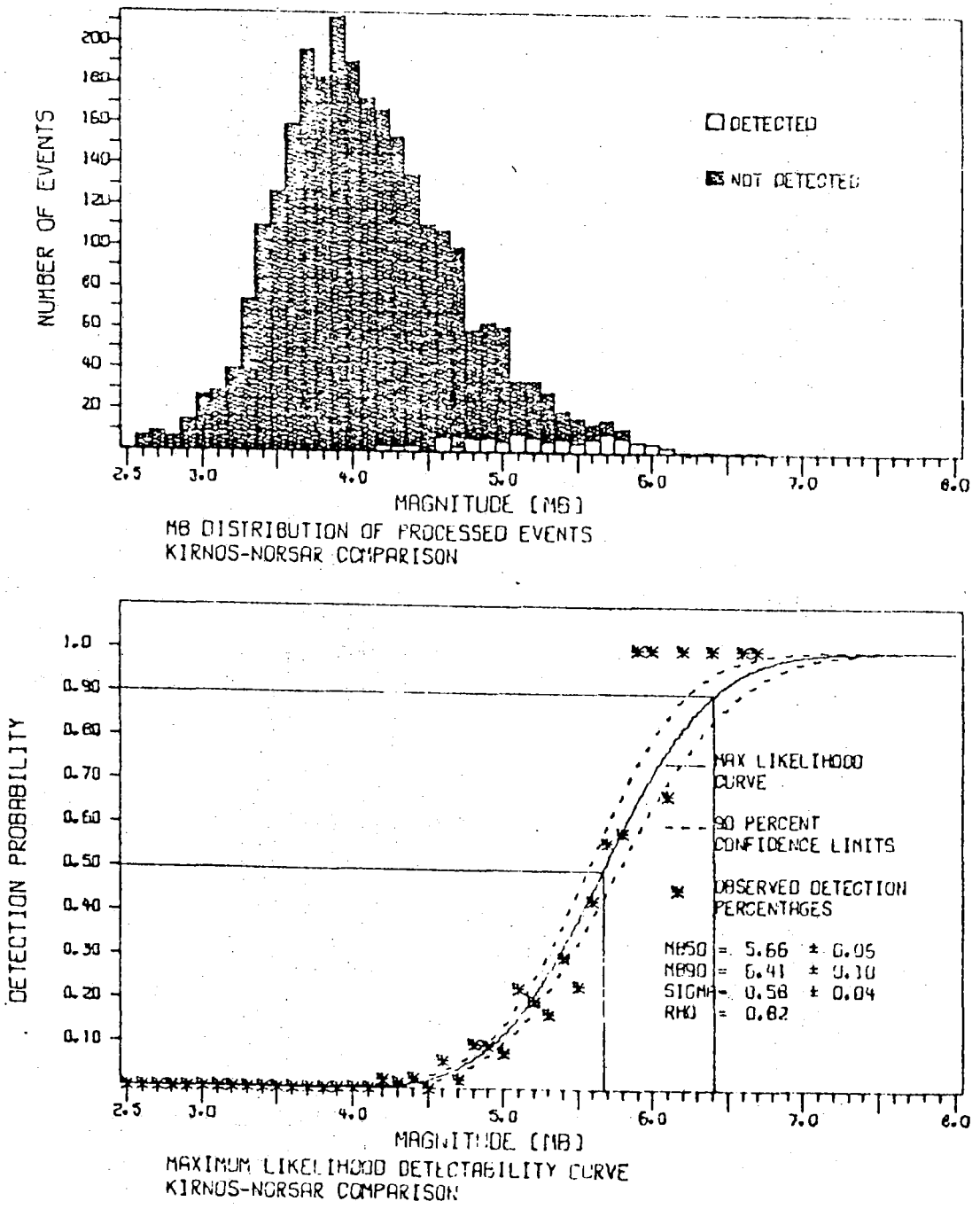

Fig. M.2 Kirnos detection statistics for the total number of events identified (all phases included).

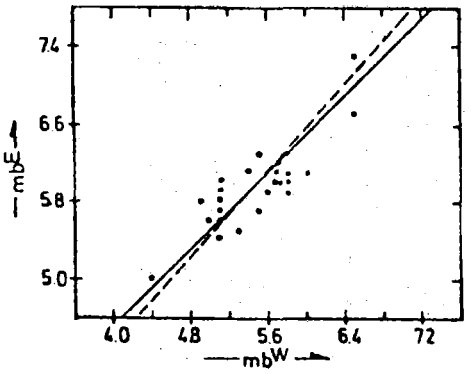

Fig. M.3 Kirnos m_b^E versus Hall-Sears m_b^W. Dotted line: 'Eastern'-'Western' magnitude relationship by Marshall et al (1972). Solid line: E-W magnitude relationship by Davies (1968).

found this relationship to be magnitude dependent, yielding

$$m_b^E = 1.12\ m_b^W - 0.15$$

Both these curves are given in Fig. M.3, and the data is not inconsistent with either.

The results obtained in this study support the conclusion that the main cause of the discrepancy between 'Eastern' and 'Western' measurements of magnitude is the difference in frequency responses of the seismographs employed. A rough estimate of the slope b of the frequency-magnitude relationship for the Kirnos gives a much lower value than reported for 'Western' narrowband instrumentation (Richter, 1958; Marshall et al, 1972). Thus by extrapolation, 'Western' data predicts more small shocks and fewer great shocks than 'Eastern' broadband data collected by Kirnos instruments. The Kirnos event detectability is poor, as the noise level imposes a serious limitation on this broadband system. In

conclusion, it should be stressed that in the present context a minimum requirement for a useful broadband seismograph system should include magnetic tape recording to permit such operations as frequency filtering.

More details from this project are to be found in the report of Dahle (1975).

A. Dahle

REFERENCES

Dahle, A. (1975): A Kirnos seismograph in the NORSAR Seismic Array, Internal Report No. 4-74/75, NTNF/NORSAR, Kjeller, Norway.

Davies, D. (1968): Seismic methods for monitoring underground explosions, Almquist & Wiksell, Sweden.

Marshall, P.D., R.F. Burch and A. Douglas (1972): How and why to record broadband seismic signals, Nature, 239, No. 5368, 154-155.

Richter, C.F. (1958): Elementary Seismology, W.H. Freeman & Company, San Francisco and London.

N. SIGNAL-NOISE CLASSIFICATION

When an event has triggered the NORSAR automatic event detector, the analyst is faced with the problem of deciding whether this is earthquake- or explosion-generated seismic signals or just correlated noise. His data are the seismograms from the 22 subarrays, filtered and time-shifted according to the estimated epicenter, and the array beam, the phased sum of the sensors, which has a signal-to-noise ratio about 13 dB better than the individual subarrays. Together with this he uses his experience about the signal shape, the subarray amplitude distribution, detectability and seismicity in the actual area. In most cases the signal-to-noise ratios on the subarray level are high enough to see the incoming P-wave on all or some of the subarrays, and the decision is easily made. But when the signal-to-noise ratio is so low that only the beam and maybe a few subarrays have a visual signal, then the analyst must use other information as a basis for a decision.
As an aid to the analyst, three different statistical tests were implemented in the Event Processor in December 1974 to test the hypothesis whether the triggering wavelet is correlated noise or a real seismic signal. The test statistics are calculated for events with signal-to-noise ratios in an interval just above the (time-varying) pre-threshold. One test statistic considered is the Sign-bit Semblance test which checks on the signal similarity between subarrays. Another is a Binomial test which checks on the sign distribution of least square amplitude weights calculated for the subarray beam traces. The third test statistic is a Student's t-test which checks on the distribution and size of subarray beam amplitude weights.

The amplitude weights are an estimate of the amplitude factor, γ_j, in the model $Y_j = \gamma_j S + n_j$, where Y_j is the recorded data on the j-th sensor, S a signal part and n_j a noise part (Fyen et al, 1975). For noise wavelets, the amplitude weights will be random in sign and size, while for P-waves the $\hat{\gamma}_j$-weights are expected to match the amplitude pattern in the region in question. However, for events with a signal-to-noise ratio as small as 3.6-4.0 units, the $\hat{\gamma}$-weights contain reliable amplitude information for the "best" subarrays only, and the correspondence between the observed $\hat{\gamma}_j$-weights and the known amplitude pattern for larger earthquakes is small, a problem which will be investigated further. Also for some extreme cases, noise has the same characteristics as an earthquake signal, as seen in Fig. N.1 where the test statistics accepted the event, but these cases may be eliminated by the anlyst due to his experience of earthquake occurrence and signal shape.

Another type of events which give test statistics results high above the thresholds are events with magnitudes below 4.0 located on the west coast of America and mid-Atlantic Ridge, where NORSAR normally only detects earthquakes above magnitude 4.6. These events are correctly classified by the analyst as being correlated noise and represent most of the statistical false alarms. For events having their origin to the east of NORSAR, we did a case study of weak Japan events. A list of events located in the Japan area, including both cases classified as noise and cases classified as earthquakes, was sent to Japan Meteorological Agency (JMA). Out of 36 events listed, 20 NORSAR-reported earthquakes were confirmed by JMA-stations, and 5 of these earthquakes were classified as noise by the test statistics (missed detections). Out of the remaining 16 events, 11 were not reported in the NORSAR bulletin, nor reported by any JMA-station, and 4 of these were classified as signals by test statistics (false alarms). The 5 other events were out of range for the JMA-stations. After 5 months of processing experience there has been no significant increase in the number of earthquakes

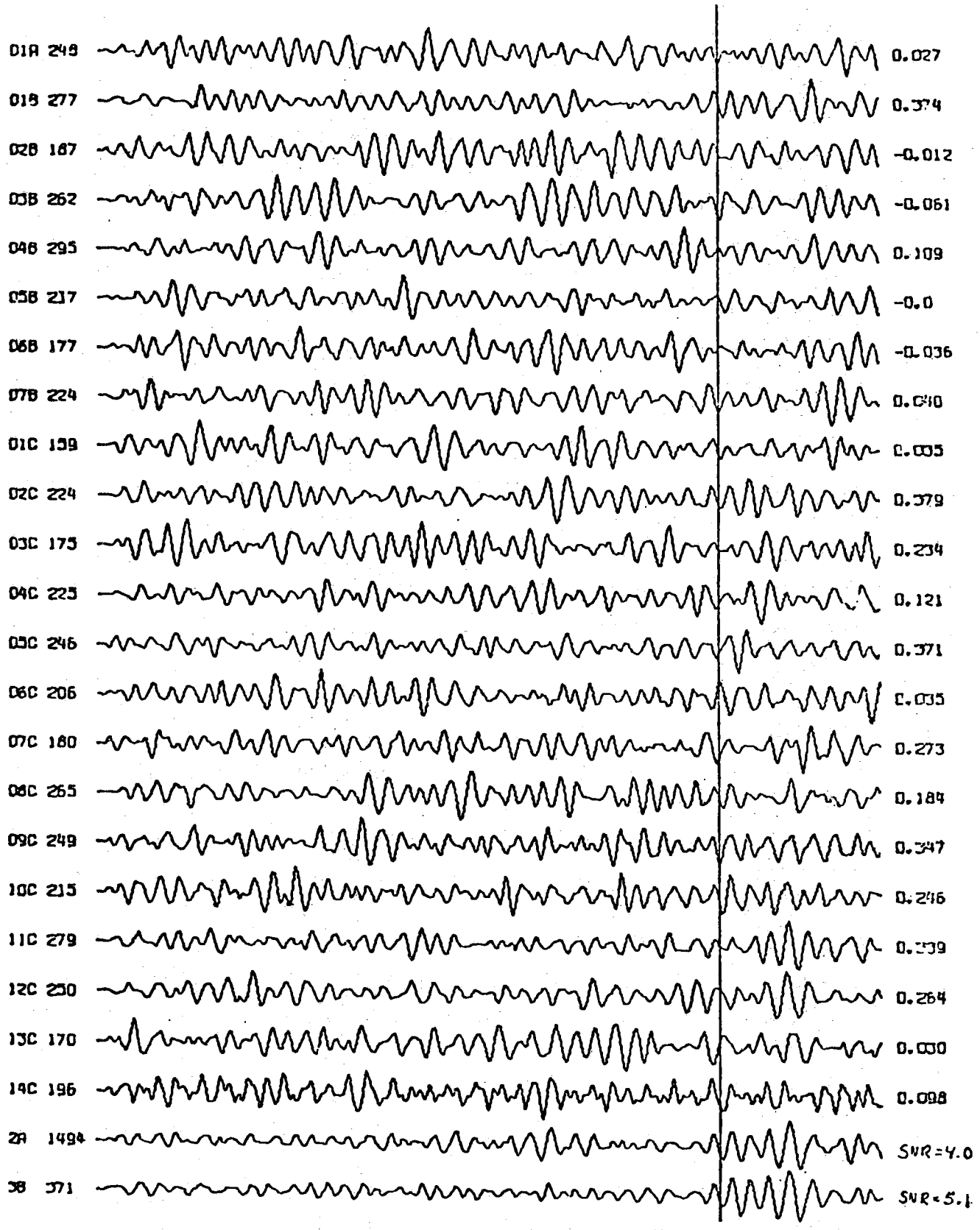

Fig. N.1 Example of extreme noise wavelets. The column to the right gives the $\hat{\gamma}_j$-weights. 2A and 3B denote array and weighted array beam respectively, pointing south of Honshu, Japan. The test results give high signal similarity and non-random sign and size of the amplitude weights, but a check with the amplitude pattern rejects this event as being an earthquake in Japan area.

reported by the analyst due to the test statistics. However, the tests are still considered as a good aid for the marginal cases, and also help the analyst to check whether the line-up of the subarray traces is good, i.e., giving correct time-delays for epicenter determination.

J. Fyen

REFERENCES

Fyen, J. E.S. Husebye and A. Christoffersson (1975): Statistical classification of weak seismic signals and noise at the NORSAR array, Geophys. J.R. Astr. Soc., 42, in press.

O. PRELIMINARY RAYLEIGH WAVE STUDIES NORTH OF SCANDINAVIA

Surface wave dispersion measurements taken to periods of the order of 100 sec or more have proved to be diagnostic of the properties of the upper mantle to depths of the order of about 0.5 λm for Rayleigh waves, where λm is the longest wave length.

The results obtained from great-circle passages are not representative of any particular ocean, shield or tectonic province. Instead they represent the averages of a variety of each of the three types of structural provinces (Dziewonski, 1971). Knopoff (1972) has described in detail the advantages of pure-path regional studies compared with "great circle decomposition" methods.

To overcome the difficulties of determining the initial phase of the source which is encountered in the single-station phase velocity measurements (Knopoff and Schwab, 1968) the two-station method is used. Under the assumption that the angle between the great-circle path between the earthquake and the stations on the one hand and the great-circle connecting the stations on the other hand is small (less than about 7°), the effect of the initial phase of the source is eliminated. The two-station method was first used by Brune and Dorman (1963) with peak-and-trough analysis and subsequently with machine Fourier analysis by Knopoff, Mueller and Pilout (1966).

To obtain phase velocities, the seismograms and the instrument responses of each station are digitized at a fixed interval of 2 sec, an interval sufficiently short to avoid aliasing problems for this study. The technique of Pilout and Knopoff (1964) and Knopoff et al (1966) for bandpass, digital filtering of detrended, digitized seismograms was applied to minimize the interference effects of multipath transmission. This procedure significantly improves the signal-to-noise ratio for complex records. The numerical window

centered at the group arrival time is in the form of a half cycle of a sine function. Fourier analysis of each of the filtered seismograms gives the phases in the frequency band of the numerical filters. In Fig. O.1 an example is shown of the raw, filtered, and filtered-windowed time series.

For two stations on the same great-circle and recording the same event, the phase velocity at a given period T is given by

$$C(T) = \frac{D_2-D_1}{T[N+(\phi_2-\phi_1)]}$$

where D_2-D_1 is the station separation, $\phi_2-\phi_1$ is the difference in the phase shifts (in circle) between the two recordings, taking into account instrumental phase shifts; the arbitrary integer N is determined by making the phase velocity geophysically suitable at long periods and extending the phase continuously into the short period regime.

It should be noted that a systematic bias exists in the Love wave observations due to interference between fundamental and I higher mode in the range 30-90 secs. For this reason Rayleigh waves are more convenient for this type of study. Fundamental Rayleigh wave phase velocities were obtained with the previous technique for the path KBS-KRK shown in Fig. O.2, analyzing the event occurring at 06:26:15.8 the 28th of December 1967.

Unusually high values were found (Fig. O.3). They are compared with the values obtained by Noponen (1966) in Finland. The agreement between the two sets of data is good and we

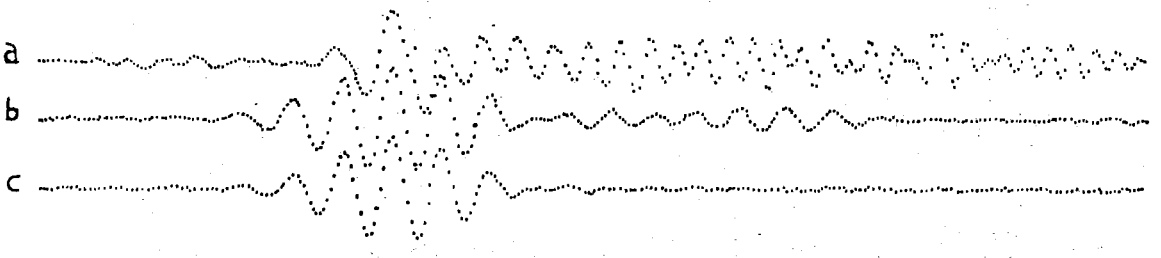

PASS BAND 25-35 sec

Fig. O.1 Example of raw, filtered and filtered-windowed time series.

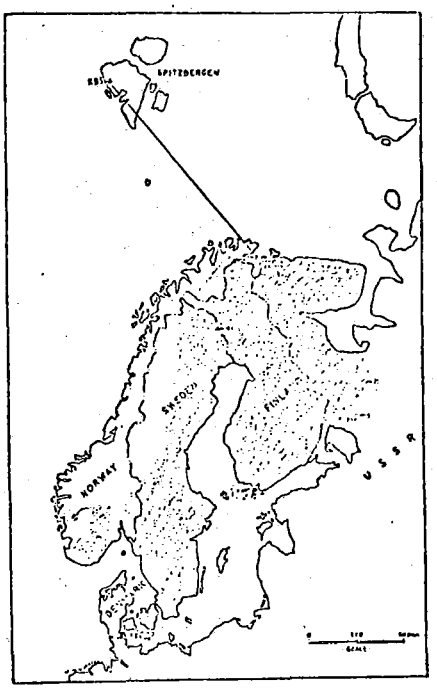

Fig. O.2 Baltic shield and profile considered in this study.

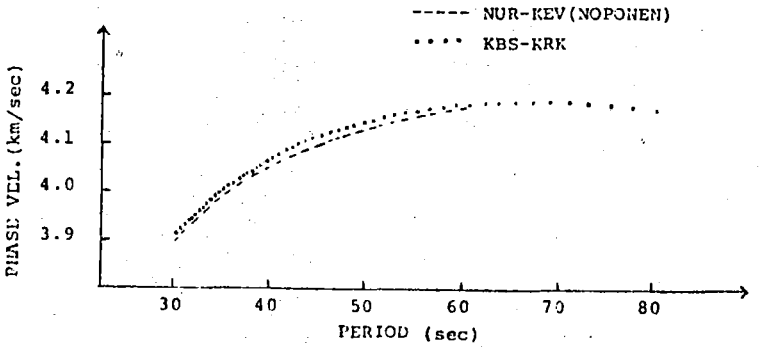

Fig. O.3 Rayleigh wave phase velocity vs. period
experimental : dots
NUR-KEV (Noponen) : dashed line

may infer that the uppermost mantle is similar in the two regions.

Work is now in progress aimed at a more detailed interpretation of the experimental data.

G. Calcagnile

REFERENCES

Brune, J., and J. Dorman (1963): Seismic waves and earth structure in the Canadian shield, Bull. Seism. Soc. Am., 53, 167-210.

Dziewonski, A. (1971): Upper mantle models from "pure-path" dispersion data, J. Geophys. Res., 76, 2587-2601.

Knopoff, L. (1972): Observation and inversion of surface-wave dispersion, The Upper Mantle, ed. A.R. Ritsema, Elsevier Publ. Co., Amsterdam, Tectonophysics, 13, 497-519.

Knopoff, L., S. Mueller and W.L. Pilout (1966): Structure of the crust and upper mantle in the Alps from the phase velocity of Rayleigh waves, Bull. Seism. Soc. Am., 56, 1009-1044.

Knopoff, L., and F.A. Schwab (1968): Apparent initial phase of a source of Rayleigh waves, J. Geophys. Res., 73, 755-760.

Noponen, I. (1966): Surface wave phase velocities in Finland, Bull. Seism. Soc. Am., 56, 1093-1104.

Pilout, W.L. and L. Knopoff (1964): Observations of multiple seismic events, Bull. Seism. Soc. Am., 54, 19-39.

P. HIGHER MODE SURFACE WAVES

Higher mode surface waves are valuable for probing the structure of the uppermost mantle on account of their selective depth sampling. Attempts to exploit higher modes are generally frustrated by the necessity for long, homogeneous paths and by limitations in the dynamic range of most recording devices. However, NORSAR's siting and digital recording is such that higher modes are commonly well-recorded from sources in Sinkiang, Central Russia, Southern Europe and Novaya Zemlya.

It has been suggested previously (Crampin, 1966) that higher mode propagation over much of Eurasia exhibits mode coupling which apparently finds no satisfactory explanation in isotropic Earth models. Crampin (1967) suggested an interpretation involving a thin layer of aligned crystalline anisotropy in the uppermost mantle, and has subsequently explored theoretically the implications of such an interpretation (Crampin, 1970; Crampin and Taylor, 1971; Crampin, 1975). The principal features include distinctive particle motion, differences in phase (wave) and group direction, and the generation of Love waves by atmospheric explosions.

NORSAR is potentially (and perhaps uniquely) suitable for a detailed examination of higher mode propagation in Eurasia; the spatial sampling of the NORSAR configuration offers the possibility of multiple analyses of particle motion as well as of direct estimation of phase and group direction. A data base of some 14 events with well-recorded higher mode wave trains has been assembled and representative examples from 2 events are plotted in Fig. P.1. These data commonly exhibit mode coupling between vertical and horizontal transverse components over extended sections of the higher mode trains. Phase velocities and directions of higher mode and fundamental mode arrivals are being estimated using high-resolution f-k analysis, and have revealed significant

($\sim 10^{o}$) differences in phase direction between the two wave groups along some paths (e.g., Sinkiang). Attempts to measure group velocity and direction of fundamental mode waves by fitting a least squares wavefront to interpolated peaks of envelopes formed from narrow band Gaussian filtered data have yielded encouraging results and may provide determinations sufficiently reliable for comparison with phase determinations.

Finally, NORSAR recorded Love waves of peak amplitude only slightly less than the Rayleigh waves from a large atmospheric explosion in southern Sinkiang in June, 1974. The possibility of explaining this observation in terms of mode conversion after propagation in an anisotropic region is being explored.

D.W. King and S. Crampin

REFERENCES

Crampin, S. (1966): Higher modes of seismic surface wave: Propagation in Eurasia, Bull. Seism. Soc. Am., 56, 1227-1239.

Crampin, S. (1967): Coupled Rayleigh-Love second modes, Geophys. J., 12, 229-235.

Crampin, S. (1970): The dispersion of surface waves in multilayered anisotropic media, Geophys. J., 21, 387-402.

Crampin, S., and D.B. Taylor (1971): The propagation of surface waves in anisotropic media, Geophys. J., 25, 71-87.

Crampin, S. (1975): Distinctive particle motion of surface waves in anisotropic media, Geophys. J., 40, 177-186.

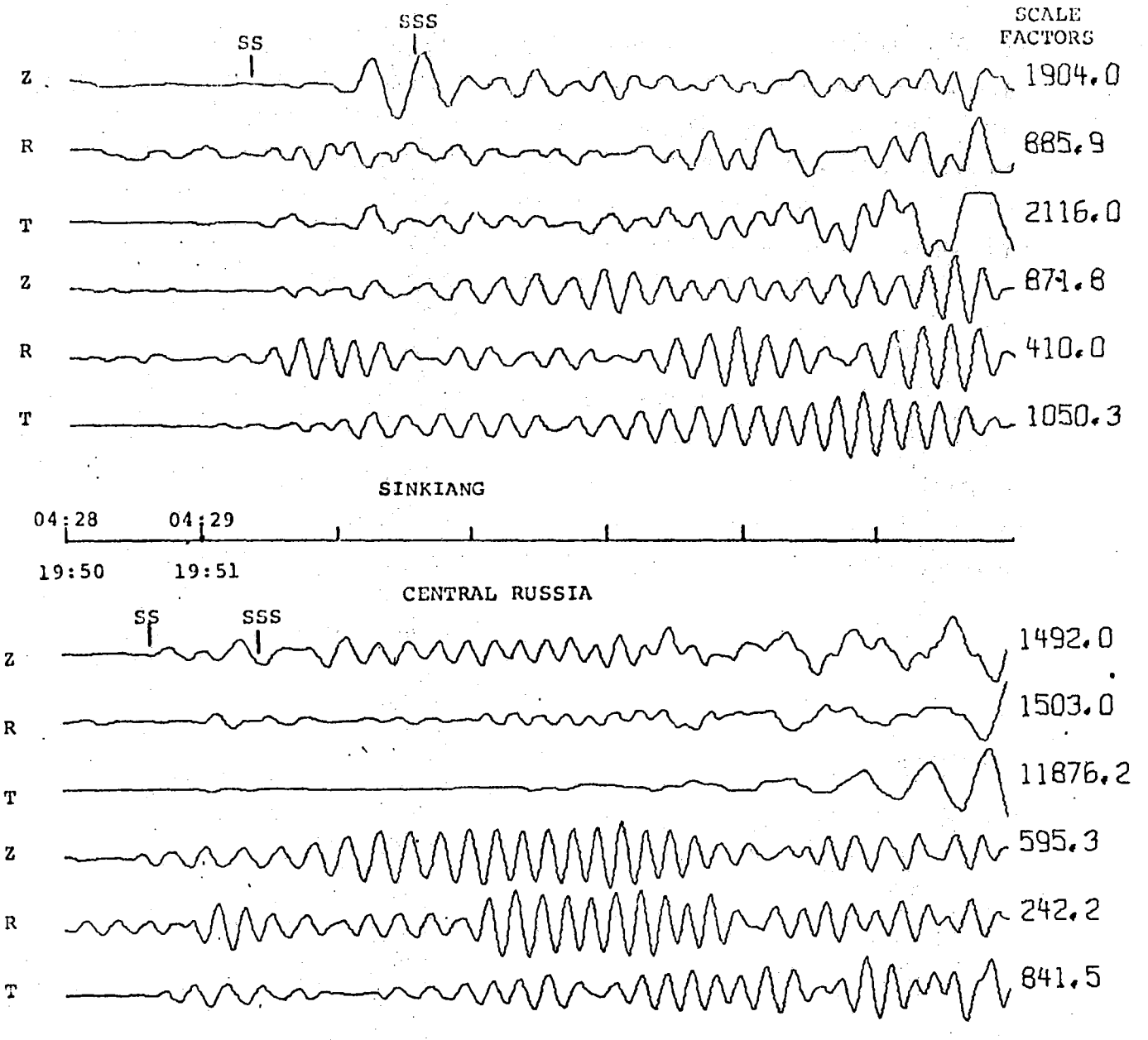

Fig. P.1

Higher mode wavetrains from events in Sinkiang (April 9, 1972, 04:10:50.7) and Central Russia (August 24, 1971, 16:33:22.7). For each event, both unfiltered and 8-17 sec bandpass filtered Z, R, T data from Subarray 01A is plotted. Approx. JB times of body phases SS and SSS are marked.

Q. SOURCE-SPECTRAL SCALING AND CORNER FREQUENCIES

Q.1 Earthquake Love-wave Spectral Ratios

The scaling of earthquake source spectra has been known in an approximate way for some years, largely through the work of Haskell (1964, 1966) and Aki (1967). In the present work, the source factor of the far-field spectrum of Love waves is being studied using the ω-square or ω-cube model (Aki, 1967) as a starting point but not assuming the principle of similarity to the same extent. The spectral ratio method (Berckhemer, 1962) is applied wherein two or more earthquakes with virtually the same focal location are used and ratios of pairs of their Love-wave spectra are determined, cancelling out instrument and path factors.

Aki's (1967) source spectral model was of one parameter, presuming a one-to-one correspondence of M_s and m_b. In this study a two-parameter model is assumed. This modified model allows for M_s and m_b to vary independently. It is expressed as

$$|A(\omega)| = \frac{k_o L^p}{[1+k_1\omega^2L^2]^s\,[1+k_2\omega^2L^2]^{\frac{1}{2}}} \qquad (Q.1)$$

where p and L are parameters and where $s = \frac{1}{2}$ or 1 according as the ω-square or the ω-cube model is chosen as a starting basis.

The expression for source spectral ratio then has four independent parameters. The estimate of these four parameters is then found from an algorithm which minimizes the variance of the model spectral-ratio values with respect to the values computed from the Fourier transforms of the two Love phases. This has been done assuming a modified ω-square model as well as a modified ω-cube model.

Although the theoretical spectral ratio is flat at high and low frequencies, its steepness at intermediate frequencies depends on the exponent of ω in the high-frequency asymptote. When we apply the model of equation (Q.1) (actually the ratio of two such expressions) to a group of deep-focus Bonin Islands earthquakes, we get a better fit for s=1 (ω-cube) than for s=½ (ω-square). An example of this is shown in Figures Q.1 and Q.2. In these figures the frequency range, which extended to 0.5 Hz for the Fourier transform output, is restricted to below 0.2 Hz because for higher frequencies one of the spectra is predominantly noise. The curves are extrapolated to 0.5 Hz but have no significance beyond 0.2 Hz. They should in fact level off just above the 1-level.

From Equation (Q.1), the corner frequencies of an event, ω_1 and ω_2, are defined as $(k_1L^2)^{-\frac{1}{2}}$ and $(k_2L^2)^{-\frac{1}{2}}$, respectively. If these two corner frequencies (for one earthquake) differ, then we have (assuming s=½) an intermediate ω^{-1} behaviour as is present in models of Brune (1970) and Savage (1972), among others. For the present data, however, ω_1 and ω_2 come out virtually equal, implying that we have $k_1 \approx k_2$ in equation (Q.1).

The corner frequencies determined so far agree in order of magnitude with those of the ω-square and ω-cube models (Aki, 1967) at magnitudes around 5½ to 6, but there is some indication that p in equation (Q.1) may be greater than 3, its value in Aki's models. This would imply a steeper corner-frequency locus, that is, less variation of corner frequency with earthquake size. This kind of behaviour has in fact been incorporated into Aki's (1972) revised model A.

Q.2 Explosion Source Spectra and Discrimination

Clearly, the fundamental difference between earthquakes and nuclear explosions is the difference in source mechanisms. This ought to manifest itself in the source spectra and indeed models of such for explosions (e.g., those of von Seggern and Blandford, 1972) differ significantly from those for earthquakes (e.g., those of Aki, 1967).

The Love-wave spectra from a group of Novaya Zemlya (presumed) explosions have been determined and an example of their spectral ratio is shown in Fig. Q.3. It is fundamentally different from the ratios of Figs. Q.1 and Q.2.
No attempt has been made to fit the modified ω-square or ω-cube models to this data -- these models assume, as a source, slip dislocation on a planar surface which is obviously inapplicable to an explosion source.

R.J. Brown

REFERENCES

Aki, K. (1967): Scaling law of seismic spectrum, J. Geophys. Res., 72, 1217-1231.

Aki, K. (1972): Scaling law of earthquake source time-function, Geophys. J. R. Astr. Soc., 31, 3-25.

Berckhemer, H. (1962): Die Ausdehnung der Bruchfläche im Erdbebenherd und ihr Einfluss auf das seismische Wellenspektrum, Gerl. Beitr. z. Geophys., 71, 5-26.

Brune, J.N. (1970): Tectonic stress and the spectra of seismic shear waves from earthquakes, J. Geophys. Res.,75, 4997-5009.

Haskell, N. (1964): Total energy and energy spectral density of elastic wave radiation from propagating faults, Bull. Seism. Soc. Am., 54, 1811-1842.

Haskell, N. (1966): Total energy and energy spectral density of elastic wave radiation from propagating faults, 2, A statistical source model, Bull. Seism. Soc. Am., 56, 125-140.

Savage, J.C. (1972): Relation of corner frequency to fault dimensions, J. Geophys. Res., 77, 3788-3795.

von Seggern, D., and R. Blandford (1972): Source time functions and spectra for underground nuclear explosions, Geophys. J.R. Astr. Soc., 31, 83-97.

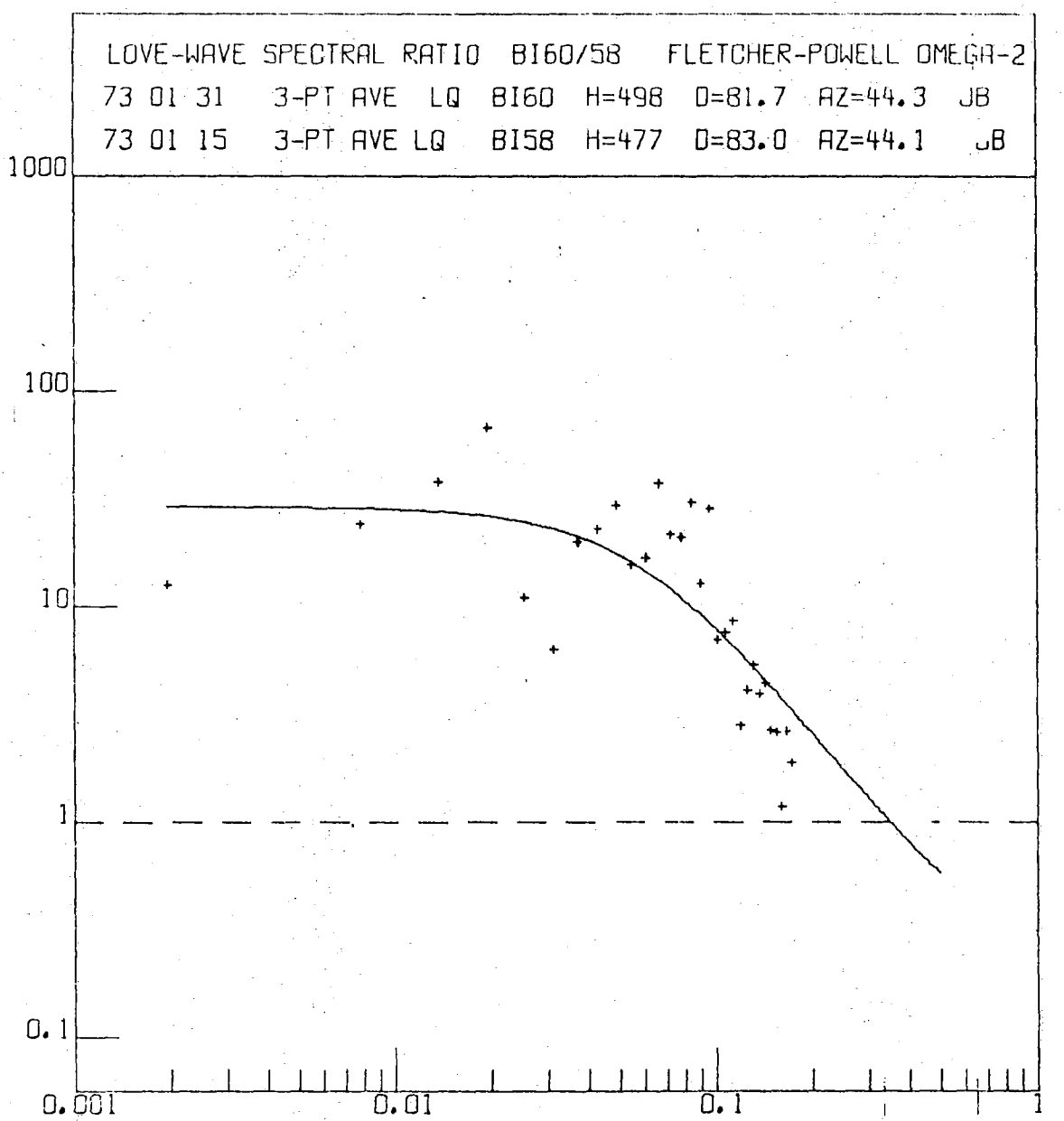

Fig. Q.1 Love-wave spectral ratio of two deep Bonin Islands earthquakes plotted versus frequency in Hz; computed by Fourier analysis of long period NORSAR Love-wave beam and group-averaged with three points to a group (plus signs); the curve is the least squares best fit assuming the modified ω-square model; S-wave corner frequency for the larger event (BI60) at 0.06 Hz.

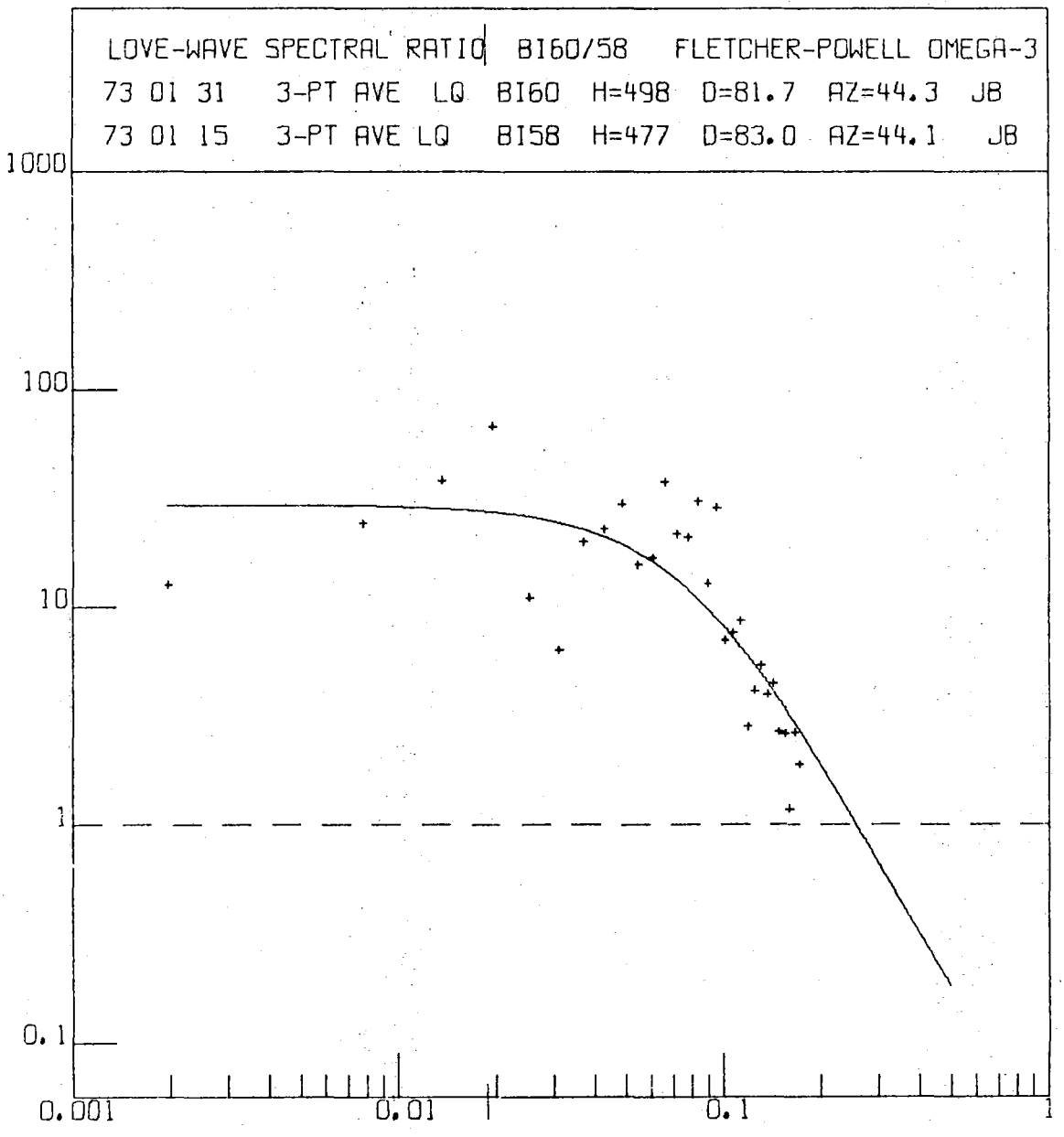

Fig. Q.2 Same as Fig. Q.1, but for the modified ω-cube model; S-wave corner frequency of BI60 at 0.08 Hz.

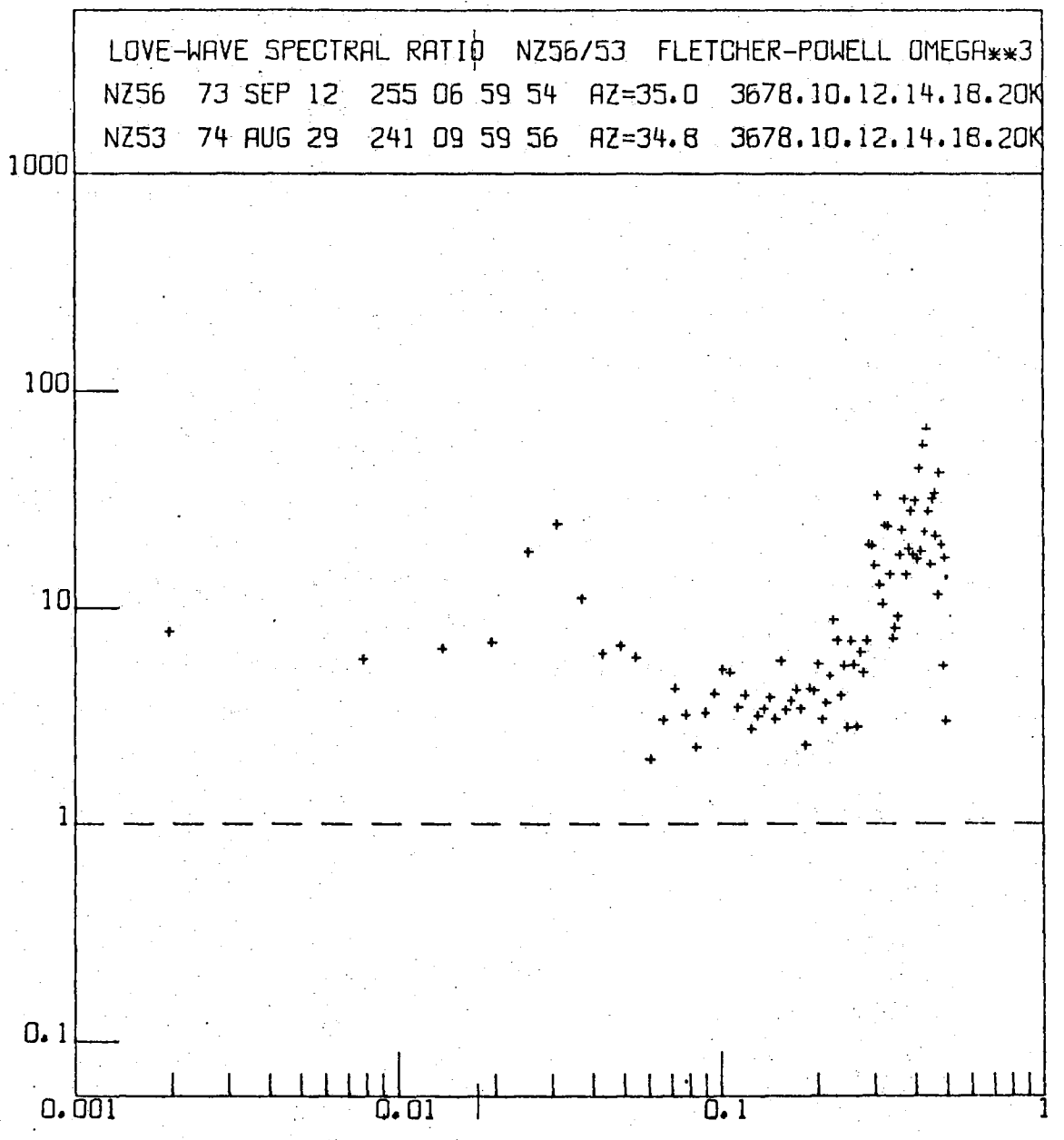

Fig. Q.3 Same as Figs. Q.1 and Q.2 for two Novaya Zemlya explosions; no model fit has been tried.

R. IN SITU STRESS MONITORING

It has been known for some time now that several narrow spectral peaks in the NORSAR short period recordings have their origin in hydroelectric power plants in the vicinity of the array. The exact nature of the generating mechanism is not known, but it is characteristic that the seismic spectral component is found at the very frequency of the revolving mass, which is typically a few hundred tons. A slight eccentricity in that mass could therefore account for the leaked energy.

The most prominent contribution in this respect is obtained near subarray 14C from the Hunderfossen power plant, which has been found to generate a strong spectral component at 2.78 Hz, corresponding to 166 2/3 rpm. The location of this steady-state energy source together with the closest seismometers is shown in Fig. R.1, where it is seen that the distances range from 4 to 14 km. In the initial analysis of the data it was discovered that the frequency of the desired spectral component was not stable; there were in fact relatively rapid variations within the frequency range 2.774 to 2.781 Hz, so that an extensive Fourier analysis was required just in order to locate the spectral peak. In order to circumvent this problem, and to get a noise-free source channel, a unit was built (at the University of Copenhagen) which uses as input the 50 Hz, 220 v power, and outputs a signal which is divided 18 times in frequency, to 2.78 Hz, and scaled down to a voltage of $\pm$ 4.6 v. This unit has now been hooked on to channel 14C05, thereby replacing the seismic data with a 2.78 Hz sine wave representing the source of the narrow spectral component.

The analysis of the data has so far only been preliminary, involving spectral analysis of consecutive 3- minute intervals over a time span of a few hours. It is noteworthy that the

introduction of the source channel reduced the required computer time by almost a factor of 10, since a running estimate of the frequency is now easily available; previously it had to be estimated from the seismic data. Even with very little blocking of data, we have obtained phase estimates for the closest channels (1 and 2) with a stability of about $\pm 1^0$, which corresponds to a precision of about $\pm 10^{-3}$ for the distances involved in this experiment. In order to monitor phase velocities, we have to study phase angle differences, and Fig. R.1 shows that there are a number of

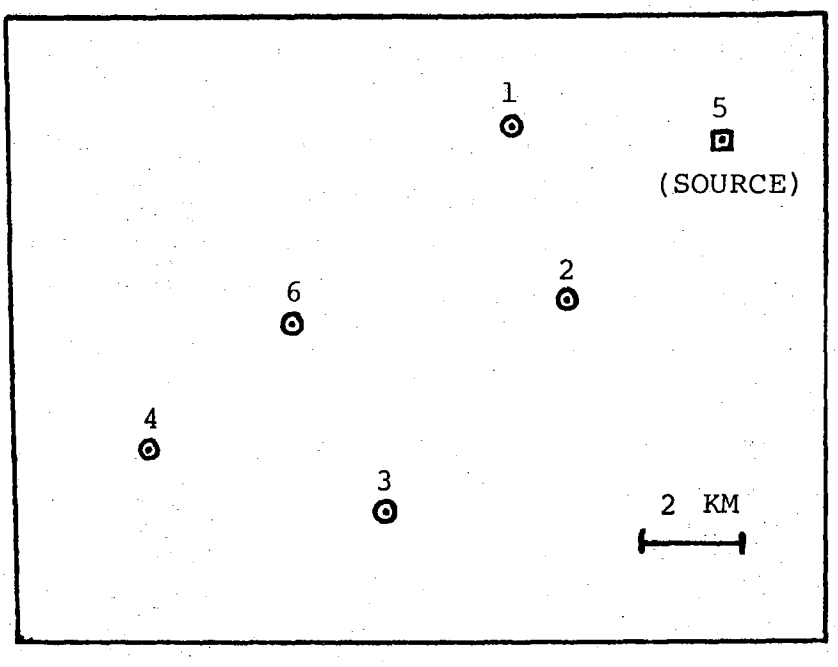

Fig. R.1 The relative locations of the Hunderfossen power plant (source) and the 5 channels currently giving short period seismic data from subarray 14C (circles). Seismometer no. 5, which used to be located in the NW part of the subarray, has been replaced by a sine wave representing the source (see main text).

possible combinations. The most stable results have been obtained using channels 1 and 2 in combination with the source channel (5), even though there is an unknown phase difference between the revolving mass and the generated current, which we use as reference. For the other channels (3 and 6) the loss in signal-to-noise ratio seems to be about compensated for by the increased distance, yielding the same relative stability.

By studying the distribution of the phase velocity differences versus travel distance, it is not possible to find any particular phase velocity which fits all the data well. However, a velocity of about 5 km/s appears to give the best overall fit. Because of the frequency variation of the source we also get an independent estimate of phase differences versus frequency, yielding group velocity, and the few data obtained so far have given estimates around 3 km/s both for combinations 1-5 and 2-5 (see Fig. R.1).

A computer program has now been developed which computes the horizontal tidal strain in any particular direction for the area around subarray 14C. We plan to continue this experiment by looking for possible phase velocity differences for different strain situations. The results obtained so far indicate that by adding much larger amounts of data, it could be possible to obtain phase difference estimates with a precision closer to 10^{-4}.

H. Bungum,
K. Aki (Cambridge, U.S.A.)
T. Risbo (Copenhagen, Denmark)

S. EARTHQUAKE ACTIVITY IN FENNOSCANDIA, 1497-1973

The systematic collection of macroseismic data on earthquake occurrence in Fennoscandia began in the 1880's when the use of questionnaires was initiated. Prior to that time macroseismic information is fragmentary and incomplete although the essential data on the larger earthquakes during another 300-400 years have been preserved. Using all pertinent macroseismic and seismograph data available, we have constructed new seismicity maps for Fennoscandia covering the time interval 1497-1973. Since the quality of macroseismic as well as instrumental data is a function of magnitude, we have constructed these maps for different magnitude intervals. Fig. S.1 shows the epicenter distribution for earthquakes with magnitude above 4.5, and the activity has been subdivided in four broadly defined zones; the Telemark-Vänern, the Western Norway, the Bothnian and the Lappland zones. There is no clear correlation between available geological and geophysical information and the earthquake occurrence, and this also applies to the Oslo Graben region. The on-going tectonic processes causing the earthquakes are not at all well-understood, and particularly so since fault plane solutions have not been obtained for any Fennoscandian earthquake.

E.S. Husebye, H. Gjøystdal,
H. Bungum

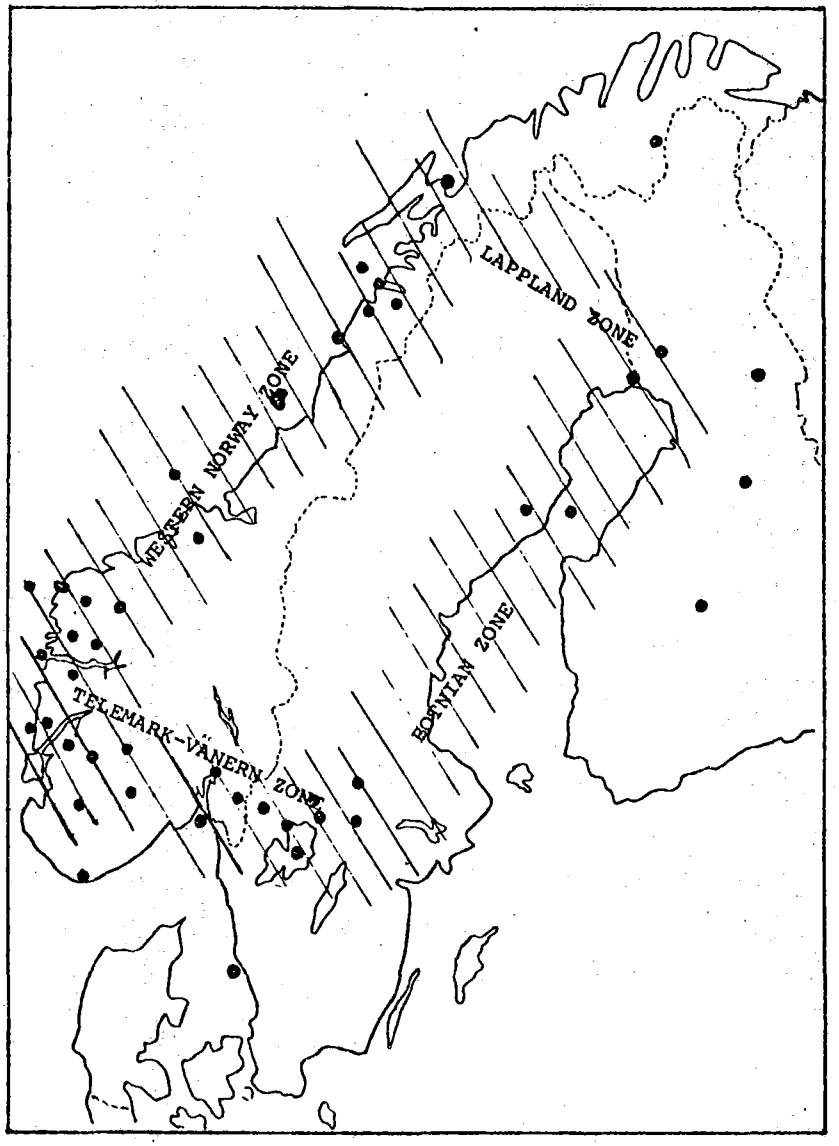

Fig. S.1 Epicenter map of Fennoscandian earthquakes (magnitude $\geq$ 4.5) for the period 1497-1973. Hatched areas indicate the proposed major seismicity zones.

T. DETECTION PROCESSOR OPERATION

The Detection Processor system has been run and operated with the goal of having minimal system down time within the reporting period. The up time percentage is thus 99.2% for this period, as compared to 97% for the last reporting period (January - June 1974). The causes of breaks in the recording have mainly been hardware problems. A floating threshold procedure has been introduced, computing periodically a noise stability estimate. The low priority message task has been split into overlays, to obtain space for future additions to DP.

T.1 Data Recording and DP Down Time

Fig. T.1 and the accompanying Table T.1 show the daily DP down time in hours for the days between 1 July 1974 and 30 June 1975. The monthly recording times and percentages up are given in Table T.2. The most significant break, as seen from Fig. T.1, occurred on June 26, when a power failure had introduced an error in the SPS hardware. The DP went down 3 times, giving a total down time of 3 hours on the 25th and a little more than 11 hours on the 26th. On March 10 a case of "SPS interrupts not received by the DP" caused the system to be down more than 6 hours. On August 9, 1974, the SPS went down, indicating high temperature (THERM - FR 1 on), giving a break of 5½ hours.

Additionally, we have a relatively even spread of down time throughout the period. However, if we look at the column giving "DAYS WITH BREAKS", we will see that this number has been low after January this year. Since repeated breaks within a day very often have the same cause, the decrease of this number indicates better conditions towards the end of the period. The 130 breaks listed in Table T.1 can be separated into the following groups, according to the cause of the break:

SPS problems	: 23
Software problems	: 22
TOD problems	: 21
Other hardware (CPU, 2701, etc.)	: 15
Power breaks & jumps	: 12
Tape drive problems	: 10
Disk drive problems	: 7
CE work	: 7
Program change	: 6
Tests	: 3
ARPANET TIP	: 2
Unknown	: 2

The "Software problems" category consists mainly of situations when, for some reason not yet understood, the system timing printed out on the 1052 console typewriter is completely wrong. To correct this, the system has to be taken down and up again. A malfunctioning Time-of-Day (TOD) unit was the cause of many recording irregularities and breaks, until the error was tracked down and fixed in the beginning of February this year. It has worked correctly since that time. Apart from these two categories, the predominant causes of DP going down have been hardware problems. The case of the SPS not sending an interrupt when it should is the major single cause of DP going down. The total down time for this period was 74 hours 15 minutes. The over-all mean time between failures, which is the sum of the uptime intervals, divided by the number of breaks plus one, was 2.8 days, as compared with 1.7 days for the last reporting period (January - June 1974).

T.2 DP Algorithms and Parameters

Two changes have been performed in the programs making up the Detection Processor. The Low Priority Message task has been implemented as a set of overlays, in order to make room

for the future implementation of the Network Control Program task. A floating threshold procedure has been coded into the detection task. An estimate of the noise stability is computed periodically, to be ultimately passed to the Event Processor in a signal arrival record.

D. Rieber-Mohn

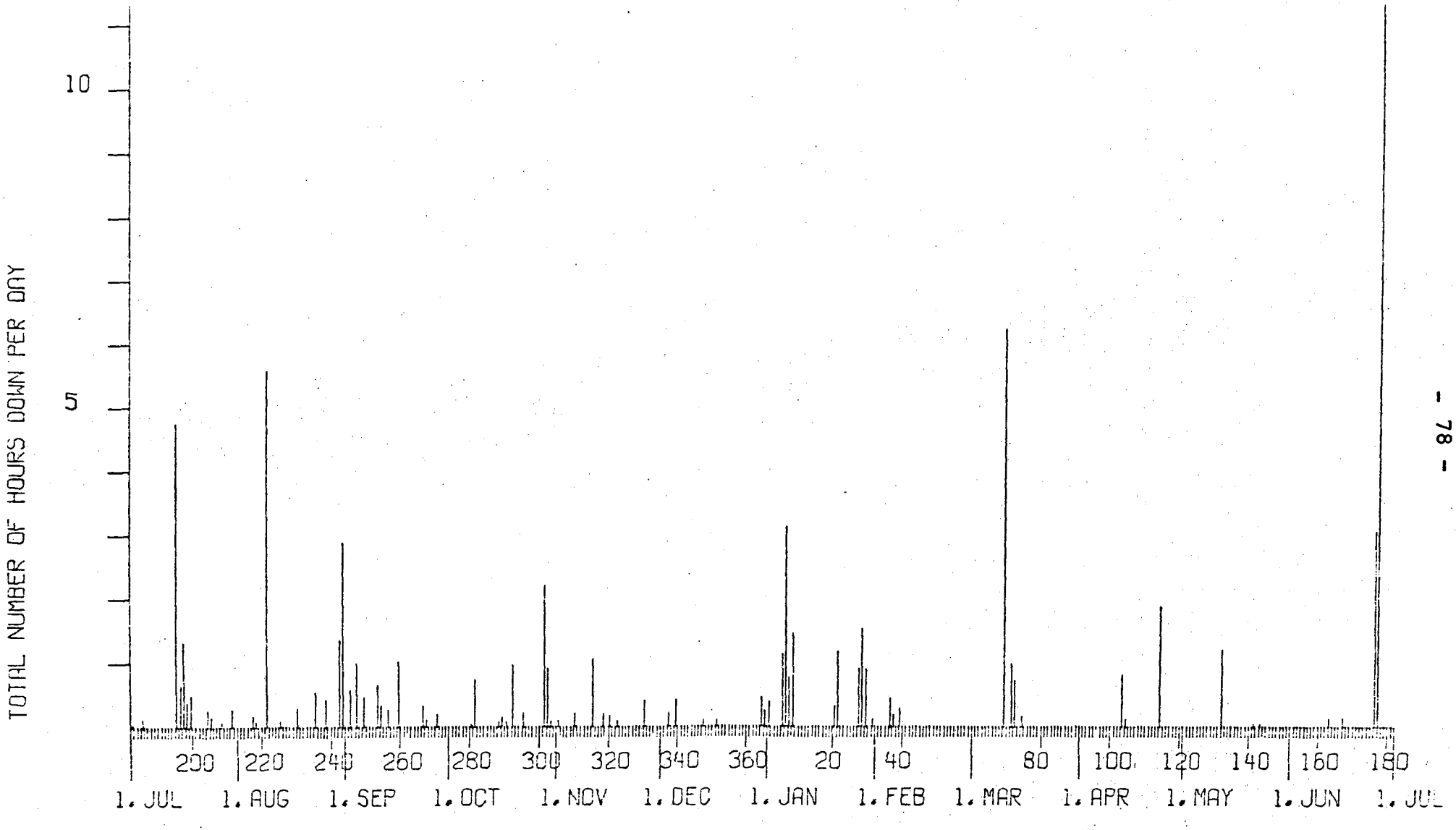

Fig. T.1 Detection Processor down time in the period 1 July 1974 - 30 June 1975.

TABLE T.1

List of breaks in DP processing in the period 1 July 1974 - 30 June 1975.

LIST OF BREAKS IN DP PROCESSING THE LAST YEAR

DAY	START		STOP		COMMENTS.....
182	9	55	9	57	CHANGE OF TAPE UNITS
185	12	3	12	11	CHANGED TOD UNIT
195	11	29	14	35	POWER BREAK
195	20	55	22	14	CPU FAILURE A TO B
196	9	24	9	38	POWER FAILURE ON B
196	15	12	15	37	SPS INTER NOT RECIVED
197	1	53	2	37	POWER ON A CAUSE B STOP
197	20	39	21	15	2701 FAILURE
198	22	25	22	48	2701 POWER TROUBLE
199	7	4	7	11	2701 FAILURE
199	13	33	13	47	270. FAILURE.SPS I.N.R.
199	17	16	17	27	TOD FAILURE
204	14	30	14	46	POWER JUMP
205	3	33	3	43	1052 TIMING WRONG
208	8	19	8	24	1052 TIMING WRONG
211	15	25	15	42	1052 TIMING WRONG
217	0	41	0	52	SPS INTER NOT RECEIVED
218	12	25	12	30	PROGRAM CHANGE
221	0	17	0	55	SPS HIGH TEMPERATURE
221	1	17	6	15	SPS HIGH TEMPERATURE
225	8	35	8	41	1052 TIMING WRONG
230	1	28	1	46	TOD ADJUSTMENT
235	3	25	3	33	2701B POWER FAILURE
235	11	53	12	13	PROGRAM TEST
238	9	56	10	12	TAPE INDICATE ON 183
238	10	27	10	37	POWER FAILURE
242	21	57	23	19	POWER OFF FOR 8
243	18	16	21	11	CHANNEL 1 HANGING
245	8	2	8	13	BAD TAPE UNIT 252
245	9	5	9	29	TEST ON TAPE UNIT 272
247	10	51	11	5	SPS INTER NOT RECEIVED
247	12	9	12	30	PROGRAM ERROR
247	12	47	12	58	PROGRAM ERROR
247	13	56	14	12	PROGRAM ERROR
249	13	4	13	32	PROGRAM ERROR
253	8	8	8	28	PROGRAM ERROR
253	14	16	14	35	PROGRAM ERROR
254	13	14	13	35	PROGRAM ERROR
256	10	26	10	43	PROGRAM ERROR
259	20	26	21	27	POWER BREAK
266	8	0	8	20	CHANGE OF TAPE DRIVES
267	9	9	9	15	PROGRAM CHANGE
270	11	44	11	56	PARAMETER CHANGE
280	9	15	9	18	CHANGE OF TAPE DRIVES
281	16	15	16	59	1052 TIMING WRONG
288	8	56	9	1	1052 TIMING WRONG
289	9	59	10	9	CHANGE OF TAPE DRIVES
290	7	26	7	31	1052 TIMING WRONG
292	12	58	13	56	T.U. 270 CAUSED HANGUP
295	17	54	18	8	PUNCH UNIT CHECK
301	8	56	9	10	T.U. 252 CAUSED HANGUP
301	18	50	20	25	DISK DRIVE IAO TROUBLE
301	22	56	23	19	DISK DRIVE IAO TROUBLE
302	6	51	7	6	DISK DRIVE IAO TROUBLE
302	8	31	9	11	DISK DRIVE IAO TROUBLE
303	9	25	9	30	CHANGE OF DISK PACK
305	12	0	12	6	CHANGE OF DISK DRIVES
310	7	52	8	5	CE WORK
315	3	48	4	52	POWER FAILURE
318	12	52	13	5	CE WORK

LIST OF BREAKS IN DP PROCESSING THE LAST YEAR

DAY	START		STOP		COMMENTS.....
320	0	1	0	12	DISK DRIVE TROUBLE
322	17	30	17	36	TOD ADJUSTMENT
330	14	22	14	47	CE CAUSING MACHINE CHK
337	8	54	9	2	PROGRAM CHANGE
337	10	43	10	49	PROGRAM CHANGE CORR.
339	10	11	10	15	CHANGE OF TAPE DRIVES
339	20	33	21	0	CHANNEL HANGUP
347	6	42	6	48	1052 TIMING WRONG
351	6	56	7	2	PROGRAM CHANGE
364	9	45	10	13	CE WORK
365	23	45	24	0	TOD ADJUSTMENT
1	0	0	0	10	TOD ADJUSTMENT
1	1	14	1	20	1052 TIMING WRONG
1	3	2	3	10	1052 TIMING WRONG
5	3	24	4	32	CPU ERROR A TO B
6	6	0	6	10	UNKNOWN
6	10	46	10	54	TOD FAILURE B TO A
6	11	29	11	45	TOD FAILURE
6	13	55	14	14	CPU ERROR A TO B
6	16	23	18	12	CE WORK
6	18	39	19	0	CE WORK
7	11	43	11	53	TOD ADJUSTMENT
7	17	35	18	8	TOD ADJUSTMENT
7	18	13	18	16	SPS INTER NOT RECEIVED
8	7	19	7	35	TOD ADJUSTMENT
8	10	36	11	3	TOD ADJUSTMENT
8	11	24	11	37	TOD UNIT CHANGED
8	14	9	14	40	TOD ADJUSTMENT,B TO A
20	9	28	9	33	TIP POWER OFF
20	12	32	12	47	ARPANET INTERFACE TEST
21	9	45	10	35	POWER FAILURE A TO B
21	13	40	13	52	INTERFACE TEST B TO A
21	14	39	14	49	TIP POWER OFF
27	12	32	12	49	TOD INCORRECT
27	14	47	14	58	TOD INCORRECT
27	15	21	15	48	TOD INCORRECT
28	21	35	23	7	POWER JUMP
29	8	20	8	56	TOD INCORRECT
29	13	6	13	24	TOD INCORRECT
31	13	2	13	10	TOD ADJUSTMENT
36	10	56	11	25	POWER JUMP
37	9	7	9	10	TOD ADJUSTMENT
37	12	56	13	5	SPS C3 FRAME 1 POWER
39	12	8	12	26	CE WORK
69	3	55	10	12	SPS INTER NOT RECEIVED
71	14	37	14	47	SPS INTER NOT RECEIVED
71	19	32	19	37	SPS INTER NOT RECEIVED
71	20	16	20	47	SPS INTER NOT RECEIVED
71	23	47	24	0	SPS INTER NOT RECEIVED
72	0	0	0	8	SPS INTER NOT RECEIVED
72	1	6	1	22	SPS INTER NOT RECEIVED
72	2	38	2	44	SPS INTER NOT RECEIVED
72	3	48	4	1	SPS INTER NOT RECEIVED
74	10	20	10	30	UNKNOWN

Table T.1
Sheet 2 of 3

LIST OF BREAKS IN DP PROCESSING THE LAST YEAR

DAY	START		STOP		COMMENTS.....
103	8	17	8	28	SPS INTER NOT RECEIVED
103	8	49	9	26	SPS INTER NOT RECEIVED
104	1	33	1	40	SPS ERROR,WRONG TODTIME
114	13	47	13	56	SPS INTER NOT RECEIVED
114	14	10	14	32	SPS INTER NOT RECEIVED
114	14	34	14	56	SPS INTER NOT RECEIVED
114	15	11	15	34	SPS INTER NOT RECEIVED
114	15	42	16	0	SPS INTER NOT RECEIVED
114	20	29	20	47	SPS INTER NOT RECEIVED
132	4	26	5	38	1052 ERROR A TO B
141	11	32	11	35	B TO A
143	10	17	10	29	POWER JUMP
163	8	0	8	8	LINEPRINTER BAD,A TO B
167	7	50	7	58	B TO A
176	20	58	24	0	SPS ERROR,POWER FAILURE
177	0	0	1	3	SPS ERROR,POWER FAILURE
177	1	30	2	50	SPS ERROR,POWER FAILURE
177	4	58	13	56	SPS ERROR,POWER FAILURE

Table T.1
Sheet 3 of 3

TABLE T.2

DP and EP Computer Usage 1 July 1974 - 30 June 1975.

Month	DP Uptime (hrs)	DP Uptime (%)	No. of DP Breaks	No. of Days with DP Breaks	DP MTBF	EP Uptime (hrs)	EP Uptime (%)
Jul 74	738	99.1	16	11	1.9	336	45.2
Aug 74	733	98.5	12	9	2.6	264	35.5
Sep 74	715	99.3	15	10	2.0	200	27.8
Oct 74	739	99.3	13	10	2.4	225	30.2
Nov 74	718	99.7	7	7	4.3	218	30.3
Dec 74	742	99.8	88	6	3.9	191	25.7
Jan 75	732	98.4	29	11	1.1	175	23.5
Feb 75	671	99.9	4	3	7.0	198	29.5
Mar 75	736	98.9	9	4	3.4	166	22.3
Apr 75	717	99.6	9	3	3.3	233	32.4
May 75	743	99.8	3	3	10.3	167	22.4
Jun 75	705	98.0	5	4	5.9	236	32.8
Total	8688	99.2	130	81	2.8	2609	29.8

U. EVENT PROCESSOR OPERATION

U.1 General Considerations

The operation of the Event Processor system (EP) has in this period been somewhat hampered by malfunctioning hardware (Tape drives, 2260 console, disk drives) and improper input data from disk files and tapes. Since the EP is strongly tape-dependent, the recurring problem of tape read data check causes a deterioration in the performance.

U.2 Computer Utilization

During the period July-December 1974 the EP was up 32.5% of the time, and for January-July 1975 the percentage was 27.2, which is the lowest ever recorded. Two changes in the EP programs in this last year have influenced the processing time: Firstly, a new package has been developed which is executed for some of the events in order to perform some statistical tests and a possible weighted beamforming. This should increase the computer time per event, while the statistics show that the time per processed detection and especially the time per accepted event has never been smaller. This can be explained by the second change, namely, the floating EP acceptance threshold. Although the number of processed detections is still about the same, the number of false alarms has decreased and the relative number of accepted events has increased. Since the false alarms (noise detections) always require more computer time, this can explain the increased efficiency of the EP.

U.3 EP Operational Problems

No special operational problems have occurred in this period, apart from the infrequently occurring breakdowns because of bad input data from the shared disk files or tapes. Bad detection times are especially malicious, because the effects of reading such times propagates through the system. Another source of operational problems is malfunctioning hardware, such as tape drives, disk drives and the 2260 console station.

U.4 EP Parameters and Algorithms

The following changes have been made to the Event Processor system within this period:

A new program package was added on December 2. This package (SP8) will be invoked by weak events with signal-to-noise ratios just above the pre-processing threshold. Three different test statistics will be computed, to aid the analyst in his signal-noise decision. Depending on the value of the first statstic a weighted array beamforming will be performed, using optimum subarray beam weights.

The results of the three tests and the optimum weights will be printed in the Summary Report for the event. Also, the weighted array beam is plotted on the event's plot panel.

On December 16 changes were introduced in the EP controller, in order to compute periodically a "floating" signal-to-noise ratio pre-threshold for the coherent detections. A noise stability estimate (STAB) is received with each signal arrival, as read from the Signal Arrival File on the Shared Disk pack. Together with the desired false alarm rate (FAR) inserted by the operator at start-up time, the pre-threshold value (TH) is computed as follows:

$$TH = 12.08 - 0.89 \log (FAR) - 0.18\ STAB$$

This computation is performed each time a new value of STAB differs from the earlier one, which means that the noise stability, as computed by DP, has changed. The actual computation of TH is done in a separate FORTRAN overlay phase, loaded and invoked by the EP controller each time it is used.

On January 4 an option to invoke the SP8 package for a re-run was introduced in MJRRUN, the re-run initialization program.

On March 4 a small subroutine (SPCONV) was added to the Detection Bulletin Report package. Instead of doing a dummy read statement (from data set zero) in SPRELSE, using PFIOCS and IOCS for a format conversion, the new subroutine performs just this. The earlier technique did not seem to work on all occasions and caused EP to terminate at this point.

On May 15 the Partial Array Beam list in EP Common was changed upon request from Vela Seismological Center. The Partial Array Beams (PABs) were changed to be as follows:

PAB 1 = Subarray Beam 01A
PAB 2 = " " 03C
PAB 3 = " " 07C
PAB 4 = " " 13C

At the same time the lower limit for the computed "floating" pre-threshold of coherent detections was lowered from 3.4 to 3.2.

U.5 EP Performance Statistics

Summaries of analyst decisions for each of the two half years in this reporting period are given in Tables U.1 and U.2. The only significant change from previous reporting periods is the drop in the number of false alarms after the floating threshold procedure was implemented late in December 1974. The main effect there, however, is not so much on the total number of false alarms but on the distribution: there is now about equally many false alarms every day regardless of noise conditions. This avoids the

processing of a large number of noise detections during microseismic storms, and normally it should also pick up some additional events during quiet periods. As mentioned above, it has resulted in a more efficient utilization of the computers: the EP up time per accepted event is now at an all time low.

The number of reported events on a monthly basis is given in Table U.3, and the distribution on a daily basis is shown in Fig. U.1. The large number of events in August 1974 is due to an earthquake swarm from the Tadshik-Sinkiang region, while swarms from Japan and the Kuriles can explain the large number of events in June 1975.

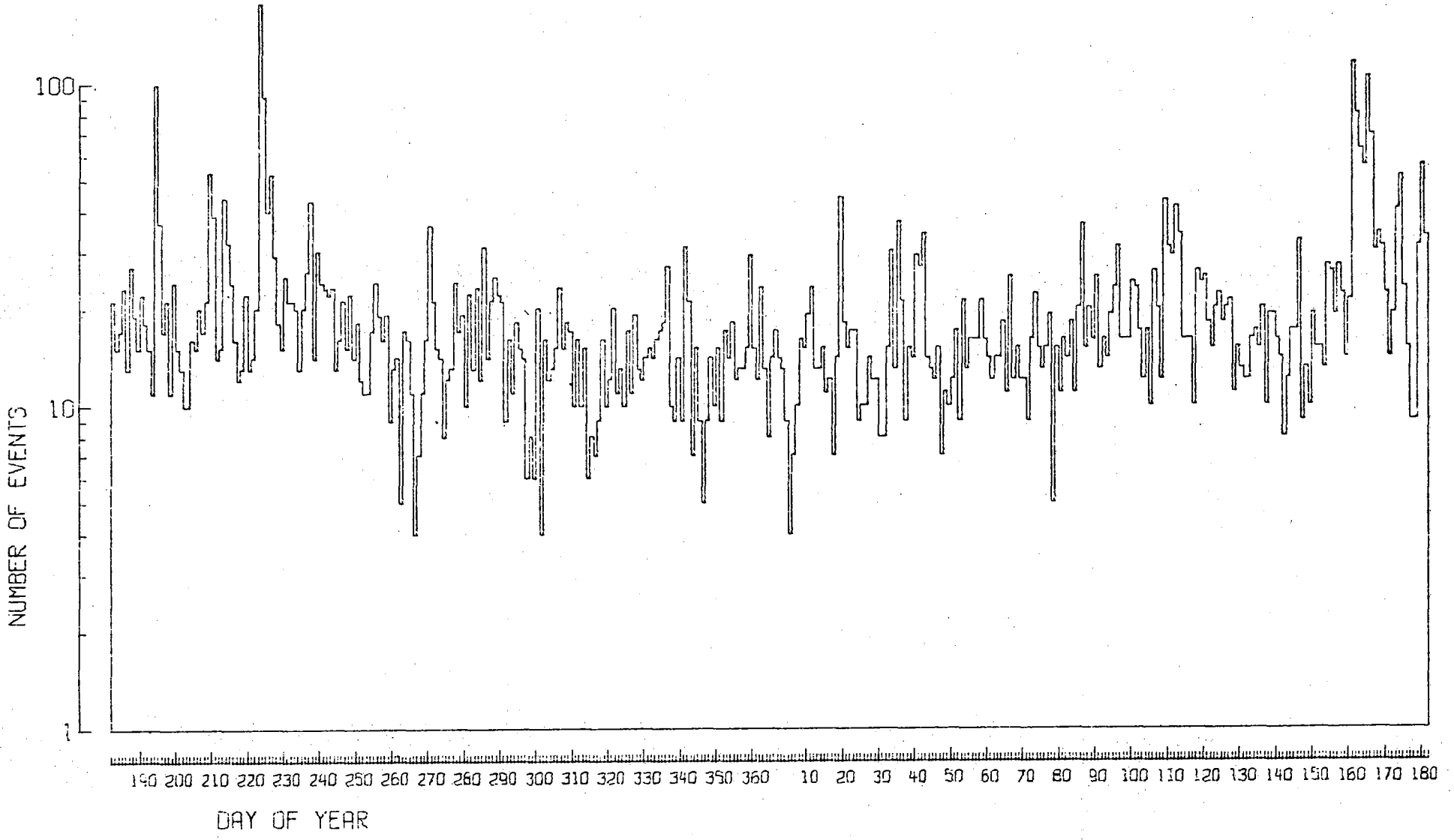

Fig. U.1 Number of events as a function of day of year July 1974-June 1975.

TABLE U.1

Analyst decisions for detections processed by EP during the time period July-December 1974.

Analyst Classifications	Number of Processings	Percentage
Accepted as events	3798	48.4
Rejected as being		
- Poor SNR or noise	1910	24.3
- Local events	905	11.5
- Double processings	796	10.2
- Communication errors	436	5.6
Sum Processed	7845	100.0

TABLE U.2

Analyst decisions for detections processed by EP during the time period January-June 1975

Analyst Classifications	Number of Processings	Percentage
Accepted as events	3929	53.2
Rejected as being		
- Poor SNR or noise	1039	14.1
- Local events	1213	16.4
- Double processing	723	9.8
- Communication errors	476	6.5
Sum Processed	7380	100.0

TABLE U.3

Number of teleseismic and core phase events reported during the time period July 1974-June 1975.

Month	Teleseismic	Core	Sum
Jul 74	532	151	683
Aug	851	106	957
Sep	374	83	457
Oct	394	81	475
Nov	318	91	409
Dec	369	79	448
Jan 75	346	80	426
Feb	391	92	483
Mar	401	89	490
Apr	525	111	636
May	402	93	495
Jun	1003	80	1083

V. PROGRAMMING ACTIVITY

The programming group consisted of 5 persons at the outset of this period, but was reduced to 4 at the start of 1975. A further reduction of one person occurred at the end of this period. The group has been involved in the following activities:

- new programming developments
- maintenance and improvement of existing programs and program systems
- routine processing of utility and application programs
- consultation support
- use of the ARPA network and related studies.

The maintenance of the program systems and the use and study of the ARPA network is described elsewhere in this report.

V.1 Development of New Programs

The following programs have been designed and coded in this period:

- a program that, based on a card-punched input of the DP down time history of a certain period, computes various parameters and plots a diagram giving down time each day (N/PD-69, DPDWN),
- a FORTRAN compatible tape write routine for writing binary records of arbitrary length on a tape (N/PD-70 WRTREC),
- A FORTRAN compatible routine for forward or backward spacing of files on a multifile tape (N/PD-71, POSTAP),
- a program for computing channel responses for given frequencies, based on a model parameter set or a set given by the user (N/PD-72, DCRESP),

- a set of programs designed to extract NR-records from NORSAR Low Rate tapes and copy them onto NORSAR Data Retention Low Rate tapes (N/PD-73, LRINPUT/LRSTACK/LRLSTPCH),
- a set of FORTRAN disk pack I/O routines that makes it convenient to store and retrieve real data, using a disk pack (N/PD-74, SKRIV/LES),
- a program that plots 3 - component long period NORSAR data for up to 22 subarrays, and optionally performs azimuthal rotation and zero phase filtering (N/PD-75, LPSUBS),
- a program that plots the data on the recording tapes from the Kongsberg High-gain, Broadband, Long Period Seismograph Station (N/PD-76, KBPLOT),
- a program for plotting time series from High or Low Rate tapes, from various sources (NORSAR, LASA, or ALPA), filtered or unfiltered (N/PD-77, TSPLOT),
- a subroutine for converting data from gain ranged to integer format (N/PD-78, FIXIT),
- a program for code conversion of punched card source decks (N/PD-79, CONVRT),
- a subroutine that reads NORSAR Long Period data from NORSAR Low Rate tapes (N/PD-80, LOWRAT),
- a subroutine that reads LASA or ALPA Long Period data from NORSAR Low Rate tapes (N/PD-81, LASA).
- In addition other programs for various applications have been developed. Programs received from other institutions have been adapted for use at NORSAR, as for instance a program received from SDAC for checking out a Special Host Interface Unit, a program for three-dimensional plotting (Algorithm 420 in CACM vol 15, no. 2, Feb 1972), and the international Mathematical and Statistical Library's Utility Program, UBLIBM.

V.2 Routine Processing

Various forms of routine processing have been undertaken by members of the Programming group, to monitor the following activities:

- maintenance of the NORSAR Tape Library directory
- discrimination tests and explosion data compilation
- data retention for High Rate, Low Rate and Detection Log data. This involves selecting data to be saved permanently, and stacking them on so-called data retention tapes, at the end of the original retention period.
- supervision and execution of sporadic run requests for different programs, from scientists, visitors and other institutions.

D. Rieber-Mohn

W. THE NORSAR ARPANET CONNECTION

The Terminal Interface Processor (TIP) located in the NORSAR Data Processing Center is a node in the ARPA Network. Two terminals (Tektronix 4010-1 and Data Dynamics 390) have been attached to the TIP during this period.

The NORSAR bulletin has routinely been converted to paper tape and inputted through the Data Dynamics 390 terminal, to be transmitted to the message file of the U.S. Geological Survey on the OFFICE-1 Host computer at Stanford, California, thus speeding up delivery and keeping the bulletin in a format which is directly machine-readable.

The terminal access has also been used for information exchange with other institutions (Seismic Data Analysis Center, Lincoln Laboratory's Seismic Discrimination Group, U.S. Geological Survey, Vela Seismological Center, etc.). This activity is based on our account on the SRI-ARC (Stanford Research Institute's Augmentation Research Center) computer, and the use of this system's facilities and resources. In the middle of this period our account was transferred to the OFFICE-1 computer, at the closing down of the SRI-ARC computer.

In the beginning of January, two Special Host Interface Units for the 360 machines were installed, thus physically linking the multiplexor channel of each IBM/360 machine to a corresponding General Host Interface within the TIP. A program called "WRABBIT" was received over the ARPANET from SDAC and was, with small modifications, used to check out the Host-TIP connections through the installed units.

During the last six months of the reporting period, a first version of a Network Control Program, dedicated to data exchange with the forthcoming Communications and Control Processor (CCP) has been developed to be implemented as a task in the Detection Processor System. This task has been implemented and tested out in the so-called Secondary On-line System (SOS), which actually is a copy of the Detection Processor System, used for experimental purposes. The SOS now sends error-free messages to itself over the ARPANET. Also, test sessions have been started, where we have run the SOS, to let it exchange messages with the program in the CCP, presently situated at BBN in Boston, Mass. Some minor discrepancies in the interpretation of protocol were discovered and cleared up. Also, a time discrepancy was discovered.

We are now ready to start up these test sessions again, and expect to test the NCP-task in a more realistic environment, with full processing load on DP at the same time as we exchange messages over the network. A plan for implementation of a Network Control Program of the off-line (B) computer has been worked out, in which we expect to use 7 man-months to perform this job. With the anticipated staff reduction for the next period, this work load estimate may turn out to be too small.

D. Rieber-Mohn

X. NORSAR DATA PROCESSING CENTER (NDPC) OPERATION

X.1 Data Center

No substantial change in equipment configuration occurred in the period, except for the installation of two ARPANET/ IBM 360 interface units (see Section W).

Operation and maintenance continued in accordance with established routines and schedules. Two new operators were hired as replacements for personnel leaving the project.

In spite of a more intensive care of the equipment, rather frequent failures and malfunctions occurred, in particular of peripherals. Also, a tendency towards more frequent stops of the Special Processing System (SPS) has been observed.

The Time-of-Day (TOD) generator has caused some concern, mainly due to periodic absence of the accurate comparison signal from the nearby Air Force base, caused by faulty equipment. Further experiments have been made with the WWV receiver and various antennas, however, usable signals cannot be obtained due to bad local reception conditions.

X.2 Communications

A summary of communication outages is given in Table X.1. The high outage of 01C is caused by a power outage (broken ground cable) rather than communication failure. Otherwise, the average outage is about "normal". Lines with degraded performance are defined as those having between 20 and 200 errors in a 16-minute interval as seen on the printout. More than 200 errors in the same interval causes masking and outage of the subarray.

TABLE X.1

Communications, degraded performance/outages. Monthly figures in hours. Month= 4 or 5 week period as indicated.

Sub-array	JUL(4)		AUG(5)		SEP(4)		OCT(5)		NOV(4)		DEC(4)		Total ½ year		Per cent ½ year	
	>20	>200	>20	>200	>20	>200	>20	>200	>20	>200	>20	>200	>20	>200	>20	>200
01A	2.5	0.7	1.0	0.8	0.3	0.7	1.7	2.7	2.0	--	0.7	--	8.2	4.9	0.2	0.1
01B	1.8	2.5	2.0	0.8	1.0	0.3	3.7	3.0	1.8	--	1.5	--	11.8	6.6	0.3	0.2
02B	2.0	0.7	1.3	0.8	1.0	0.3	1.0	2.5	1.5	--	1.3	31.6	8.1	35.9	0.2	0.8
03B	2.2	0.7	1.7	0.8	0.3	0.3	1.3	2.5	1.2	--	1.0	1.7	7.7	6.0	0.2	0.1
04B	1.8	1.7	1.0	0.8	0.7	0.3	1.8	11.4	1.5	--	1.3	--	8.1	14.2	0.2	0.3
05B	14.8	2.9	12.8	13.8	18.5	9.9	30.7	7.2	59.3	0.7	24.2	0.8	160.3	35.3	3.7	0.8
06B	5.7	3.9	4.0	4.0	1.5	8.2	1.8	6.6	2.7	1.5	2.7	4.7	18.4	28.9	0.4	0.7
07B	7.2	20.3	3.9	78.3	3.0	7.2	2.2	6.9	2.5	1.5	2.5	1.5	21.3	115.7	0.5	2.6
01C	2.7	115.0	2.7	4.4	1.8	13.8	2.2	9.2	1.5	43.3	1.7	1.3	12.6	187.0	0.3	4.3
02C	14.3	2.4	12.1	7.7	6.2	2.9	16.6	3.0	9.2	2.5	8.1	1.3	66.5	19.8	1.5	0.5
03C	8.2	87.7	1.0	0.8	0.7	1.5	1.3	2.9	1.5	0.5	2.9	1.2	15.6	94.6	0.4	2.2
04C	2.2	108.2	2.7	0.8	--	0.3	0.7	3.2	0.8	16.5	0.7	--	7.1	129.0	0.2	3.0
05C	1.5	396.1	1.2	2.2	0.3	1.0	1.0	2.5	1.8	0.7	1.8	2.7	7.6	405.2	0.2	9.3
06C	0.7	0.3	1.0	45.9	0.7	1.3	0.7	16.4	1.5	40.5	1.0	2.7	5.6	107.1	0.1	2.5
07C	37.0	3.5	60.6	3.7	18.3	1.0	0.3	1.5	1.7	4.0	0.3	--	118.2	13.7	2.7	0.3
08C	--	--	1.8	1.2	2.5	7.1	4.5	16.3	8.7	15.6	4.4	8.7	21.9	48.9	0.5	1.1
09C	4.9	22.0	2.5	3.7	1.8	6.9	2.9	6.6	2.2	2.2	2.0	1.3	16.3	42.7	0.4	1.0
10C	--	672.0	2.2	337.0	4.0	12.8	1.5	85.0	2.5	1.8	1.8	1.2	12.0	1109.8	0.3	25.4
11C	5.4	4.0	4.2	3.7	0.8	7.1	1.7	6.9	2.5	1.8	2.2	4.2	16.8	27.7	0.4	0.6
12C	7.4	4.2	4.5	4.4	0.8	8.7	1.5	6.9	1.8	1.5	2.2	7.4	18.2	33.1	0.4	0.8
13C	20.3	273.5	5.0	4.0	2.2	26.5	2.5	31.4	49.9	6.6	131.9	54.4	211.8	396.4	4.8	9.1
14C	3.0	41.8	1.8	56.6	0.3	13.9	2.0	9.4	6.0	3.0	2.2	1.8	15.3	126.5	0.4	2.9

TABLE X.1

Sub-array	JAN (5) >20	JAN (5) >200	FEB (4) >20	FEB (4) >200	MAR (4) >20	MAR (4) >200	APR (4) >20	APR (4) >200	MAY (5) >20	MAY (5) >200	JUN (4) >20	JUN (4) >200	Total ½ year >20	Total ½ year >200	Per cent ½ year >20	Per cent ½ year >200
01A	5.9	--	0.3	0.3	0.8	0.7	--	0.3	1.2	0.7	0.3	--	8.5	2.0	0.2	--
01B	4.2	0.3	1.7	0.3	1.8	1.3	0.3	0.3	1.5	0.7	0.3	--	9.8	2.9	0.2	0.1
02B	5.2	--	1.7	15.6	1.2	1.3	0.7	1.0	2.2	3.7	0.3	--	11.3	21.6	0.3	0.5
03B	4.5	--	1.0	15.6	1.8	1.3	0.7	1.0	3.0	45.5	0.3	--	11.3	63.4	0.5	1.5
04B	6.0	--	1.3	--	1.5	1.3	0.3	0.3	1.8	1.5	0.7	--	11.6	3.1	0.5	0.1
05B	125.8	85.3	83.5	43.0	90.7	148.3	3.4	32.4	1.8	10.4	0.3	1.2	305.5	320.6	7.0	7.3
06B	26.9	4.0	8.2	22.7	1.8	9.7	8.6	34.3	4.5	11.2	0.3	1.2	50.3	83.1	1.2	1.9
07B	4.7	234.0	5.4	22.2	3.0	6.6	3.9	33.6	2.5	18.8	--	1.2	19.5	316.4	0.4	7.2
01C	22.2	153.2	12.3	36.3	2.5	6.7	--	640.8	--	840.0	--	672.0	37.0	2349.0	0.8	53.8
02C	5.0	1.0	3.9	6.6	3.7	1.7	199.2	199.8	4.9	22.3	--	--	216.7	231.4	5.0	5.3
03C	5.7	--	--	0.3	2.4	1.8	0.3	0.7	1.5	3.0	0.7	--	10.6	5.8	0.2	0.1
04C	4.5	0.3	0.3	24.9	1.2	1.3	1.0	0.3	1.8	3.5	1.0	--	9.8	30.3	0.2	0.7
05C	3.7	--	1.3	16.8	0.8	2.7	1.2	1.5	1.8	1.3	0.3	--	9.1	22.3	0.2	0.5
06C	3.9	--	0.7	126.2	1.5	9.6	--	1.3	1.2	1.5	--	--	7.3	138.6	0.2	3.2
07C	15.1	9.4	1.0	--	2.9	0.3	0.3	--	2.2	3.9	6.2	143.0	27.7	156.6	0.6	3.6
08C	3.5	30.7	1.5	2.9	0.3	--	--	0.8	--	--	--	58.6	5.3	93.0	0.1	2.1
09C	9.9	46.7	16.3	47.7	2.9	6.7	21.8	36.6	4.4	18.5	11.4	16.8	66.7	173.0	1.5	4.0
10C	54.4	5.5	8.4	41.5	2.2	82.7	19.3	38.0	6.0	14.1	5.2	115.1	95.5	296.9	2.2	6.8
11C	33.8	3.0	18.3	28.9	2.5	7.1	9.1	92.2	1.8	36.3	1.3	--	66.8	167.5	1.5	3.8
12C	32.3	2.9	9.6	51.4	1.7	6.7	8.2	35.8	51.9	53.8	1.5	--	105.2	150.6	2.4	3.4
13C	302.4	48.6	122.8	122.8	2.4	115.6	6.4	194.5	0.7	36.1	0.3	--	435.0	517.6	10.0	11.8
14C	23.7	5.0	28.1	28.1	2.2	4.9	13.6	37.3	2.7	5.0	0.3	--	70.6	80.3	1.6	1.8

TABLE X.1

Sub-array	TOTAL YEAR >20	TOTAL YEAR >200	PER CENT YEAR >20	PER CENT YEAR >200
01A	16.7	6.9	0.2	0.1
01B	21.6	9.5	0.2	0.1
02B	19.4	57.5	0.2	0.7
03B	19.0	69.4	0.2	0.8
04B	19.7	17.3	0.2	0.2
05B	465.8	355.9	5.3	4.1
06B	68.7	112.0	0.8	1.3
07B	40.8	432.1	0.5	4.9
01C	49.6	2536.0	0.6	29.0
02C	283.2	251.2	3.2	2.9
03C	26.2	100.4	0.3	1.1
04C	16.9	159.3	0.2	1.8
05C	16.7	427.5	0.2	4.9
06C	12.9	245.7	0.1	2.8
07C	145.9	170.3	1.7	1.9
08C	27.2	141.9	0.3	1.6
09C	83.0	215.7	1.0	2.5
10C	107.5	1406.7	1.2	16.1
11C	83.6	195.2	1.0	2.2
12C	123.4	183.7	1.4	2.1
13C	646.8	914.0	7.4	10.5
14C	85.9	206.8	1.0	2.4
AVERAGE	108.2	373.4	1.2	4.3
LESS 01C		270.4		3.1

Y. ARRAY MONITORING AND FIELD MAINTENANCE

This section includes a review of actions of remote array monitoring at NORSAR Data Processing Center (NDPC) and maintenance accomplished at the subarrays and the NORSAR Maintenance Center (NMC) by the field technicians.

Y.1 Subarray Monitoring Schedule

The planned schedule for the remote array monitoring (AM) has been well met. No changes have been made in the schedule in the reporting period. The schedule is presented in Table Y.1. The off-line computer requirement for AM is on the average approximately 20 hours per month. Including the on-line tests, the on-line computer time requirement is approximately 77 hours.

TABLE Y.1

Monitoring rates for AM programs.

Biweekly	Monthly	Bimonthly	Quarterly	Annually
LPCAL	SLEMTEST	MISNO	CHANEVLP	SACPLP
RSA/ADC Test		CHANEVSP		
		SACPSP*		

*Subarrays with newly overhauled seismograph amplifiers are analyzed every four months.

Y.2 Maintenance Visits

Fig. Y.1 shows the number of visits to the different subarrays in the period. Excluding visits caused by troubles in the communications system, the subarrays have on the average been visited 7.5 times. The large difference from average for subarrays 03B, 04B, 06C, 07C and 10C is explained in Table Y.2.

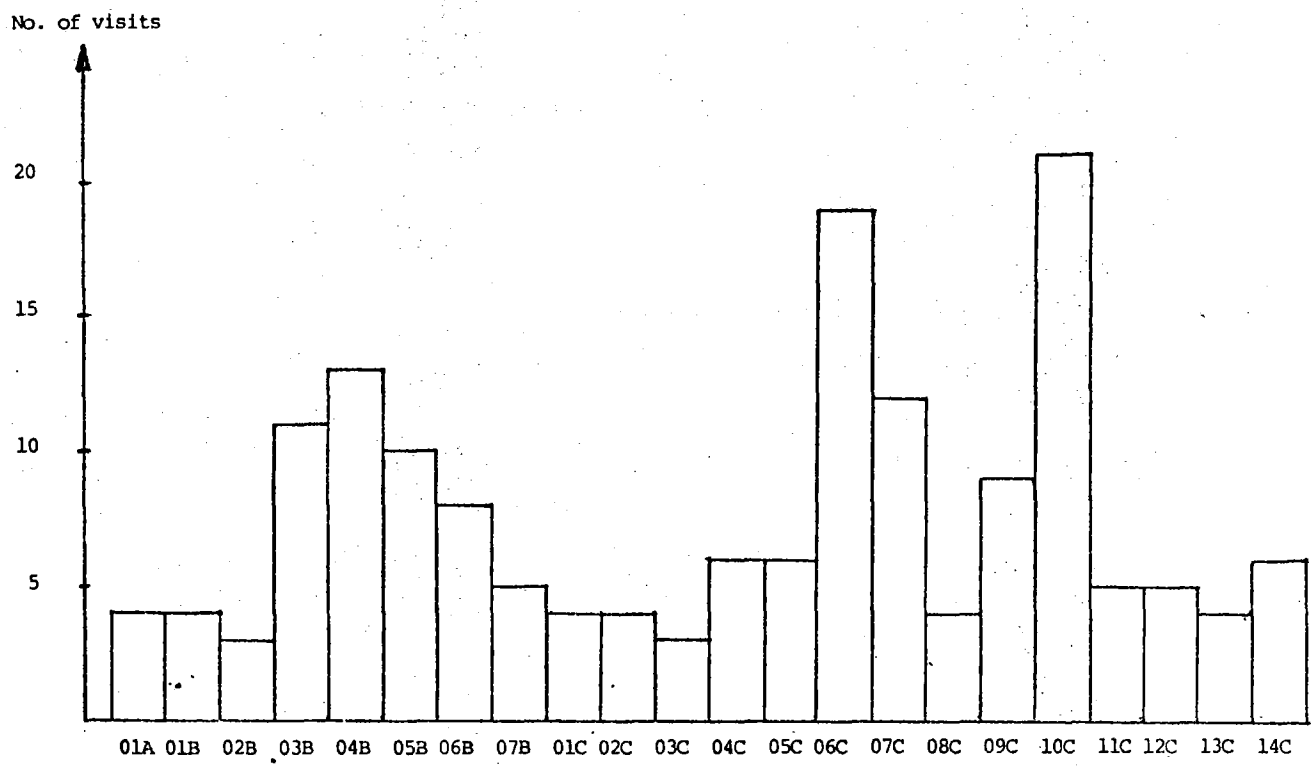

Fig. Y.1 Number of maintenance visits to the NORSAR subarrays 1 July 1974 - 30 June 1975.

TABLE Y.2

Tasks accomplished at 03B, 04B, 06C, 07C and 10C

Sub-array	No. of Visits	Maintenance Visits on: Power/ rectifier	Cable breakage	LP ch's incl. RCD	BE Card	Other Maint.	Comments
03B	11			8		3*	* LTA discrepancies and ch. gain adj.
04B	13		4	3	1	5*	* 2 RA-5's with distortion (3 visits) and CMR/ch. gain.
06C	19	2	5	3	5	4*	* Faulty RA-5's (3 visits) EM cal. circuit faulty
07C	12	1	4		3	4*	* RSA/ADC faulty (1 visit) DCO unadjustable and ch gain (2 visits). RA-5 faulty.
10C	21		16		2	3*	* Routine replacement of RA-5's to prevent power decay (2 visits). Test generator faulty.

Y.3 Preventive Maintenance Projects

Work accomplished as part of this type of the preventive maintenance of NORSAR is described in Table Y.3. The work at WHVs consisted of maintenance such as painting of the wood frame, replacement of RA-5 amplifiers and control of all circuits at the site. The new RA-5's installed had been fully overhauled with new power batteries mounted.

TABLE Y.3

Preventive maintenance accomplished at NORSAR during the period.

Unit	Action	No. of Channels Accomp.	Remaining	Comments
SP Seism.	Adjustment of damping	3	-	10C06,02C05,06 (10C03 remaining from last period has drifted within tolerance limits).
RA-5	Modification of RA-5 input card	1	1[1]	10C04 (remaining 12C05)
LTA	Adjustment of SP DC offset to positive bias[2]	94	-	Whereof 4 LP ch.
	Modification of DC offset adjustment range (R12)[2]	102	30	Remaining: 04B, 01C,08C,13C,14C.
WHV and RA-5	Construction maintenance	11	9	04C03,04;10C01,02, 03,04,06; 02C03,04, 05,06
	RA-5 replacement	10	11	10C01-06; 02C03, 04,05,06 (remaining:12C01-03,05,06; 14C)

1) Modified for noise supression, but variable damping resistance is lacking.

2) Refer Larsen and Nilsen, 1974.

Y.4 Disclosed Malfunctions on Instrumentation and Electronics

Table Y.4 gives the number of accomplished adjustments and replacements of field equipment in the total array with the exception of those mentioned in Table Y.3.

TABLE Y.4

Total number of required adjustments and replacements in the NORSAR data channels, 1 July 1974 to 30 June 1975.

Unit	Characteristic	SP		LP	
		Repl.	Adj.	Repl.	Adj.
Seismometer	Damping		3		7
	Nat. Freq.	2			
	Sensitivity	1			
	Distortion				
	RCD			18	4
Seismometer	Gain	2	2		
Amplifier	Distortion	2			
RA-5	Cal.amp. inop.	2			
LTA	Ch. gain	1	45		3
	Filter discr.	12			
	DCO	4	12		
	CMR	2	9		
	K2 relay fault	4			
BE card		43			
SLEM					
BB gen.		3	2		
SP gen.		1			
LP gen.		1			
RSA/ADC		2	5		
EPU		1			
DU			1		

Y.5 Malfunction of Rectifiers, Power Loss, Cable Breakages

Malfunction of the rectifiers and power loss requiring action of the field technicians are reported in Table Y.5.

TABLE Y.5

Faults disclosed in subarray rectifiers and power loss.

Sub-array	Fault	Period of inoperation	Comments
02B	Main AC power break	8-9 Dec	
01C	Rectifier failed to go into "High Charge" battery power low.		Restarted manually
06C	Main AC power break		Main fuses replaced
	-"-	4-5 Mar	
07C	Rectifier continuous in "High Charge"		Timer coil burned
10C	Main AC power break		Main fuses replaced
14C	Rectifier trafo M2 burned, diode failure on M2 card.	10-13 Aug	

In the period 27 cable breakages have occurred in all types of cables. The field maintenance personnel spent 77 days' work on 17 of the breakages, the rest were repaired by NTA. The status as of 30 June was:

01C: Power cable broken 31 March 75. Repair will be completed in August 75 including modification from 10 KV to 1 KV network.

07C: 04 cable broken 24 March. Repair has been delayed due to agricultural activity. Approximately 600 meters of cable have to be spliced in and buried in a depth of two meters.

09C: 03 cable broken by lightning 16 June 75.

10C: 04 cable was broken again 30 April after repair 14 March 75. 05 cable has been broken since 2 October 74. After 8 days' work the repair had to be postponed due to bad snow conditions. The cable repair is expected to be time-consuming, but should be completed in July 75.

Y.6 Workshop Repairs

All units removed from the field (refer Repl. columns in Table Y.4 and Table Y.3 - RA-5 replacement) this and previous reporting period have been repaired, with the exception of a few SP seismometers. Also remaining unrepaired at NMC are:

1 DC/DC converter
6 RA-5 input cards
11 BE protection cards
1 Code Converter 02

Thirteen LTA cards with presampling filter faults are stored at NMC. Repair (replacement of the presampling filter) is not planned in the near future, as the number of spare LTA cards is good.

Y.7 NMC Facilities and New Instruments

The NMC workshop and storage were slightly damaged by fire 24 November 1974. The cleaning up and repair work engaged the field technicians several weeks. The communication line between NDPC and NMC was broken during the fire and has not been re-established. In order to save funds investigations were initiated to achieve alternative solutions to the permanent line. After installation of the short period analog SP station at NMC/04B05 there is a two-pair line connection between NMC and the CTV at 04B through 04B05. The experiments and measurements made are promising, but line equilizers should be constructed before the line may be taken in regular use.

One Hewlett-Packard 5035T logic lab including logic test probes were acquired in April 1975.

Y.8 Improvements

The status of a number of investigations to prepare lasting solutions to problems or time-consuming maintenance of certain units experienced during the operation of NORSAR is as follows:

- Depression of noise in SLEM discrete inputs and - Too low surge rating of BE protection card	Proposed modifications have been tested and are described in Larsen, Falch and Pettersen, 1975. We are now awaiting approval.
- False triggering of CTV water monitor	Investigations have shown that only marginal improvements can be gained by a modification. Recheck of the "turn on" point is expected to be completed on all subarrays this year.
- Trends towards negative DC offset in the SP/LTA	Modification (refer Larsen and Nilsen, 1974) is accomplished on 77% of the channels.

Y.9 Short Period Analog

The short period analog station located at subarray 05C with the recording drum in the NORSAR Data Processing Center (NDPC) was moved to the subarray 04B/NORSAR Maintenance Center (NMC) in November 1974. The recording station is placed in a room in the office building at NMC, the seismic signals are received from seismometer 04B05 with a separate RA-5 seismometer amplifier through a buried cable. The

station is operated continuously and the seismograms are forwarded to NDPC once a week. The technical layout is given in Larsen, 1975. Note that explanations to the Figs. 1 and 2 in the report are interchanged.

Y.10 Experimental Broadband Analog (Kirnos)

The cooperative Nordic research project involving the operation of a Kirnos station at NORSAR concluded 20 September 1974, and the instrumentation was re-shipped to Finland 30 October. The installation and calibration of the instrument are described in detail by Pettersen and Larsen (1974). An evaluation of the station is given in section M in this report.

Y.11 Conclusion

Except for one remark described below, the field instrumentation has operated satisfactorily throughout the period and the facilities are in good standard. Compared with the previous year (refer Bungum, 1974a and b) an increasing number of replaced LP RCD's is observed. The most common fault is corrosion and rust on the RCD's caused by moisture in the LP tanks making the RCD's immovable. But otherwise there has been less moisture in the LPV's after implementation of the routine of not visiting the LPV's except for corrective maintenance. The cause of the damping ratio of the LP channels which have an increasing trend is planned investigated next year. The SLEM units have been more stable this period compared with the previous period, also the number of burned out BE protection cards has been less (43 compared with 68).

The preventive maintenance program for the WHV's and RA-5's has been delayed as priority has been given to the corrective maintenance. Eleven channels are now remaining and will be completed this summer.

The array average DC offset of the SP channels which was nominal one year ago is now plus one quantum unit and is explained by the fact that the modification program of the DC offset trim range of the LTA's is nearly completed. The offset is adjusted to a positive bias of three millivolts to compensate for the negative trend. Because of relatively high noise level the short period data from subarray 14C has been masked since 16 May.

Alf Kr. Nilsen

REFERENCES

Bungum, H. (1974a): Semiannual Technial Report, NORSAR Phase 3, NORSAR Scientific Report No. 4-73/74, NTNF/NORSAR, Kjeller, Norway.

Bungum, H. (1974b): Semiannual Technial Report, NORSAR Phase 3, NORSAR Scientific Report No. 6-73/74, NTNF/NORSAR, Kjeller, Norway.

Larsen, P.W. (1975): Reinstallation of NORSAR SP Analog Station (NAS), NORSAR Internal Report No. 5-74/75, NTNF/NORSAR, Kjeller, Norway.

Larsen, P.W., and A. Kr. Nilsen (1974): DC offset trim modification of NORSAR short period line terminating amplifier, NORSAR Internal Report No. 8-73/74, NTNF/NORSAR, Kjeller, Norway.

Larsen, P.W., K. Falch and R. Pettersen (1974): Modification proposals on SLEM and associated equipment, NORSAR Internal Report No. 3-74/75, NTNF/NORSAR, Kjeller, Norway.

Pettersen, R., and P.W. Larsen (1974): Installation and Calibration of KIRNOS instrumentation, NORSAR Internal Report No. 7-73/74, NTNF/NORSAR, Kjeller, Norway.

ABBREVIATIONS

AC	-	Alternate current
ADC	-	Analog-to-Digital Converter
BB	-	Broad band
BE Card	-	Lightning Protection Card
CMR	-	Common Mode Rejection
CTV	-	Central Terminal Vault
DC	-	Direct current
DCO	-	DC offset
DU	-	Digital Unit
EPU	-	External Power Unit
LP	-	Long period
LPV	-	Long Period Vault
LTA	-	Line Terminating Amplifier
NTA	-	Norwegian Telegraph Administration
RCD	-	Remote Centering Device
RSA	-	Range Scaling Amplifier
SLEM	-	Seismic Short and Long Period Electronics Modules
SP	-	Short period
WHV	-	Well Head Vault